Tissue Engineering Cartilage with a Composite Electrospun and Hydrogel Scaffold

Lee D. Wright

Dissertation Submitted to the Faculty of the
Virginia Polytechnic Institute and State University
In fulfillment of the requirements for the degree of

Doctor of Philosophy
In
Biomedical Engineering

Committee Members:

Joseph W. Freeman (Chairman)
Aaron S. Goldstein
Yong W. Lee
Cristin M. Ferguson
M. Nichole Rylander

March 23, 2011
Blacksburg, VA

Keywords: cartilage, osteoarthritis, electrospinning, hydrogel, tissue engineering

Tissue Engineering Cartilage with a Composite Electrospun and Hydrogel Scaffold

Lee D. Wright

Abstract

Osteoarthritis is the most prevalent musculoskeletal disease in humans, severely reducing the standard of living of millions of people. Osteoarthritis is characterized by degeneration and loss of articular cartilage which leads to pain, and loss of joint motility and function. Individuals suffering from severe osteoarthritis are commonly treated with full knee replacements. The procedure does eliminate the problem of degrading cartilage tissue; however, it does not fully restore function and its lifetime can be limited. To overcome the disadvantages of current treatments, tissue engineering has become a focus of research to regenerate cartilage. Tissue engineering attempts to repair or replace damaged tissue with cells, biomaterials, and/or molecular signals. Biodegradable scaffolds serve as a temporary replacement for the tissue until it has regenerated. Two types of scaffolds that have been used in tissue engineering are electrospun scaffolds and hydrogels. We have proposed and fabricated a scaffold for cartilage tissue engineering that incorporates an electrospun cylinder and a thermosetting hydrogel in order to provide improved properties compared to either individual material.

Electrospun cylinders were created by sintering electrospun mats that include salt pores. The addition of salt pores decreased the mechanical properties of the electrospun materials while also improving the capability of cells to infiltrate into the scaffold. The sintering process involved the connecting of one electrospun mat to an adjacent one. Specifically, poly(d,l-lactide) was capable of sintering to an adjacent electrospun mat when exposed to either heat (near the glass transition temperature) or tetrahydrofuran vapor. The sintering process did not deteriorate the structure or function of the electrospun material. Sintering allowed the creation of unique structures of electrospun material that previously could not be produced.

A thermosetting hydrogel was added to the scaffold to replicate the function of proteoglycans present in articular cartilage. A composite scaffold of electrospun polymer and hydrogel showed improved mechanical properties and better integration of the scaffold *in vivo* compared to an electrospun scaffold with no hydrogel. In conclusion, the composite electrospun and hydrogel scaffold could become an excellent tissue engineering scaffold to treat patients suffering from osteoarthritis.

Acknowledgements

I would like to thank several people for their help during my time at Virginia Tech. First I would like to thank my advisor, Dr. Joseph Freeman, for his guidance and support during my graduate career. He has been a great mentor for the last five years. I would like to thank Dr. Aaron Goldstein for serving on my committee, providing advice, and helping introduce me to electrospinning. I am grateful to Dr. Yong Woo Lee for being on my committee, access to his laboratory equipment, and advice with respect to cell studies. I would also like to thank Dr. Nichole Rylander for being on my committee, for her support, and access to her laboratory equipment. I am also grateful to Dr. Cristin Ferguson for serving on my committee and providing a clinical perspective on my project. I would also like to thank Dr. Lakshmi Nair and Dr. Zhanwu Cui at the University of Connecticut for providing the chitosan hydrogel and performing the in vivo rat study.

I am especially grateful to all the members of the Muskuloskeletal Tissue Regeneration (MTR) Laboratory. In particular I would like to thank my fellow doctoral canidates Tea Andric, Kristin Fischer, and Albert Kwansa. Over the last few years they have helped me immensely in determining the best course of action for my project and helping me solve problems that have developed. I would also like to thank my family for their support throughout my school career. They have always believed in me and supported my decision to attend Virginia Tech for graduate school. Most importantly I would like to thank my wife, Beth Wright, for her support and, in particular, her humor reminding me to enjoy life.

This work was funded by the Walter H. Coulter Foundation.

Table of Contents

List of Figures

List of Tables

List of Abbreviations

Osteoarthritis (OA)

Extracellular matrix (ECM)

Glycosaminoglycan (GAG)

Phosphate buffered saline (PBS)

Cyclooxygenze (COX)

Non-Steroidal Anti-Inflammatory Drugs (NSAIDS)

Autologous chondrocyte implantation (ACI)

poly(2-acrylamido-2-methylpropanesulfonic acid) (PAMPS)

poly(N,N-dimethylacrylamide) (PDMAAm)

Polyethyleneoxide (PEO)

Self-assembling peptide (KLD)

Insulin-like growth factor-1 (IGF-1)

Transforming growth factor β-1 (TGF β-1)

Bone marrow stromal cells (BMSCs)

Poly(d,l-lactide) (PDLA)

Poly(l-lactide) (PLLA)

Poly(lactide-co-glycolide) (PLGA)

Polycaproloactone (PCL)

Dichloromethane (DCM)

Tetrahydrofuran (THF)

Dimethylformamide (DMF)

Minimal Essential Medium (MEM)

CellTiter 96 AQueousOne Solution Cell Proliferation (MTS) assay

Optimal cutting temperature (OCT)

Glass transition temperature (Tg)

Deionized (DI) water

Scanning Electron Microscopy (SEM)

Dulbecco's Modified Eagle Medium (DMEM)

Dimethylmethylene blue (DMMB) assay

Chapter I: Introduction

1.1 Osteoarthritis

Osteoarthritis (OA) is the most prevalent musculoskeletal disease in humans [1], causing pain, loss of joint motility and function, and severely reducing the standard of living of patients. OA is common within the joints of the hand, foot, knee, spine, and hip. This condition affects quality of life of nearly 27 million Americans [2] and is projected to affect nearly 67 million people by 2030 [3]. OA is estimated to have raised the aggregate annual medical care expenditures in the U.S. by $185.5 billion [4]. OA is characterized by degeneration and loss of articular cartilage. Primary OA (idiopathic) is considered to be the result of insidious age-related 'wear and tear' processes, whereas secondary OA develops following acute trauma [5,6]. In both processes, the disease is associated with excessive biomechanical stress [7,8], although the mechanisms by which biomechanical joint trauma leads to OA remain poorly understood.

1.2 Cartilage Biology and Function

Cartilage is a fibrous, dense connective tissue with no blood vessels. The nonvascular nature of cartilage dictates that all nutrients must diffuse or convect through the extracellular matrix (ECM) to the cartilage cells (chondrocytes). Three major types of cartilage exists: hyaline cartilage, elastic cartilage, and fibrocartilage [9].

1.2.1 *Types of cartilage*

Hyaline cartilage is the most abundant type of cartilage; it contains up to 40% of collagen type II by dry weight and is found in the trachea, larynx, fetal skeleton, and the diarthroidal joints of the adult. The fetal skeleton is composed mostly of hyaline cartilage, also called "temporary" cartilage, which becomes calcified cartilage and is later replaced by bone. In addition hyaline cartilage composes the growth plates by which long bones grow during childhood. The specific structure and function of articular cartilage (cartilage within the adult diarthroidal joints) will be discussed in Section 1.2.2 [9].

Elastic cartilage also has a high proportion of collagen type II; however, it also contains a dense network of branching elastin fibers. The elastin allows the cartilage to be more elastic compared to hyaline cartilage in addition to cartilage's inherent stiffness. Thus, elastic cartilage

is important in keeping tubular structures open (i.e. auditory eustachian canals and larynx) and in allowing tissues to expand like the rib cage during respiration [9].

Fibrocartilage is arranged in a fibrous matrix that is similar to fibrous connective tissue. Fibrocartilage is found in areas requiring tough support or great tensile strength. Such areas include intervertebral discs, the pubic symphysis, and sites connecting tendons or ligaments to bone. In addition, when hyaline cartilage is damaged, it is often replaced with fibrocartilage despite it being a poor substitute [9].

1.2.2 *Articular cartilage structure and function*

Articulating cartilage (a form of hyaline cartilage) is well designed for both reducing friction within the joint and transmitting load effectively through the joint. Cartilage is best described through a multiple layer approach because of both structural changes through the depth of the cartilage, and functional differences between each layer. As a result, an effective design approach to creating an artificial articulating cartilage construct is to create layers that replicate the function and structure of each natural cartilage layer and fuse them into the final construct. Therefore, each layer of cartilage must be well understood to replicate the function of cartilage as a whole.

The most superficial layer of articulating cartilage is called the superficial zone. This layer contains the highest concentration of both cells and collagen type II with respect to the other layers. Collagen content is high in this layer because this is the surface at which articulation occurs; this surface experiences the highest amounts of shear, tensile, and compressive forces. The collagen fibers are arranged in planes parallel to the joint surface which helps improve resistance to shear stresses [9-11]. Cell content is high due to an important function that cells at the surface must perform: secretion of the protein lubricin, also called superficial zone protein, which does not occur at any other layer within articulating cartilage. Lubricin is very important for reducing the friction of the articulating surfaces [10]. The content of proteoglycans within the superficial zone is also significantly different compared to the other layers. Decorin and biglycan are at their highest concentrations within the superficial zone, while aggrecan is at its lowest concentration. The high concentrations of decorin and biglycan are believed to be important in fibrilligenesis, resulting in closely knit, smaller molecules of

collagen within the superficial zone [10]. The result is a collagen network more suited to handle the tensile, compressive, and shear forces found within the superficial zone [9,10].

Proteoglycans constitute the 2nd largest portion of the solid phase (15-30% dry weight) in articular cartilage and are composed of glycosaminoglycan (GAG) chains bound to a protein core [9,12]. Aggrecan (aggregating proteoglycans) composes 90% of cartilage total proteoglycan mass and binds to hyaluronan (HA) and link protein; aggrecan consists of a protein core bound to keratan sulfate and chondroitin sulfate GAG chains [9,11]. These chains become negatively charged when in contact with interstitial fluid to attract cations. Small proteoglycans including decorin and biglycan make up approximately 3% of the total proteoglycan mass [11]; they bind to matrix molecules helping to stabilize the matrix. Biglycan and decorin specifically are two forms of dermatan sulfate proteoglycans and are important for fibrilligenesis in the superficial layer of articular cartilage reducing the diameter of collagen fibrils [9-11].

Below the superficial zone lies the midzone. This layer contains lower densities of collagen and cells. The collagen fibrils are larger and more randomly oriented, while the cells take on a rounder morphological shape compared to the superficial layer [9-11]. Unlike the superficial layer, aggrecan concentration is very high [10,11]. Aggrecan's role in cartilage is to modulate the compressive forces that the tissue experiences. Aggrecan performs this task through the hydration of its chondroitin sulfate and dermatan sulfate chains [10]. As compressive forces increase, water is forced out of the tissue relinquishing much of the energy introduced from the compressive load [10]. Thus, aggrecan performs the role of a dashpot (shock absorber), resisting motion through viscous friction.

The third layer of cartilage is the deep zone. The deep zone contains the lowest concentration of cells and collagen fibrils and the highest concentration of the proteoglycan aggrecan [10,11]. The collagen fibrils that are present in the deep zone are greater in diameter compared to the other zones in cartilage. The deep zone, like the midzone, is very important in resisting compressive forces due to its high concentration of aggrecan. The deep zone also serves as a transition layer between cartilage and the subchondral bone [12]. Thus, this layer provides a mechanical buffer between the stiff subchondral bone and the viscous dominated mechanical properties of the other cartilage layers [9,10,12].

Articular cartilage's function is to transmit load from one bone to another while also allowing adequate motion at the joint. Therefore, two of the most important features of cartilage are its frictional properties at the joint surface and its compressive properties. Osteoarthritis treatments can be limited by an inability to reestablish appropriate compressive mechanical properties of the cartilage. Articular cartilage plugs with subchondral bone have been measured to possess a compressive modulus of approximately 10 MPa when tested at 10% strain/minute at 37°C in phosphate buffered saline (PBS) [13].

1.3 Current Treatments for Osteoarthritis

Treatment of individuals suffering from OA is currently very limited. Some individuals take dietary supplements like chondroitin sulfate and glucosamine to reduce the severity of OA or to help prevent OA; however experts currently disagree on the effectiveness [14]. Chondroitin sulfate and glucosamine supplements are derivatives of natural components of healthy cartilage tissue. The goal of this treatment option is to provide component molecules of healthy cartilage to help prevent the degradation of the cartilage; however, this desired effect is unverified. Other individuals simply treat the primary symptom of OA, pain, through traditional pain relievers or, if necessary, prescription medications including NSAIDs (Non-Steroidal Anti-Inflammatory Drugs). Pain drugs, such as NSAIDs, analgesics, and specific COX-2 inhibitors, are widely applied to inhibit cyclooxygenase (COX), the key enzymes that metabolizes arachidonic acid to prostaglandins [15]. Prostaglandins are pain mediators primarily associated with inflammatory reactions within the body. Relieving the pain of OA, however, is not a long term solution since the individual is only treating the symptoms and not the underlying cause. Thus, over time more drastic treatments are often required.

One drastic treatment option is total knee replacement. This treatment replaces the knee joint with a metal and polymeric artificial joint [16] (Figure 1.1). This procedure does eliminate the problem of degrading cartilage tissue; however, the treatment does not fully restore function for an active individual and for younger patients, this artificial knee joint cannot be expected to last throughout their life. In particular, McClelland *et al*. showed that patients had a reduced range of motion within the knee after total knee replacement which is considered to be an important determinant of patients' functional abilities after surgery [17]. After several years the implant may require a revision surgery due to loosening of the implant. The survivorship of a

total knee replacement after 10 years is 83% for individuals 55 and younger compared to 94% for patients over 70 [18]. The most likely cause of the reduced survivorship for the younger population is higher levels of activity that could lead to increased wear and loosening [18].

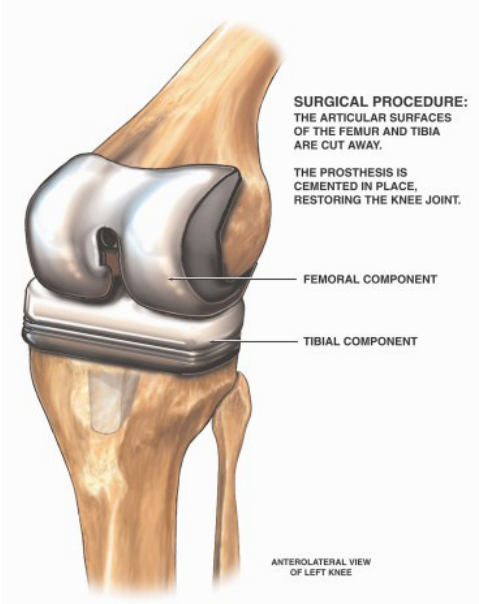

Figure 1.1. Diagram of a total knee replacement [19]. [fair use]

Less drastic surgical treatment options are marrow stimulation techniques. The goal of this technique is to recruit primitive mesenchymal cells by penetrating and stimulating the subchondral bone to utilize its regenerative capability [12]. Microfracture surgery, a descendent of the marrow stimulation technique, employs arthroscopic awls to perforate the subchondral bone of focal articular cartilage surface lesions [20]. However, the success of microfracture surgery is limited because the restored tissue is fibrocartilage instead of hyaline cartilage, which is mechanically inferior [12]. Microfracture surgery has been most effective for young patients with small lesions and strong compliance with rehabilitation protocol [20].

Osteochondral autograft transfer involves the transfer of intact hyaline cartilage and subchondral bone to a load bearing lesion [12,21]. Typically the osteochondral plug is harvested from a nonweightbearing region of the knee and can effectively treat lesions up to 3-4 cm diameter. The most common donor site is the femoral intercondylar notch and the periphery of the lateral femur [20]. This technique is most notably limited by inadequate graft volume and donor site morbidity [22,23].

In contrast to the osteochondral autograft, an allograft provides larger constructs of viable subchondral bone and viable cartilage from cadaveric donors [12,20]. Therefore, large osteochondral lesions typically require allografts that can repair lesions as large as 2.5cm^2 [20]. The current routine involves the use of fresh (not frozen) osteochondral allografts implanted within days of harvest [12]. A longer the delay to implantation increases the death of chondrocytes which can reduce the regeneration capability of the graft. Graft availability, immunogenicity, and potential disease transmission are some additional disadvantages of allografts [20]. The survivorship of allografts is approximately 71% after 10 years with early failure being more common in individuals over 50 [24].

Another popular set of treatment techniques currently being researched are tissue engineering techniques. Tissue engineering approaches involve utilizing cells, biomaterials (scaffolds), and bioactive molecules to encourage regeneration. The scaffold or cell carriers are intended to degrade over time and be replaced by new tissue as time progresses. Only one tissue engineering approach is FDA approved, the Carticel® or autologous chondrocyte implantation (ACI) [25]. This technique is typically considered after other restorative techniques (microfracture and autograft transplantation) have failed [20].

Carticel® or ACI is a relatively simple methodology. Autologous cells are removed from the patient. The cells are then expanded *in vitro* and then reimplanted into the patient at the defect site [12,25,26]. The cells are not placed into a scaffold but instead are injected into the space of the defect and are capped by periosteum from the proximal medial posterior cortex of the tibia; sutures and fibrin glue are used to prevent leakage (Figure 1.2). In some patients, neo-hyaline cartilage is observed, and a large proportion of patients do gain better function and lessening of pain [20]. The rehabilitation after implantation is quite severe, however. Return to normal living and light sporting activity, for instance, cannot occur for 4-6 months [20,27,28]. In addition, many patients are never capable of returning to heavier sporting activity [29]. The purpose of the implant is to simply encourage the formation of new tissue in the defect site from the addition of cultured autologous cells. Loading of the implant immediately after implantation would probably result in the death of the implanted cells or displacement of the cells from the injury site, destroying any possibility of improved function.

Figure 1.2. Photograph of a completed Carticel® graft [30]. [fair use]

Similar to ACI, other researchers are investigating the treatment of injured articular cartilage with autologous bone marrow mesenchymal cells in the femoral condyle and the patellae [31-33]. Cells are obtained from autologous bone marrow (iliac crest), culture expanded, embedded into a collagen gel, and then transplanted into the defect. Matsumoto *et al*. initially performed the technique on rabbits. The results showed that after 24 weeks the subchondral bone was completely repaired without loss or alteration of the overlying cartilage. The procedure was also applied to human patients suffering from cartilage damage. The bone marrow mesenchymal cells were embedded in the collagen gel, transplanted into the defect in the patella, and covered with autologous periostieum. The tissue that formed was typically softer than surrounding articular cartilage, but the repair tissue appeared to be hyaline-like (semi-metachromatic staining). Commonly patients reported improved clinical symptoms; however, the technique is limited because the repaired cartilage was not hyaline cartilage. The authors proposed that the procedure has similar effectiveness to ACI [31,33].

Both of these techniques are only designed for the treatment of small osteochondral defects. They are designed to treat damage resulting primarily from acute injury; they cannot treat the progressive loss of cartilage tissue experienced by many with OA (large cartilage defects or thinning of the entire cartilage tissue). For example, individuals receiving ACI for large osteochondral defects have a high need for later arthroscopic procedures [34]. Due to a lack of mechanical structure, ACI cannot be considered for improving cartilage function for an

entire knee. Thus ACIs are not suitable for individuals requiring a total knee replacement (i.e., patients with severe osteoarthritis). Although it provides hope for the future of treating OA, tissue engineering is not currently capable of treating patients with significant OA.

1.4 Tissue Engineering of Cartilage

Tissue engineering methodologies attempt to repair or replace damaged tissue with cells, biomaterials, and/or molecular signals. Often these techniques intend to leave no artificial device or material in the patient after a certain period of time. Tissue engineering prefers to allow for regeneration of the tissues by the patient that will resume function at some later point in time. Therefore, the goal of a successful tissue engineered implant is to temporarily replace the function of the lost tissue, encourage regeneration of the replaced tissue, and eventually allow the regenerated tissue to fulfill the role of the replaced tissue [35].

A biomaterial is any material that has a medical application. Various materials have been used for medical applications including ceramics, polymers, and metals. Tissue engineering, however, typically utilizes polymers as biomaterials because many are degradable and can have properties similar to native tissues, except in the case of bone tissue engineering which also utilizes ceramics [36].

Biomaterials have been processed by numerous different techniques to create scaffolds for tissue engineering including casting, particulate leaching, gas saturation, electrospinning, melt spinning, fiber extrusion, solid free form fabrication, etc [36,37]. Solvent casting and particulate leaching, solid free form fabrication, electrospinning, and hydrogels formation have been the most commonly investigated techniques for cartilage tissue engineering. Solvent casting and particulate leaching creates sponges of the polymer that have very controllable porosities. An example of this is dissolving a polymer in solvent and then adding salt particles to the solution. The solvent is allowed to evaporate, drying the solution, and then the salt particles are leached out with deionized water to yield the porous structure [38]. The gas saturation technique utilizes gases to produce similar polymer sponges [37,39]. In both cases, the sponges created, however, often have poor mechanical performance and have minimal viscoelastic properties.

Solid free form fabrication methods are defined as a set of manufacturing processes that are capable of producing complex-free form parts directly from a computer-aided design (CAD) model of an object. 3-D printing of a binder molecule on a powder bed can be used to create a polymeric scaffold layer by layer [40]. This technique gives great flexibility in the design and structure of the scaffold to be created. Currently, 3-D printing techniques must be improved in both accuracy and mechanical properties of the materials to become an effective fabrication technique; presently, this technique can only be used for hard materials [40,41]. Electrospinning and hydrogels and their applications in cartilage tissue engineering will be discussed in Sections 1.4.1 and 1.4.2 respectively.

Each processing technique has advantages and disadvantages for tissue engineering applications, but no one technique has been capable of producing a scaffold that can replace and encourage repair of large three dimensional tissues like cartilage. Two specific polymer processing techniques, electrospinning and hydrogel formation, will be utilized in this project because they have very specific advantages that are important for the tissue engineering of cartilage: 1) electrospinning creates polymeric fibers similar to the collagenous ECM and 2) hydrogels imbibe water similar to cartilage tissue, however both techniques have disadvantages that must be overcome.

1.4.1 *Electrospinning*

Electrospinning utilizes an electric field to produce a solid fiber from a viscous polymer solution [42-44]. Continuous stretching, due to the electrostatic repulsion between the charged nanofibers and the evaporation of the solvent, leads to nanofiber formation [45]. Electrospinning is capable of creating long continuous nanofibers and is much more efficient than other nanofiber fabrication techniques. As the diameters of polymeric fibers decreases from several micrometers to nanometers, the materials obtain some very unique characteristics. The nanofiber material has significantly higher surface area to volume ratios and superior mechanical performance compared to any other form of the material [43]. Therefore, creating polymeric fibers within the nanofiber scale has become a very popular processing technique for biomedical applications.

1.4.1.1 The electrospinning process

Electrospinning requires five components: polymer dissolved in a solvent (or in the form of a melt), a syringe and needle, syringe pump, electrostatic field, and a collector/grounded surface [42]. A syringe pump ejects the polymer through a syringe and needle at a constant rate. An electrostatic field is then applied to the polymer as it exits the needle [43,46]. The force of the field overcomes the cohesive forces of the solution, which is dominated by surface tension, causing the polymer to erupt from the needle to form a jet [43,46,47]. As the polymer jet moves from the needle it becomes unstable resulting in a whipping action of the polymer stream. The whipping action leads to stretching and thinning of the polymer solution. During this period the solvent evaporates leaving behind a long, thin fiber of polymer as it reaches the collector [43]. The polymer is deposited on the collector in a random fashion, creating a nonwoven mat.

Many factors influence the electrospinning process. Those which can be easily controlled include the polymer viscosity, solvent(s) utilized, rate of extrusion, strength of the electrostatic field, and the distance from the needle to the ground/collector [43]. The polymer viscosity and solvents used are dictated when preparing the polymer for electrospinning. The molecular weight and concentration of polymer in solution dictate the viscosity of the solution. If the viscosity is too low electrospraying will occur causing the deposition of polymer spheres instead of fibers [43]. If the viscosity is too high the electrostatic field will not be able to overcome the viscosity and the polymer solution will only drip from the syringe. The polymer viscosity also has an important impact on the size of the fibers produced; as the viscosity increases, the fiber diameters also increase [43,47,48]. In addition, a higher polymer concentration decreases bead morphology by reducing their relative size and their likelihood of formation [49]. Only certain solvents can be used for electrospinning. The polymer must dissolve in the solvent(s) at the intended concentration and the solvents must evaporate before the polymer reaches the collector. The solvent(s) used often has a large impact on the distance from the needle to the collector; some solvents require greater distances to evaporate than others.

The rate of extrusion of the polymer from the needle (adjusted by the syringe pump), the strength of the electric field, and the distance from the needle to the collector/ground can be easily adjusted to affect the performance of the electrospinning process. The rate of extrusion of the polymer depends predominantly on the choice of polymer and solvent(s). High extrusion

rates can lead to more prevalent bead formation [48]. The strength of the electrostatic field must be high enough to overcome the cohesive forces of the polymer solution, but not so high as to cause electrospraying. In addition, increasing the voltage can decrease fiber diameter size and can increase bead formation [47,48]. Lastly, the distance from needle to ground can be adjusted to affect the material produced. If the distance is not large enough the solvent will still be present when it reaches the collector producing wetter fibers. Increasing the distance can also decrease the formation of beaded structures [48].

Some other parameters that affect electrospinning are not easily controlled. Environmental factors of temperature, humidity, and air velocity can have significant impacts on electrospinning [43]. High humidity or lower temperatures, for instance, can prevent proper drying and cause entangling of the fibers on the collector [50,51]. In addition, increased humidity can cause the formation of pores on electrospun fibers through "breath figures" [48,52]. Higher temperatures (70°C) were shown to increase uniformity of electrospun fiber diameters compared to those at room temperature [49]. The best solution to overcome the environmental affects is to place the electrospinning process in an environmental chamber where these factors can be controlled and kept consistent.

1.4.1.2 Electrospinning history

Electrospinning was first developed and patented in 1934 by Formhals [53]. He described the process and apparatus for producing artificial filaments using electrical charges. The techniques, however, gained little attention until many years later. Taylor in 1964 developed studies to describe and understand the jet formation process [54]. Due to his work, the conical shape of the jet (often seen at the end of the syringe) was later named after Taylor (the Taylor cone) by other researchers. In 1978 Annis *et al.* first published a paper utilizing electrospun materials for biomedical applications [55]. They created tubes of electrospun material to replace lengths of the thoracic aorta in mini-pigs. The paper began the process of reinvigorating an old technique for new applications. Electrospinning became more prominent in the 1990s as several applications for nanofibers were developed including filtration systems, protective clothing, catalyst substrates, photonics, sensors, and tissue engineering [45]. Interest in electrospinning was further revived when Reneker demonstrated that a multitude of polymers

could be electrospun [56]. Specifically, according to Huang *et al*. over 100 different natural and synthetic polymers have been electrospun [43].

1.4.1.3 Electrospinning variations

The increase in electrospinning research has led to numerous procedural developments. Generally, these developments change the extrusion process, affect the whipping action of the polymer while traveling to the collector, or change the method of collection. These techniques are intended to improve the functionality of the electrospun material for specific purposes. The most common technique employed is the use of a rotating cylinder, often called a mandrel, to collect the electrospun polymer. The rotating mandrel mechanically aligns the electrospun material in a specific direction [57-59]. As the linear speed of the rotating device increases, the alignment of the fibers increases [60-62]. The aligned electrospun material has anisotropic mechanical properties and is often used to orient cells in specific directions for tissue engineering applications [57-59].

Another technique also creates very well aligned electrospun fibers. This method, often termed the 'gap method', uses parallel plates as a collector and ground which are placed a few centimeters apart [63,64]. Fibers accumulate between the two parallel plates creating well aligned fibers. Although, this method creates the most aligned fibers, this practice is not capable of producing thick electrospun materials, limiting its applications.

Electrospinning into a liquid (water) and then drawing out the electrospun material can create long yarns made up of small electrospun fibers [65,66]. The drawing process aligns the fibers producing a continuous yarn of aligned fibers. These yarns could then be further processed into larger structures, e.g. woven into fabrics, or could be used in tissue engineering applications of ligaments and tendons.

Different polymer extrusion techniques can be utilized to create unique fiber morphologies. Two coaxial capillaries can be used to co-electrospin two different polymers creating a core/shell morphology [67-69]. The inner polymer can also be removed to create hollow nanofibers. Another approach removes one component of a two phase polymer blend creating a porous structure in the individual electrospun fibers. This technique significantly

enhances the surface area of the material and could be beneficial for catalysis, filtration, absorption, fuel cells, solar cells, batteries, or tissue engineering applications [45].

Another variation of electrospinning improves the deposition area of electrospun materials. The whipping action of the polymer within the instability region can cause the polymer to be deposited in a large area. For certain applications (e.g. electrospinning on a small diameter rotating collector) a wide deposition area causes a large amount of the polymer to not be collected on the intended target. Deitzel *et al*. utilized a series of electrically charged rings to focus the polymer into a smaller deposition area; the rings constrained the whipping action of the polymer [46]. This technique can be used to improve the deposition efficiency of electrospinning under some conditions.

The porosity and pore size distribution of electrospun materials is very important to many of their applications. To better control and increase the porosity of electrospun materials, porogens have been utilized during the process. Porogens, e.g. NaCl, can be added during electrospinning and become incorporated into the final product [70,71]. The porogen can then be removed creating a void that would not have been present otherwise. The size of the porogen can be adjusted to control the porosity and pore distribution of the electrospun product. Controlling the pore parameters can be important for cell infiltration into tissue engineered scaffolds. Nam *et al.* used this technique to improve cellular infiltration for an electrospun scaffold [70].

1.4.1.4 Cartilage tissue engineering by electrospinning

Electrospinning can produce scaffolds with similar structures to the collagen component of articular cartilage. As a result, several researchers have electrospun both natural and synthetic polymers to attempt to tissue engineer articulating cartilage. Mathews *et al*. electrospun collagen type II to create scaffolds 300μm thick. Normal human articular chondrocytes were then cultured on the electrospun scaffolds. The cells were able to infiltrate into the scaffold, presumably by remodeling the ECM locally [72]. Similarly, human articular chondrocytes were cultured on electrospun silk scaffolds with transforming growth factor-β1 (TGF-β1). The cells attached to, proliferated and redifferentiated in the scaffolds and showed upregulation of chondrogenic markers [73].

Subramanian *et al*. electrospun a combination of chitosan and polyethyleneoxide (PEO) to produce a scaffold for articular repair. The electrospun material had a higher elastic modulus than cast films of the chitosan and PEO. In addition, cell viability was higher on the electrospun scaffolds compared to the cast films [74]. Similarly, Li et al. electrospun polycaprolactone (PCL) to create a scaffold for cartilage tissue engineering. Adult bone marrow derived mesenchymal stem cells (MSCs) were cultured on the nanofibrous scaffold. With the addition of TGF-β1 the MSCs differentiated into a chondrocyte phenotype and produced ECM similar to natural cartilage proteins [75].

1.4.1.5 Limitations of electrospinning

Despite showing considerable promise, electrospinning must overcome several limitations to become a successful processing technique for tissue engineering. As mentioned previously, pore size continues to be a limitation of the electrospinning process. Cells can require pore sizes of 300μm and larger to be able to affectively infiltrate a biomaterial [76]. Although, the use of porogens does provide promise for overcoming this limitation, the reduction of mechanical properties associated with increases in pore size may limit its application. In addition, stringent control of porogen embedding will be required to produce electrospun structures with consistent large pores throughout the electrospun material.

Another limitation of electrospinning is the inadequate number of three dimensional structures that can be produced by the process. Currently electrospun materials have only been produced in sheets, tubes, and bundled fibers. Many tissues will require unique scaffold architectures that are often larger than electrospinning can efficiently produce to become successfully tissue engineered. Cartilage, for instance, would require a structure approximately 2mm thick whose zonal properties change from the surface of articulation to the bone interface. The fibers in cartilage orient differently according to zone: parallel to the joint surface at the articulating surface and perpendicular to the joint surface near the bone surface. Electrospinning is not currently capable of creating such complex fiber arrangements [77]. Electrospinning provides an excellent raw material for tissue engineering of cartilage; however, improvements must be made in processing and fabrication for electrospinning to become an effective technique used in tissue engineering.

1.4.2 *Hydrogels*

A hydrogel is composed of a network of hydrophilic polymer chains that imbibe a large amount of water within their network [78,79]. A large number of common materials are composed of hydrogels including contact lenses and Jell-O®. Hydrogels have been highly investigated for tissue engineering purposes because they are easy to manufacture, have a high porosity, and numerous different polymers can be used [78,79]. Since hydrogels can be fabricated from many different polymers in numerous ways the properties of a scaffold can be well controlled for a particular purpose. In addition hydrogels are capable of delivering molecules locally to improve the regenerative capability of a tissue engineered scaffold. Hydrogels are also capable of maintaining a three dimensional structure because of their branched and crosslinked nature [78,79].

The capability of hydrogels to retain large amounts of water has made them very popular for the tissue engineering of cartilage in particular. Cartilage contains a large amount of water naturally; it imbibes water due to its large amount of aggrecan. The high water content is crucial to cartilage's capability to transmit and dissipate energy while under load. As the tissue is compressed, water is extruded out of the tissue dissipating energy [10]. Since hydrogels inherently have this capability due to their high water content, they have shown considerable promise for tissue engineering applications for cartilage.

1.4.2.1 Current hydrogel approaches

Although hydrogels have several properties that are conducive for tissue engineering, they also have limitations, the most prominent being their weak mechanical properties. To help overcome this obstacle, Gong et al. created double network (DN) hydrogels which are able to resist much higher loads than traditional hydrogels. These hydrogel systems are capable of resisting up to 17.2 MPa of stress compared to 0.8 MPa in compression. The compressive moduli reached 0.3 MPa for the DN hydrogels. The double network hydrogel is composed of two different polymers one of which is highly crosslinked while the other is loosely crosslinked. In addition, the less crosslinked polymer has a molar ratio 10-30 times larger than the other polymer. The highly crosslinked polymer is responsible for increasing the elastic stress while

the other is responsible for increasing the strain resistance by absorbing crack energy and preventing the growth of cracks [80].

Yasuda *et al.* placed a double network hydrogel into osteochondral defects of rabbit knees composed of poly(2-acrylamido-2-methylpropanesulfonic acid) (PAMPS) and poly(*N*,*N*-dimethylacrylamide) (PDMAAm). The defect was 4.3mm diameter and 15mm depth. The hydrogel was placed so that 2mm of defect remained at the surface after hydrogel implantation. To determine the effectiveness of the repair, hemotoxylin-eosin and safranin-o staining were used in addition to reverse transcription polymerase chain reaction (RT-PCR). The defect with no implant contained fibrous tissue and bone tissue after four weeks. The defect that contained the DN gel showed deposition of proteoglycan-rich material and collagen type II near the joint surface. An implant of polyvinyl alcohol (PVA) and ultra-high molecular weight polyethylene (UHMWPE) did not heal as well as the DN gel system [81].

Traditional hydrogels are incapable of locally adjusting their properties. Suri *et al.* created an interpenetrating network hydrogel (IPN) of collagen and hyaluronan whose properties can be adjusted on the macro and micro scale. This system involved the crosslinking of both polymers so that the separate networks became entangled. Collagen and hyaluronan were chosen because collagen serves as a structural component for natural ECM while hyaluronan is important for cell-signaling within the ECM. The properties of the IPN can be controlled by adjusting the amount of crosslinking of the networks; a more crosslinked system is more elastic while less crosslinking leads to more viscous behavior. Suri *et al.* was further able to control regional mechanical properties of the hydrogel by exposing different parts of the IPN hydrogel to different amounts of photo crosslinking. Therefore, they were capable of micropatterning the hydrogel and controlling porosity and mechanics within different zones of the hydrogel. Since many tissues, including cartilage, have varying properties within their overall structure, this technique could be very useful for better mimicking tissues [82].

One class of hydrogels that have become increasingly popular is injectable hydrogels. These hydrogel systems are liquid during implantation and then crosslink at the site of implantation. This technique allows for cells to be delivered with the hydrogel and be well dispersed within the implant after crosslinking. One example of such a system is a hydrogel composed of polyethylene glycol (PEG), gelatin, and genipin (a natural crosslinking agent) by

Miljkovic *et al*. Their hydrogel was placed into the knee defect of rats. The hydrogel was implanted, gelled, and then hydrated. This hydrogel system, however, did not stay within the defect over time as it became dislodged when not glued into place with cyanoacrylate glue [83].

Miller *et al*. used a self-assembling peptide (KLD) hydrogel injected to treat an osteochondral defect. In addition to the KLD hydrogel, they also added chondrogenic factors (dexamethasone, insulin-like growth factor-1, and transforming growth factor β-1) and bone marrow stromal cells (BMSCs) to improve the repair of the osteochondral defect. Defects implanted with KLD alone or KLD with chondrogenic factors showed improved repair compared to untreated defects. However, defects treated with KLD, chondrogenic factors, and BMSCs displayed poorer repair compared to defects with KLD alone or KLD with chondrogenic factors [84]. This hydrogel system is hampered by very low mechanical properties. After 28 days of culture in ITS/FBS medium, the constructs only reached 20-33% of articular cartilage stiffness. At earlier time points the values were much lower than 20% [85].

1.4.2.2 Limitations of hydrogels

Hydrogels have not been created with mechanical properties similar to cartilage tissue [86]. Even double network hydrogels, which display significantly improved mechanics, are not able to resist the compressive loads natural cartilage undergoes [80]. In addition, hydrogels do not have the same microarchitecture of natural cartilage tissue. Articulating cartilage is predominantly composed of the fibrillar type II collagen; however, hydrogels do not have this fibrillar architecture. As a result, cells may experience loads differently within hydrogels compared to native cartilage tissue. This difference could affect the regenerative capability of a hydrogel implant.

1.5 Project Overview

The purpose of this project is to create a composite porous 3D nanofiber and hydrogel scaffold for tissue engineering. The scaffold will have improved mechanical and biological performance because of its composite design. This project divides the task of creating and characterizing the scaffold into three steps:

1) **Creation and characterization of electrospun materials created with pores that are large enough for cellular infiltration.** NaCl particles will be introduced into electrospun mats and then subsequently leached with water. The space where the NaCl particles resided will become large pores which will improve the ability of cells to infiltrate within the electrospun material.
2) **Creation and characterization of three-dimensional electrospun structures.** A very limited number of 3D scaffolds can be created currently which includes sheets, tubes, and bundled fibers. The sintering process (with solvent vapor or heat) allows unique 3D scaffolds to be created that better replicate the natural structure of tissues like cartilage.
3) **Combining electrospun 3D material with a hydrogel to create a cartilage scaffold and characterizing its properties (mechanical and biological).** The composite hydrogel and electrospun scaffold will replicate the functions of the two predominant ECM molecules: collagen and proteoglycans. The electrospun fibers will replicate the function of the collagen fibers, resisting shear stresses and contributing toughness to the scaffold. The hydrogel will attract water into the scaffold in a similar manner as proteoglycans. The water, as in cartilage, will be extruded during compression, thereby, dissipating energy.

Chapter II: Utilizing NaCl to Increase the Porosity of Electrospun Materials

Materials Science & Engineering C-Materials for Biological Applications, 2011. **31**(1): p. 30-36. (L.D. Wright, T. Andric, and J.W. Freeman)

2.1 Abstract

Electrospinning has emerged as a popular method for creating scaffolding materials used in tissue engineering applications to repair or replace damaged tissues. To become a viable scaffold material, however, pore sizes in electrospun materials must be increased to improve cell infiltration. Deposition of NaCl crystals during electrospinning was utilized to help overcome this obstacle. The NaCl crystals are released above the rotating collection mandrel and become incorporated into the poly(L-lactide) electrospun material. The NaCl then leaches out of the electrospun material creating larger pores: average pore diameter of 48.7μm for PLLA-NaCl electrospinning versus 5.5μm for PLLA alone electrospinning. Electrospun PLLA scaffolds with NaCl pores have a lower elastic modulus (8.05 MPa) and yield stress (349 kPa) and a higher yield strain (0.04) compared to their traditional counterparts (40.36 MPa, 676 kPa, and 0.0188). Decreased elastic modulus and yield stress would be beneficial to tissue engineering of elastic tissues including skin. The presence of NaCl pores did not significantly affect the cellular proliferation of MC3T3 cells but did allow for cell infiltration into the electrospun material. Therefore, the creation of large pores through NaCl leaching can significantly improve the performance of electrospun materials for tissue engineering applications by improving cellular infiltration.

2.2 Introduction

Tissue engineering incorporates cells, biomaterials, and/or molecular signals to replace or repair damaged tissue [35,42]. Typically, a tissue engineered graft is intended to replace the tissue's function while the cells reconstitute a natural replacement. The biomaterial and scaffolding architecture are important for determining the degradation, biocompatibility, and physical and chemical properties of the graft. They must also support new tissue formation by encouraging cell migration, differentiation, adhesion, and proliferation [35,87,88]. For large tissues, including muscle and bone, cell infiltration and nutrient diffusion into the thickness of a three-dimensional (3-D) scaffold are very important for tissue repair. Cells must be able to proliferate and deposit new extracellular matrix (ECM) throughout the entire scaffold in order for the graft to be successful. In addition, the scaffold should replicate the mechanical properties of the natural tissue to provide cells the proper environment for growth and repair. The obstacle that faces tissue engineering is fully replicating the properties of the natural tissue while also encouraging cells to quickly replace the biomaterials.

Electrospinning has become a popular technique investigated for tissue engineering applications [42,89,90]. Its popularity arises from its capability to produce micron and sub-micron size fibers of various polymers (both natural and synthetic) in a nonwoven mat, which is similar to the structure of ECM in many tissues [46,63,72,91-99]. This similarity can lead to improved cellular function and better regeneration of tissue [93,96,100]. For this reason, electrospinning has been utilized in tissue engineering for numerous tissues including bone, cartilage, ligament, tendon, skin, nerves, and arteries [58,59,61,92,100-102]. Electrospinning has been most successful in replacing tissues that are naturally thin; less success has been achieved

with thicker tissues, including bone and muscle. Current electrospinning techniques are limited in creating viable scaffolds for these tissue engineering applications.

One of the limiting factors of electrospinning is relatively small pore sizes. Although electrospinning creates a structure with a very high percent porosity, the small pore sizes limit cell infiltration [42]. Estimated optimal pore sizes for many tissues, including bone and cartilage, are in the range of 100-500μm [35,76]. Pore sizes for electrospun scaffolds are typically only a few times larger than the electrospun fibers. For example, Yang *et al*. measured the porosity of poly(L-lactide) (PLLA) electrospun mats by mercury porosimetry. The porosity of their electrospun material was 78% with an average pore diameter of 21.5μm and a maximum pore diameter of approximately 140μm, however most of the pores were less than 10μm [103]. Similarly, Bhattarai produced electrospun structures of poly(*p*-dioxanone-*co*-L-lactide)-block-poly(ethylene glycol) with an average pore diameter of 8μm, maximum pores at 200μm, and most of the pores smaller than 10μm [104]. Thus, few pores in these examples were large enough to allow for effective cell infiltration. A scaffold with small pores will serve as a membrane, preventing cells from crossing the scaffold but allowing diffusion of smaller molecules. For some tissue engineering applications a membrane-like scaffold may be appropriate but for many tissues, cells need to be able to migrate into the scaffold. Cell infiltration is critical to the replacement of the degrading scaffold with new tissue [35,76].

This study focuses on utilizing NaCl crystals during electrospinning to create larger pores within scaffolds to promote cell infiltration. NaCl crystals are deposited onto the electrospinning collector and embedded into the electrospun scaffold. Kim *et al*. used the technique previously to create a fluffy, 3-D electrospun structure of hyaluronic acid and collagen with macropores [71]. Nam *et al.* also used a similar approach to improve cellular infiltration within poly(ε-

caprolactone) [70]. This study furthers this research with mechanical tests, porosimetry analysis, and *in-vitro* tests intended to describe the performance of NaCl embedded PLLA (PLLA-NaCl mats) electrospun scaffolds versus electrospun PLLA scaffolds without NaCl.

2.3 Methods and Materials

2.3.1 *Electrospinning*

PLLA (inherent viscosity of 2dl/g) was purchased from Sigma-Aldrich (St. Louis, MO, USA) and dichloromethane (DCM) and dimethylformamide (DMF) were purchased from Fisher Scientific (Pittsburgh, PA, USA). PLLA was mixed with a 3:1 ratio of DCM and DMF to yield a total polymer weight percent of 7% (w/v). This solution was then electrospun onto a rotating mandrel with a diameter of 5 cm rotating at approximately 1100 RPM. The flow rate of the polymer was 5mL/hr. An electric field was applied to the PLLA solution (12kV and -9kV) forcing the polymer from the syringe onto the rotating mandrel 5cm away. During electrospinning, NaCl crystals (with a diameter of < 710 μm) were released from a rotating drum above the collection mandrel (Figure 2.1). The release rate of NaCl was approximately 79 g/hr. The electrospun PLLA-NaCl and PLLA mats were then placed in deionized (DI) water under vacuum pressure where the NaCl was leached out for two hours; the water was changed three times. The thickness of the electrospun mats were approximately 250μm. The end result of leaching was the creation of large pores or voids where the NaCl crystals had previously been.

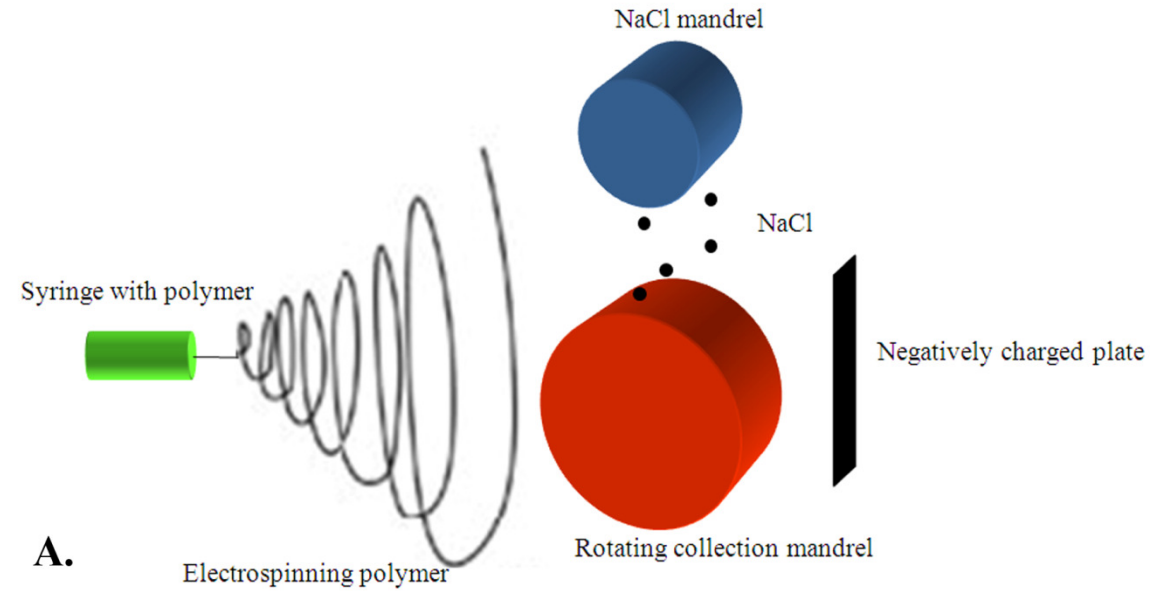

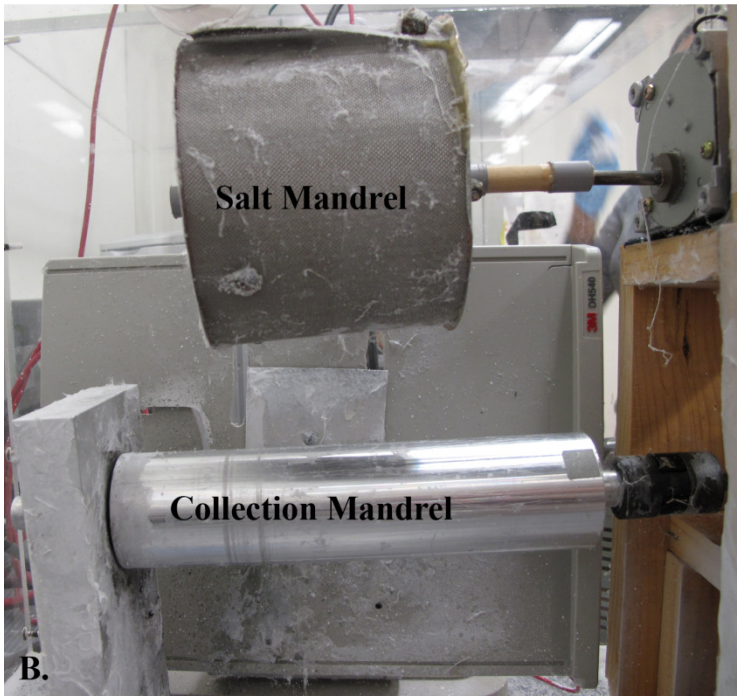

Figure 2.1. **A.** Schematic of NaCl addition during electrospinning and **B.** a picture of the salt and collection mandrels used.

2.3.2 *Porosimetry*

The porosity of electrospun PLLA and PLLA-NaCl samples was measured using a Liquid Extrusion Porosimeter (Porous Materials, Inc., Ithaca, NY, USA). Samples of

electrospun mats were cut into 3cm x 3cm x 0.025cm samples, allowed to soak in Galwick wetting fluid, and placed into the device's chamber. The porosimeter then calculated pore size distribution, pore volume, and median pore size based upon the amount of pressure required to remove the wetting fluid from the sample. The porosimeter assumes that all pores are spherical.

2.3.3 *Mechanical Testing*

PLLA (n=6) and PLLA-NaCl (n=7) electrospun samples were cut into strips (6cm x 1cm x 0.025cm) for mechanical testing. Samples were tested in phosphate buffered saline (PBS) at 37°C. The strips were tested at a rate of 3mm/min with a gage length of approximately 3cm (10% strain/min) until failure on an Instron 5869 with Biopuls Bath (Norwood, MA, USA). The yield stress, yield strain, and elastic modulus were then calculated and compared for analysis. The yield stress was defined as the stress at the end of the linear (elastic) region. The yield strain is the strain value at the yield stress. The elastic modulus was calculated by determining the slope of the stress vs. strain graph in the linear region.

2.3.4 *Cell Study and SEM Analysis*

The effect of salt pores on cellular function was determined through a cell study with MC3T3-E1 cells (ATCC, Manassas, VA, USA) which were cultured (passage 9) on PLLA and PLLA-NaCl electrospun scaffolds in 24-well tissue culture plates (Beckton, Dickinson and Company, NJ, USA). The scaffolds, diameter of 1.5 cm, were fixed to the plates by a Silastic® medical adhesive (Dow Corning, Midland, MI, USA). The affixed mats were sterilized by soaking the samples in ethanol for 30 minutes and then exposing them to UV light for 30 minutes on each side. Minimal Essential Medium (MEM) with Earl's salts and L-glutamine, 10% fetal bovine serum, and 1% penicillin/streptomycin (Mediatech, Manassas, VA, USA) was added and the mats were soaked overnight. Wells were seeded at a density of 50,000 cells/well

onto PLLA electrospun mats, PLLA-NaCl electrospun mats, and tissue culture polystyrene. Electrospun PLLA mats with MEM media but without cells were used as a negative control. Media was changed three times per week.

Cellular proliferation and cytotoxicity were determined by the CellTiter 96 AQueousOne Solution Cell Proliferation (MTS) Assay (Promega, Madison, WI, USA) (n=3) on days 3, 7 and 14. After removal of media, 100µL of the assay and 500µL of DMEM were added to each well and incubated for four hours. The light absorbance was then measured at 490 nm using a SpectraMax M2e spectrophotometer (Sunnyvale, CA, USA). After washing with PBS, scaffolds were fixed with glutaraldehyde (Sigma-Aldrich) followed by serial dilutions of methanol (Fisher Scientific). The samples were then frozen with liquid nitrogen and fractured to view cross-sections of the samples. Samples were sputter coated with gold-paladium to 20nm thick before being imaged by a FEI Quanta 600 FEG (environmental scanning electron microscope) in high vacuum mode.

Cellular infiltration was determined through fluorescent staining. Electrospun mats were embedded in Optimal Cutting Temperature (OCT) compound (Sakura, Torrance, CA, USA) after four weeks of culture with MC3T3-E1 cells. Samples were then cross-sectioned with a cryotome and placed onto slides. The cross-sections were stained with Oregon Green® 488 phalloidin (Invitrogen, Eugene, Oregon, USA) and Vectashield® with DAPI (Vector Laboratories, Burlingame, CA, USA). Images were then taken with a Leica DMI 6000B microscope (Lecia Microsystems, Wetzlar, Germany).

2.4 Results

PLLA was electrospun with and without the addition of NaCl; NaCl was then leached out with DI water to create large pores. Liquid extrusion porosimetry was used to determine the

effect NaCl has on porosity. The addition of NaCl increased the average pore diameter from 5.5µm for PLLA mats to 48.7µm in PLLA-NaCl mats. The pore size distributions are shown in the histograms in Figure 2.2. Specifically, the percentage of pores larger than 20µm is greatly increased in the electrospun mats with NaCl voids. The predominant pore sizes were 3-5µm for PLLA mats and 50-70µm for PLLA-NaCl mats. Therefore, the addition of NaCl during PLLA electrospinning drastically increased the number of large pores.

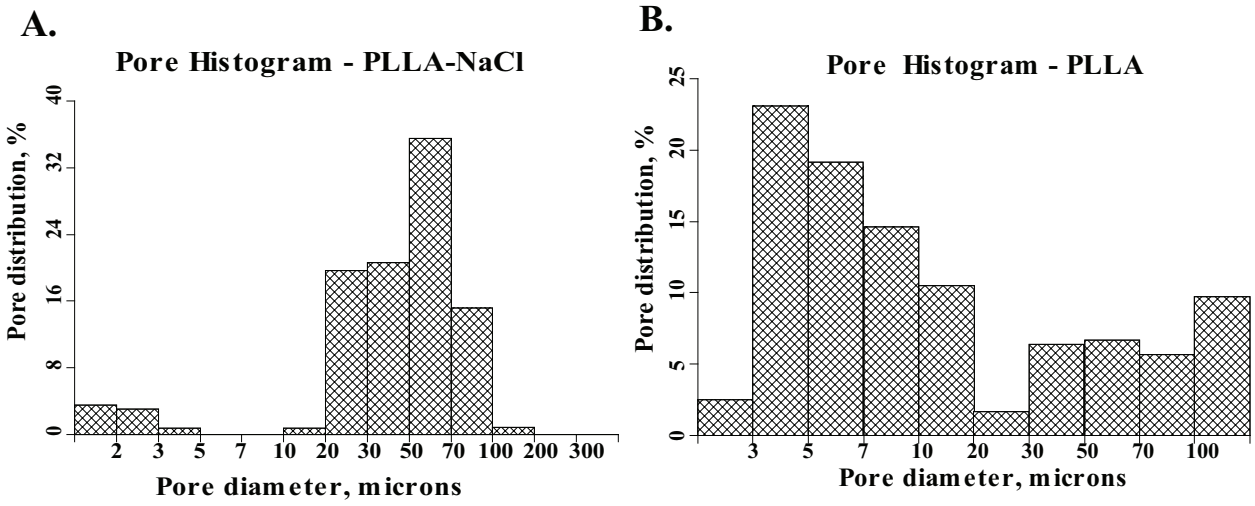

Figure 2.2. Histograms of pore sizes of polylactide electrospun mats **A.** with and **B.** without NaCl leaching

Tensile tests were performed to determine the effect of NaCl pores on the mechanical properties of PLLA-NaCl versus PLLA electrospun mats. The samples were tested at a rate of 3mm/min under physiological conditions (in PBS at 37°C). The elastic moduli of PLLA-NaCl and PLLA electrospun mats were 8.05±2.47 MPa and 40.36±17.34 MPa respectively. The yield stress for mats with NaCl voids was 349.14±111.8 kPa and 675.5±293.8 kPa for PLLA mats. The yield strains for PLLA-NaCl and PLLA electrospun mats were 0.045± 0.007 and 0.019±0.0013 respectively (Figure 2.3). Thus, both the elastic modulus and yield stress are

significantly reduced for samples with NaCl voids while the yield strain increased. Statistical significance was determined by Student's t test.

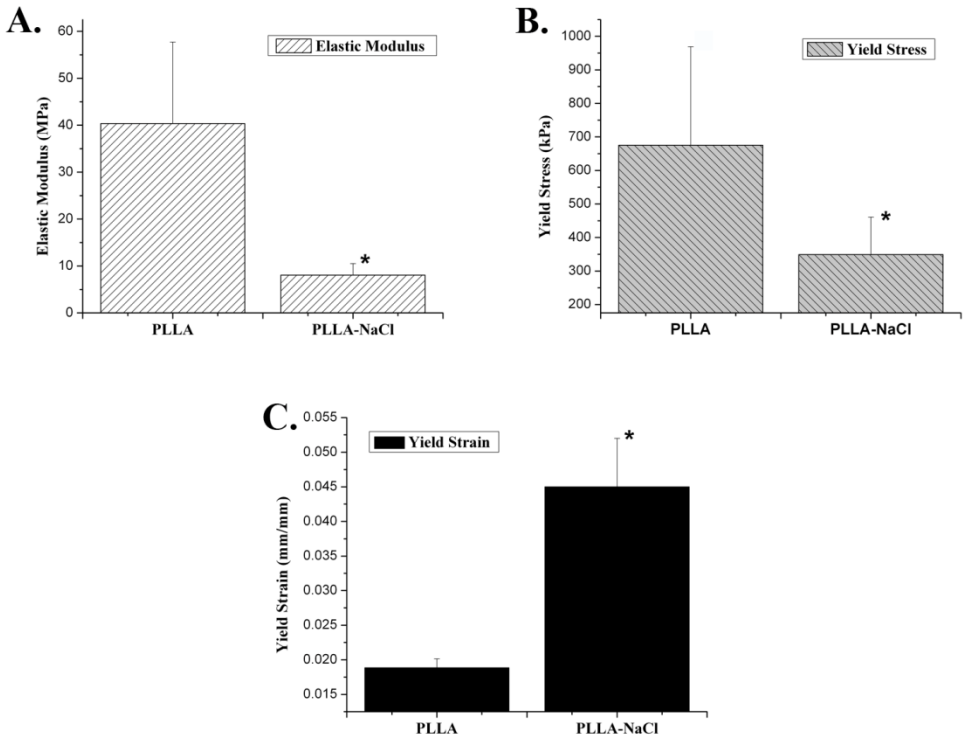

Figure 2.3. Comparison of **A.** elastic modulus, **B.** yield stress, and **C.** yield strain between electrospun mats with and without NaCl (* $p<0.05$)

Electrospun mats were cultured with MC3T3-E1 cells for two weeks. Cellular proliferation was determined by an MTS assay on 3, 7, and 14 days (Figure 2.4). For day 3, cells cultured on PLLA mats, PLLA-NaCl mats, and on tissue-treated polystyrene had average absorbance values of 1.692±0.22, 1.80±0.014, and 2.07±0.30 respectively. Day 7 values were 2.45±0.27, 2.05±0.13, and 2.43±0.54 respectively. On day 14 absorbance values were 2.40±0.31, 3.33±0.60, and 4 respectively. Day 14 absorbance of tissue-treated polystyrene has no standard deviation because all values were 4, the maximum for the spectrophotometer. The average absorbance value for the negative control (electrospun mats cultured in media without cells) was 0.39±0.06. Statistical significance was determined by ANOVA with Tukey's test.

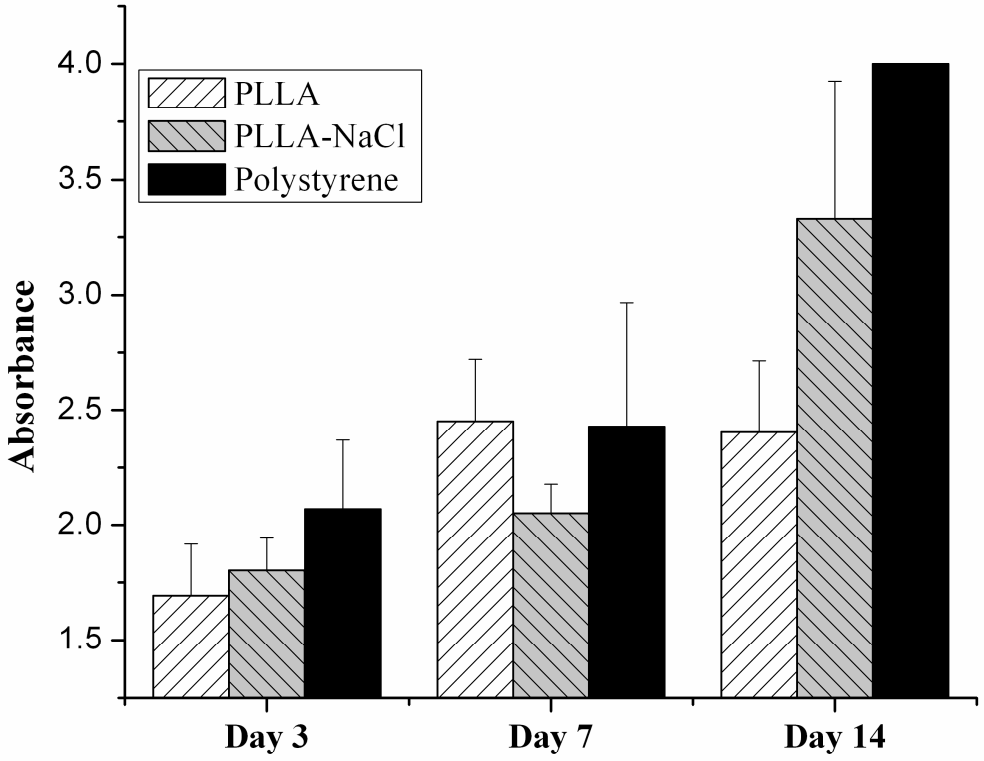

Figure 2.4. Cellular proliferation data of MC3T3 cells on electrospun mats.

After being cultured with MC3T3 cells, several samples of PLLA and PLLA-NaCl electrospun mats were fixed and imaged by SEM. Figure 2.5 displays micrographs of both types of PLLA electrospun scaffolds. Figure 2.5A is a light micrograph of a salt particle entrapped within the electrospun material. Figure 2.5B shows large pores created by NaCl leaching which are significantly larger than the pores between the electrospun fibers. Figure 2.5C and 2.5D display cells on the surface of an electrospun mat and ECM deposited on the surface of a mat. Figure 2.5E shows a cell within the cross-section of a PLLA-NaCl electrospun mat. This cell had to infiltrate through the electrospun material to reach this location which requires larger

pores than what exists for PLLA electrospun mats. Figure 2.5F is the cross-section of a PLLA electrospun mat which does not have any cells infiltrated. The rippling of 2.5F is caused by the freeze fracturing of the sample with liquid nitrogen.

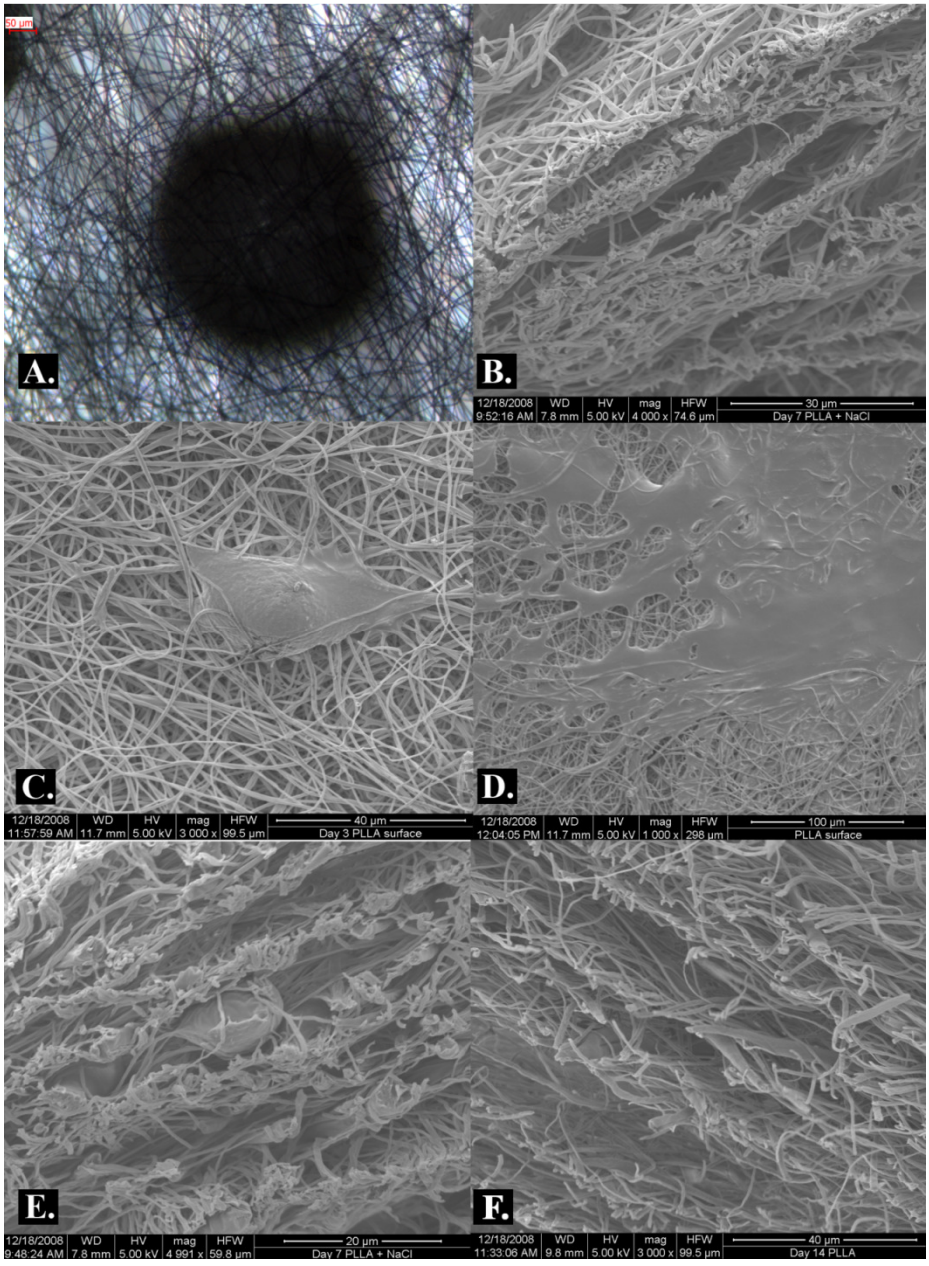

Figure 2.5. SEM and light micrographs of **A.** a salt particle within the electrospun mat, **B.** large pores created after NaCl leaching, **C.** a cell on the surface of an electrospun mat (day 3), **D.** cells and ECM on the surface of a mat, **E.** a cell within the cross-section of an electrospun PLLA-NaCl mat (day 7), and **F.** a cross-section of a PLLA mat without cell infiltration (day 14).

After four weeks of culture electrospun mats with and without salt pores were cross-sectioned and stained with DAPI and phalloidin. The DAPI stains the nuclei while the phalloidin stains the actin within the cell. The images in Figure 2.6 describe how well the cells are able to infiltrate within the electrospun material. Cells were able to infiltrate electrospun mats without salt pores up to approximately 20 microns (Figure 2.6A) whereas the cells were able to infiltrate mats with salt pores up to approximately 100 microns (Figure 2.6B).

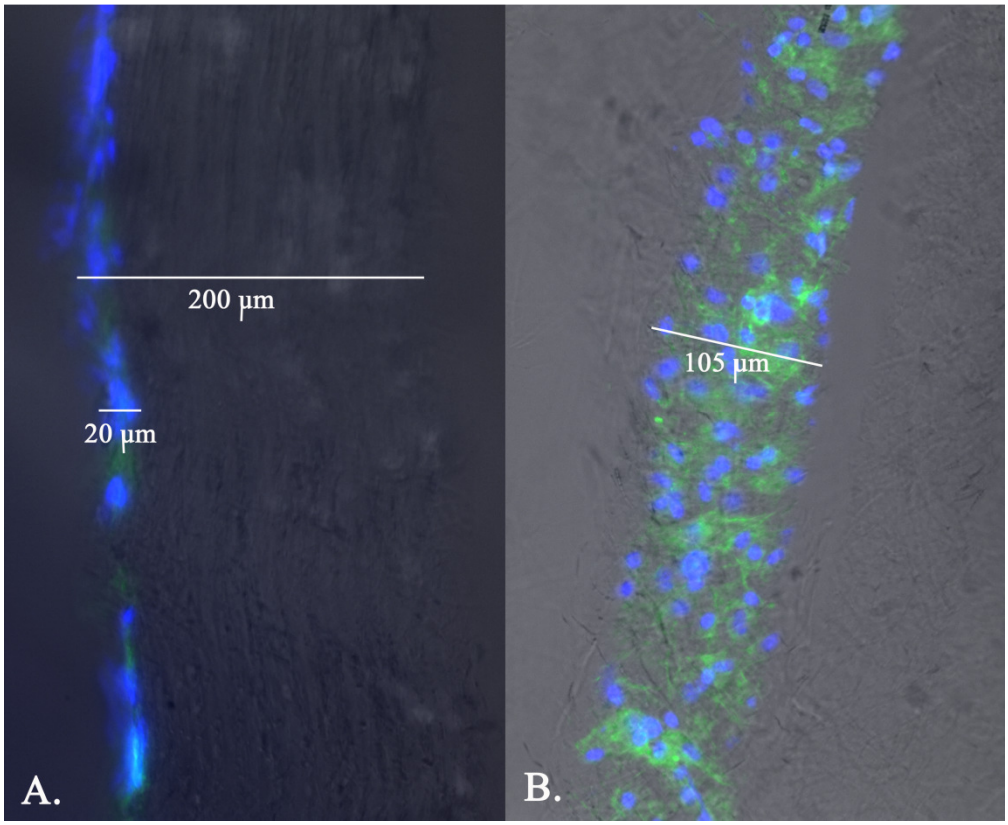

Figure 2.6. Micrographs of MC3T3-E1 cells seeded on electrospun mats **A.** without salt pores and **B.** with salt pores stained with DAPI and Oregon Green® phalloidin.

2.5 Discussion

In this study, PLLA electrospun mats were created with and without NaCl crystals. NaCl crystals were then leached out with DI water to leave behind large voids. This process created larger pores than those traditionally created when electrospinning polymers. The addition of

NaCl dramatically increased the percent of pores with a diameter above 20µm compared to electrospun mats without NaCl deposition (Figure 2.2). Although there is a possibility that moisture from the air could affect the salt crystal size during electrospinning, this was considered neglibile and was not measured in this study. Specifically, electrospun materials with and without NaCl pores had an average pore diameter of 5.5µm and 48.7µm respectively. The size of NaCl crystals was not stringently controlled for this study leading to a wide range of pore sizes. The range of NaCl crystals used could be regulated by using a sieve to separate the crystals according to size; larger crystals could also be used to further increase pore sizes. Restricting the size of the NaCl crystals would lead to greater control of the size of the pores created when the NaCl is leached out. Therefore, one could adjust the size of the pores to the needs of the specific tissue and scaffold design.

Electrospinning while concurrently releasing salt to increase porosity has a few advantages compared to other methods intended to increase pore size. This method does not affect the electrospinning process, and therefore does not affect the individual fibers produced. Adding a particle to be leached from the polymer solution could affect the individual fibers by altering the continuity of the polymer fiber and possibly reduce the mechanical strength of the electrospun material. Another technique that has been utilized to increase porosity is sacrificial fibers [105]. This method purposely removes some of the fibers within the electrospun material to increase the porosity. This technique, however, can involve the removal of a considerable portion of the fibrous material to create significant changes in porosity, which can significantly reduce the mechanical strength of the material.

The average pore diameter of our PLLA electrospun mats is smaller compared to porosimetry data obtained by other studies, including Yang *et al.*, 21.5µm [103]. However,

Yang et al. utilized a mercury porosimeter instead of a liquid extrusion porosimeter that was used in this study. The results obtained from the two different techniques are not necessarily comparable. Any actual differences in average pore diameters would most likely be due to differences in electrospinning processes. Yang *et al*. electrospun onto a flat surface versus a rotating mandrel and used a lower weight percent of PLLA [103]. A flat surface collector creates electrospun fibers with a more random orientation and larger diameters when compared to fibers electrospun onto a rotating mandrel. Randomly aligned fibers do not pack as well and can lead to larger pore sizes. Therefore, the random packing of larger fibers creates larger pores.

The addition of NaCl pores to an electrospun material creates a bimodal distribution of pores. The NaCl pores reside within the natural pores of the electrospun material, therefore, all of the NaCl pores are inherently interconnected within the electrospun mat. The natural nanoscale pores of the electrospun materials also decreased the average pore size. The large volume percent of natural nanoscale pores reduces the average size of pores that would be created by a material with exclusively salt pores, which explains the low average pore diameter of 50μm for these materials. The additional space created by the NaCl pores improves the capability of cells to infiltrate within the electrospun material. Thus cells can utilize the entire electrospun mat to proliferate and produce new extracellular matrix.

NaCl pores significantly affected other properties of the electrospun mats. PLLA-NaCl electrospun mats have a significantly reduced elastic modulus and yield stress and an increased yield strain compared to their traditional counterparts. The elastic modulus was decreased by approximately 5-fold and the yield stress by about 2-fold. The yield strain increased by about 2-fold. A concurrent decrease in elastic modulus and an increase in yield strain in electrospun mats with NaCl voids produced more elastic electrospun materials. This change in properties

may affect (positively or negatively) the electrospun scaffold's capability of being used in some tissue engineering applications. For example, decreased stiffness would be detrimental to bone tissue engineering applications, whereas this property may be beneficial for skin applications. Cortical bone has an elastic modulus of 17.0 GPa [106] which is much higher than any of the electrospun materials. Skin has elastic modulus values ranging from 4.6-20 MPa [107]; the PLLA-NaCl electrospun mats would fall within this range of elastic moduli (8.05 MPa).

The reduced stiffness and increased yield strain of the electrospun mats with NaCl pores is most likely due to fibers being less straight; the fibers are required to go around the crystals at these locations. As a result these individual fibers have to be pulled farther before they are subjected to any stresses. This aspect is very similar to an unaligned electrospun mat. Unaligned electrospun mats have been shown to possess reduced elastic moduli and increased yield strains compared to aligned electrospun mats [62]. The yield stress is decreased because strain around the created voids can lead to internal cracks or tears within the electrospun mats which will cause failure as they propagate.

Processing of the electrospun materials with NaCl pores could affect the pore size and structure. Sterilization, manipulation, and cutting of the materials could all change the pore size and structure and, therefore, impact the mechanics and cellular response to the materials. Compression of the pores is one prime example and can be seen in the SEM image in Figure 6A. Further studies will be needed to determine the impact processing may have on the mechanics and cellular response of NaCl pores in electrospun materials.

MC3T3-E1 cells proliferated well on both the electrospun scaffolds and tissue culture polystyrene. Absorbance values increased over the course of the study for PLLA mats, PLLA-NaCl mats, and the positive control; therefore, the electrospun mats are not cytotoxic. MC3T3-

E1 cells grew to confluence on the polystyrene quickly which led to the MTS assay reaching the maximum value of 4.0 when analyzed by the spectrophotometer on day 14. The PLLA-NaCl electrospun group also had one value out of three samples reach an absorbance of 4.0 on day 14. The PLLA mats and the negative control never reached this maximum. Since some of the samples had values of 4.0, significance cannot be determined because this artificially creates a smaller standard error and lowers the average. However, one can hypothesize that the cells proliferated best on the polystyrene and grew slightly better on the PLLA-NaCl mats versus PLLA mats. Additional studies will have to be conducted to confirm this hypothesis.

Although we could not test for significance between PLLA and PLLA-NaCl mats due to limitations of the spectrophotometer, we propose that PLLA-NaCl mats encourage more cell proliferation than PLLA mats without NaCl. In addition to the PLLA-NaCl group having a higher absorbance average, the group also had one sample reach the 4.0 maximum. Improved cell growth on electrospun mats with NaCl pores versus mats without NaCl pores could be ascribed to improved cellular infiltration. Improved infiltration would allow cells to better utilize the interior fibers of the electrospun mats giving them more room to proliferate. The result is a more evenly distributed and denser network of cells in a scaffold made from electrospun polymers with NaCl pores; cells were noticeable within cross-sections of the PLLA electrospun mats with NaCl pores (Figure 2.5E). No cells could be identified within the electrospun mats that did not have the larger pores (Figure 2.5F). In addition, Figure 2.6 verifies that cells are able to better infiltrate into electrospun materials with salt pores. Cells were able to infiltrate five times farther (20µm vs. 105µm) into the electrospun mat with salt pores after four weeks of culture. Therefore we believe that this new technique can lead to improved performance for tissue engineering applications by improving regeneration of the tissue by cells.

Kim *et al*. and Nam *et al.* previously used NaCl during the creation of electrospun materials. The work presented by Kim *et al*. focused on utilizing NaCl to stabilize a thick, fluffy electrospun material until cross-linking could be accomplished and to create additional pores [71]. Nam *et al*. created larger pores with the addition of NaCl which significantly increased the infiltration of cells into the thickness of their electrospun material [70]. This study expanded on the NaCl addition concept by electrospinning a different polymer, PLLA, with NaCl onto a rotating mandrel (versus flat surface). Electrospinning onto a rotating collector while depositing NaCl is significant because the process will allow us to create large pores in aligned electrospun mats. A large number of tissues require controllable nanofiber alignment to effectively replicate their ECM. In addition we have further characterized the electrospun materials noting differences in structure, mechanics, and effects on cellular proliferation.

2.6 Conclusions

This study added NaCl crystals to nanofiber meshes during electrospinning to artificially create larger voids or pores in electrospun PLLA mats. The larger pores lowered the elastic modulus and yield stress of electrospun mats while increasing the yield strain, cellular proliferation, and cell infiltration. Improved proliferation and infiltration of cells into the scaffold will increase the success of a tissue engineered graft in repairing large tissues. This suggests that the use of NaCl to create pores can help electrospinning become useful for tissue engineering applications in three dimensions.

Acknowledgements

The authors would like to thank the Walter H. Coulter Foundation for funding this study.

Chapter III: Fabrication and Mechanical Characterization of 3-D Electrospun Scaffolds for Tissue Engineering

Biomedical Materials, 2010. **5**(5): p.055006 (L.D. Wright, R.T. Young, T. Andric, and J.W. Freeman)

3.1 Abstract

Electrospinning is a polymer processing technique that produces fibrous structures comparable to the extracellular matrix of many tissues. Electrospinning, however, has been severely limited in its tissue engineering capabilities because this technique has produced few three-dimensional structures. Sintering of electrospun materials provides a method to fabricate unique architectures and allow much larger structures to be made. Electrospun mats were sintered into strips and cylinders, and their tensile and compressive mechanical properties were measured. In addition, electrospun materials with salt pores (salt embedded within the material and then leached out) were fabricated to improve porosity of the electrospun materials for tissue engineering scaffolds. Sintered electrospun poly(d,l-lactide) and poly(l-lactide) (PDLA/PLLA) materials have higher tensile mechanical properties (modulus: 72.3 MPa, yield: 960 kPa) compared to unsintered PLLA (modulus: 40.36 MPa, yield: 675.5 kPa). Electrospun PDLA/PLLA cylinders with and without salt-leached pores had compressive moduli of 6.69 MPa and 26.86 MPa, respectively, and compressive yields of 1.36 MPa and 0.56 MPa, respectively. Sintering of electrospun materials is a novel technique that improves electrospinning's application in tissue engineering by increasing the size and types of electrospun structures that can be fabricated.

3.2 Introduction

Electrospinning is a polymer processing technique capable of producing fibers with diameters on the micrometer and nanometer scales and has become a popular tissue engineering technique because the fibers formed are similar to natural ECM, in particular the fibrillar collagens [42,89,90]. Electrospun materials also are highly porous and can be utilized to orient cells, both of which are characteristics desirable for many tissue engineering applications. Electrospinning has been investigated for engineering numerous tissues, including bone, cartilage, ligament, tendon, skin, nerves, and arteries [58,59,61,92,100-102]. However, electrospinning has had limited success in repairing thicker tissues, including bone and muscle.

Electrospinning has been limited by an inability to produce large three-dimensional scaffolds, as electrospinning typically produces a flat sheet of material that is approximately 200-500 μm in thickness. Creating thicker electrospun structures requires a large amount of polymer and time and is, therefore, inefficient. As the construct increases in size, greater amounts of polymer are needed to attain a similar size increase because the density of the construct increases. In addition, as deposition of polymer increases, the polymer begins to shield the electrode from the newly deposited polymer, which can negatively impact nanofiber deposition. Also, very few unique, three-dimensional architectures have been created through electrospinning. Flat sheets, tubes, and bundled fibers are currently the only macrostructures that have been fabricated [43,66,108]. Improving electrospinning's capability to produce unique three-dimensional architectures is a vital step for the process to become a valuable tissue engineering scaffold fabrication technique because it will allow production of scaffolds for large tissues, including bone and muscle.

We have designed techniques that allow multiple electrospun mats to be combined into one large structure to remedy this problem. The processes expose the electrospun materials to solvent vapors and/or heat, which can bond the electrospun materials. This allows electrospun materials to be efficiently combined into thicker constructs and permits the creation of unique three-dimensional architectures. Electrospun tissue engineered structures have also been hampered by poor cellular infiltration, as the pores can be too small to allow adequate cell movement [70]. However, particle (salt) leaching techniques can be employed to create larger pores throughout the electrospun mats, creating a large, three-dimensional construct with increased pore sizes that will improve cell infiltration [70,109].

This study compares two different sintering techniques to examine if both are effective techniques to creating thicker electrospun scaffolds and to ascertain which process will be most effective in this task. Polylactide and polyglycolide polymers were electrospun and sintered under the two different techniques and then mechanically tested to determine the sintering processes' effectiveness. Polylactide and polyglycolide polymers were utilized because they are FDA approved [35,110], are commonly used polymers for tissue engineering and electrospinning [43,110-112], and because they can be successfully sintered with themselves or each other.

3.3 Materials and methods

3.3.1 *Electrospinning*

Poly(l-lactide) (PLLA) was purchased from Sigma-Aldrich (St. Louis, MO, USA). Poly(d,l-lactide) (PDLA) and poly(lactide-co-glycolide) (PLGA) were purchased from Lakeshore Biomaterials (Birmingham, AL, USA). Dichloromethane (DCM), dimethylformamide (DMF), and tetrahydrofuran (THF) were purchased from Fisher Scientific

(Pittsburgh, PA, USA). PLLA was mixed with a 3:1 ratio of DCM and DMF to yield a total polymer weight percent of 7% (w/v). PDLA and PLGA were each mixed in a 3:1 ratio of THF and DMF to yield a polymer weight percent of 22% (w/v) for each.

PDLA/PLLA mats were fabricated by first electrospinning PDLA onto a rotating mandrel (~1100 RPM) with a diameter of 5 cm. An electric field was applied to the PDLA solution (13kV and -10kV) forcing the polymer from the syringe onto the rotating mandrel 20 cm away. After a specified amount of PDLA (0.25, 0.5, 0.75, 1.0 mL) was electrospun onto the mandrel, 5 mL of PLLA was electrospun onto the PDLA. An applied electric field (12kV and -9kV) caused PLLA to electrospin onto the rotating mandrel (1100 RPM) 5 cm away. During PLLA electrospinning, NaCl crystals (with a diameter of < 710 μm) were released from a rotating drum above the collection mandrel onto the electrospun materials to produce some mats with salt pores, previously described by Wright *et al* [109]. PLGA mats were fabricated by electrospinning 5 mL of PLGA solution onto a rotating mandrel (~1100 RPM) with a diameter of 5 cm under the same electrospinning conditions as PDLA. The total thickness of the electrospun mats were 200-250 μm.

3.3.2 *Sintering*

The PDLA/PLLA, PDLA/PLLA-NaCl, and PLGA electrospun samples were cut into strips (6 cm x 1 cm). Vapor sintering and heat sintering were then used to fuse electrospun strips together. For vapor sintering, two PDLA/PLLA electrospun strips were overlapped (by approximately 3 cm) and held together between two aluminum meshes with magnets. Two sets of strips were then placed into the sintering chamber and exposed to THF vapor (240°C) for 10 minutes. The vapor sintering setup is shown in Figure 3.1. For heat sintering, the electrospun

strips were overlapped (by approximately 3 cm) and held together between two glass slides with magnets. Six sets of strips were sintered at one time. The samples were then placed in an oven for 30 minutes at 54°C for PDLA/PLLA samples or 46°C for PLGA samples. The temperatures and times were determined by an iterative process that established the most effective parameters. The temperatures are lower for PLGA because it is a more amorphous polymer and has a lower glass transition temperature (T_g). The PLLA fibers are unaffected during the sintering process because they have a more crystalline structure and higher T_g compared to the PDLA or PLGA. During this process, the PDLA or PLGA layer interconnects with the adjacent electrospun strip. Specifically, PDLA and PLGA fibers fuse at any fiber intersections producing a fully interlinked network of fibers from two or more different electrospun mats.

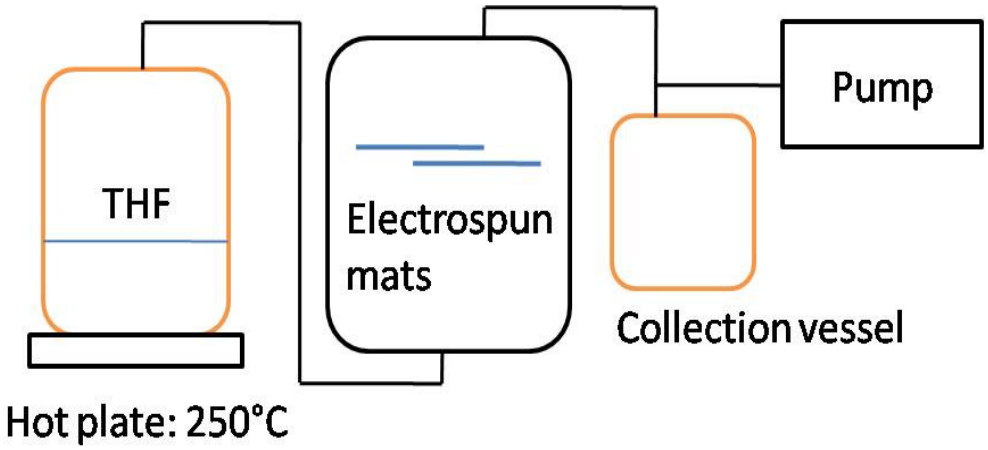

Figure 3.1. Schematic of vapor sintering process

Electrospun cylinders were built by cutting strips of PDLA/PLLA or PLGA 1 cm tall and wrapping the strip around a 20 gauge blunt tip needle until the diameter was 0.5 cm, creating a ratio of 2:1 height to diameter. If one strip was not sufficient to obtain the appropriate diameter, two strips were sintered together by heat before being wrapped around the needle. The cylinder

was then taped to prevent unwinding and heat sintered in an oven for 40 minutes at 54°C for PDLA/PLLA samples or 46°C for PLGA samples (Figure 3.2).

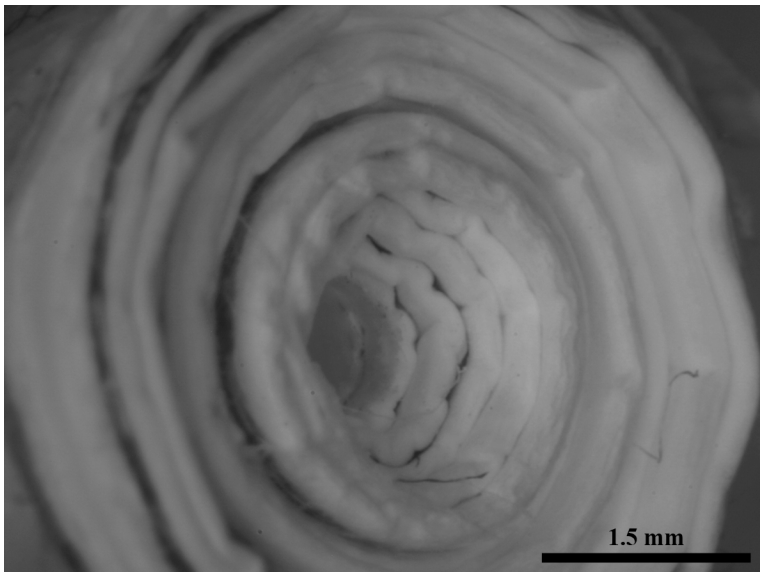

Figure 3.2. Photograph of a heat-sintered electrospun cylinder composed of PDLA and PLLA

3.3.3 *Leaching*

The electrospun mats were placed in deionized (DI) water under vacuum where NaCl was leached out for two hours; the water was changed every 30 minutes. The percent of salt within the mats by weight was calculated by comparing the mass of samples (n=7) before and after leaching. One tensile group was leached before sintering (0.75 PDLA L S) to test if the salt particles prevented an even fusion of the two electrospun strips. All compressive samples were leached before sintering. The nomenclature for the different groups with respect to tension and compression samples is listed in Table 3.1. The naming convention excludes PLLA because all samples include 5 mL of PLLA. The nonsintered controls for the tensile tests are PLLA vapor control (PLLA-VC), PLLA heat control (PLLA-HC), and PLLA heat control with salt leaching

(PLLA-SC). PLA refers to 1 mL of PDLA and 5 mL of PDLA electrospun mat for compression samples.

Table 3.1. Nomenclature of vapor and heat-sintered materials for tension and compression.

Tension	**Sintered with No Salt (NS)**	**Sintered with Salt (S)**
0.25 mL PDLA, 5 mL PLLA	0.25 PDLA NS	0.25 PDLA S
0.5 mL PDLA, 5 mL PLLA	0.5 PDLA NS	0.5 PDLA S
0.75 mL PDLA, 5 mL PLLA	0.75 PDLA NS	0.75 PDLA S
1.0 mL PDLA, 5 mL PLLA	1.0 PDLA NS	1.0 PDLA S
Leach first, 0.75 mL PDLA, 5 mL PLLA	-----	0.75 PDLA L S
5 mL PLGA	PLGA NS	----
5 mL PLGA nonsintered (control)	PLGA-C	----
5 mL PLLA nonsintered (vapor control, heat control, salt control)	PLLA-VC, PLLA-HC	PLLA-SC
Compression		
1 mL PDLA, 5 mL PLLA, Dry Test	PLA Dry	----
1 mL PDLA, 5 mL PLLA, Physiologic Test	PLA Wet	PLA S Wet
5 mL PLGA, Dry Test	PLGA Dry	----
5 mL PLGA, Physiologic Test	PLGA Wet	----

3.3.4 *Mechanical testing*

Tension samples were tested in phosphate buffered saline (PBS) at 37°C. The strips were tested at a rate of 3 mm/min with a gauge length of approximately 3 cm (10% strain/min) until failure on an Instron 5869 with Biopuls Bath (Norwood, MA, USA). The tensile yield stress, elastic modulus, shear modulus, and shear yield stress were then calculated and compared for analysis. Length, width, and thickness were measured independently for each sample with calipers to calculate the mechanical properties. Shear stress in the sintered samples was calculated by dividing the applied force by the overlapping area between the two strips. The

yield stress (tensile and shear) was defined as the stress at the end of the linear (elastic) region. The modulus (elastic and shear) was calculated by determining the slope of the stress vs. strain graph in the linear region. Statistical significance among sintered samples and nonsintered samples (controls) was tested by a Student's T test with α=0.05.

Compression samples were tested in PBS at 37°C and under dry conditions at 22°C. The cylinders were compressed at a rate of 1 mm/min (10% strain/min) until failure on the Instron 5869 with Biopuls Bath. The compressive yield stress and compressive modulus were then calculated and compared for analysis. The height and diameter were measured independently for each sample with calipers to calculate the mechanical properties. Statistical significance was tested by a Student's T test with α=0.05.

3.3.5 *Scanning Electron Microscopy (SEM)*

Sintered electrospun materials were imaged by SEM to view their cross-sections and surface. Images were taken to ensure the sintering process did not affect the fiber architecture of the electrospun materials and to verify fusion between the PDLA and PLGA fibers. Average fiber diameters were obtained by determining the fiber diameter of at least 15 fibers over at least three fields of view for both PDLA and PLLA layers. Cross-section samples were frozen with liquid nitrogen and fractured. The samples were sputter coated with gold-palladium to 20 nm thick before being imaged using a FEI Quanta 600 FEG (environmental scanning electron microscope) in high vacuum mode.

3.4 Results

Electrospun materials were sintered together by employing both heat and vapor techniques to fabricate thicker three-dimensional electrospun structures. Some of the electrospun

materials had increased porosity from leaching embedded salt from the mats. The mats had an average of 40.1±3.1% by weight of salt embedded. The salt leaching was previously shown to increase the average pore size from 5.5 μm to 48.7 μm [109]. The mechanical properties of these materials were then compared to test the effect of the sintering processes. Specifically tensile tests were performed on electrospun strips to measure the tensile elastic modulus, tensile yield stress, shear modulus, and shear yield stress (shear properties were only measured for the sintered samples). Compressive tests were performed on electrospun cylinders to measure the compressive modulus and the compressive yield stress.

3.4.1 *Tension tests*

Four different groups were vapor sintered and mechanically tested: 0.25 PDLA, 0.5 PDLA, 0.75 PDLA, and 1 PDLA without NaCl. Each of these groups included 5 mL of PLLA with varying amounts of PDLA (0.25 mL, 0.5 mL, 0.75 mL, 1 mL respectively). The control (PLLA-VC) had both the highest elastic modulus and yield stress; the modulus was significantly larger than all of the sintered groups. In the case of the yield stress, PLLA-VC was only statistically higher than the 1.0 PDLA and the 0.5 PDLA groups. Only the 0.75 PDLA shear yield stress showed any significant differences of shear mechanical properties compared to the other groups; it was significantly larger than all other groups. The vapor sintering process slightly reduced the tensile yield stress and tensile modulus with respect to the control. In addition, there seems to be no noticeable trend between the amount of PDLA used and the tensile mechanical properties (Figure 3.3).

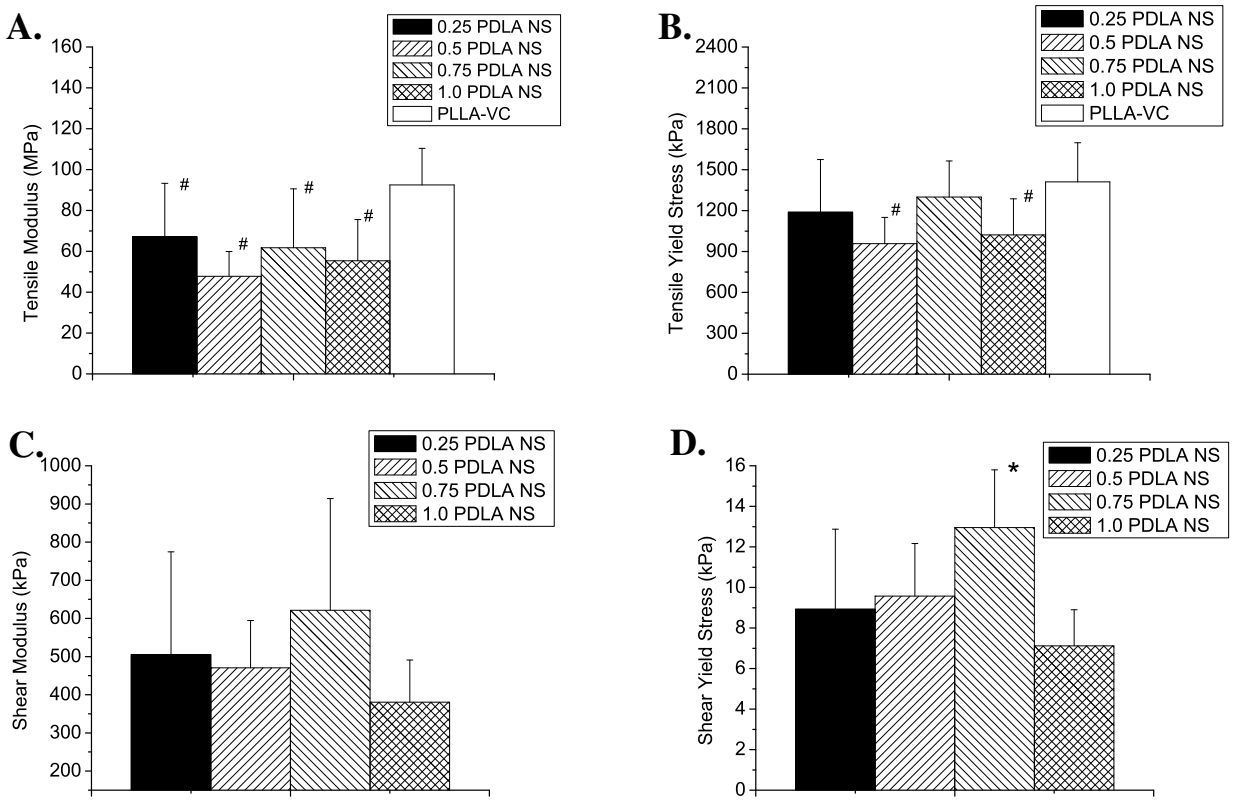

Figure 3.3. **A.** Tensile modulus, **B.** tensile yield stress, **C.** shear modulus, and **D.** shear yield stress of vapor-sintered electrospun materials. # $p<0.05$ from PLLA-VC and * $p<0.05$ from all other groups.

Eight different PDLA/PLLA groups were heat sintered and mechanically tested in tension: 0.25 PDLA NS, 0.25 PDLA S, 0.5 PDLA NS, 0.75 PDLA NS, 0.75 PDLA S, 1.0 PDLA NS, 1.0 PDLA S, and 0.75 PDLA L S (leach before sinter). All of these groups included 5 mL of PLLA with the varying amounts of PDLA (0.25-1.0 mL PDLA). The S groups were sintered before the NaCl was leached, while the NS groups had no salt within the mat. The 0.75 PDLA L S group had the salt leached before being sintered. All controls were nonsintered single electrospun mats. According to the no salt samples, the sintering process significantly increased the mechanical properties of the electrospun material compared to the control. The addition of salt, however, lowered the tensile modulus, tensile yield stress, shear modulus, and shear yield

stress of most of the electrospun heat-sintered materials. The sintered salt samples had statistically lower yield stresses compared to the salt control. However, the group that was leached before sintering (0.75 PDLA L S) had improved mechanical properties compared to the other heat-sintered salt samples and had a similar yield stress to the salt control and a modulus similar to the no salt control (Figure 3.4).

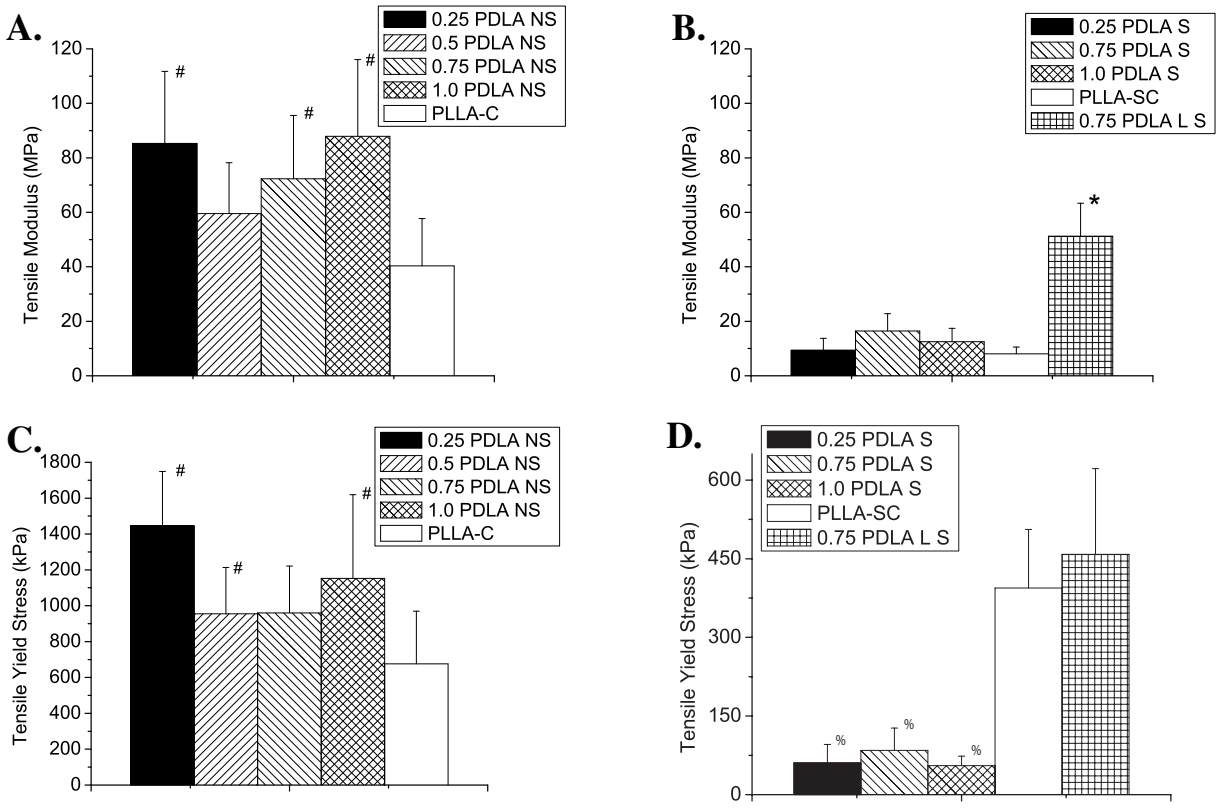

Figure 3.4. Tensile moduli of **A.** no salt and **B.** salt and yield stress of **C**. no salt and **D.** salt electrospun PDLA/PLLA materials and their controls. # $p<0.05$ from PLLA-C, * $p<0.05$ from all other salt groups, and % $p<0.05$ from PLLA-SC and 0.75 PDLA L S.

In addition, the shear mechanical properties were decreased by the addition of salt pores (Figure 3.5). Specifically, the salt samples' shear yield stress were all significantly lower than

the no salt samples. The shear moduli of the salt samples were all statistically lower than every other no salt group excluding the 0.5 NS group.

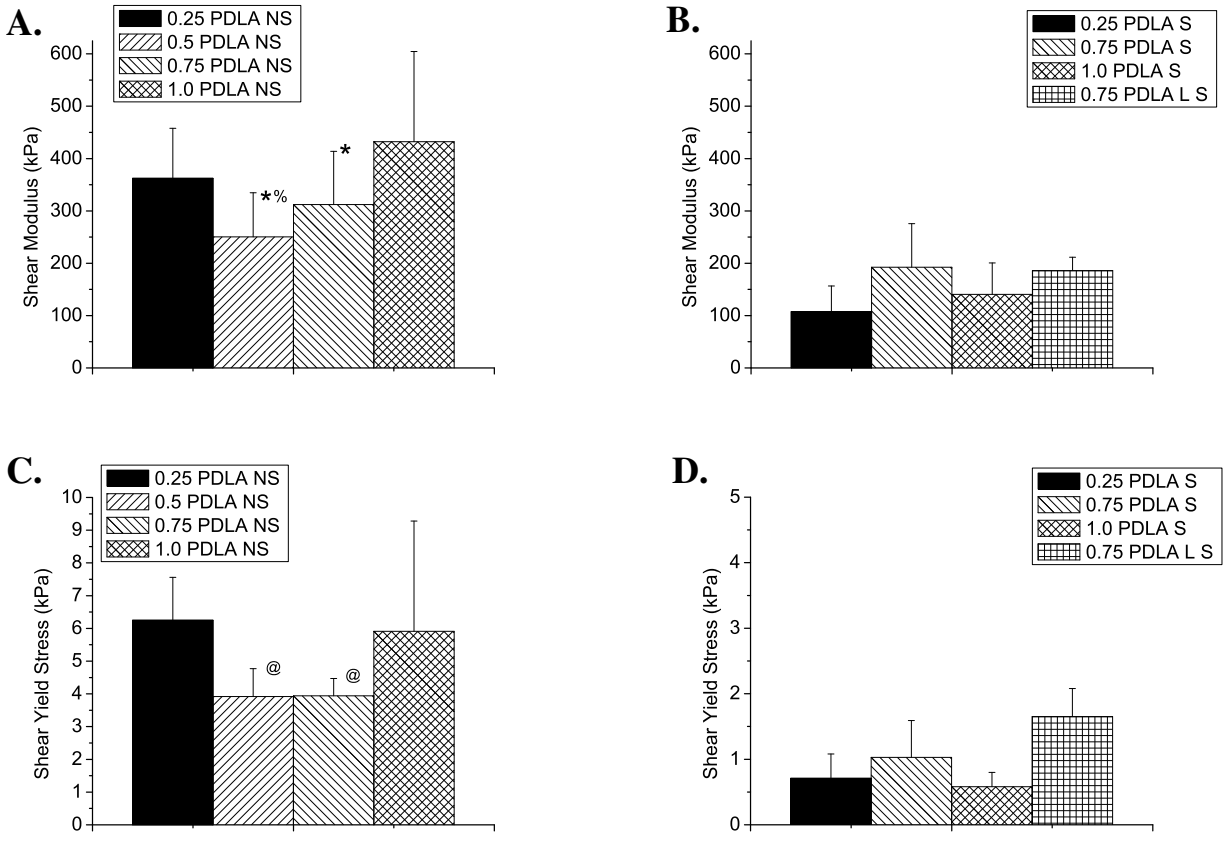

Figure 3.5. Shear elastic moduli of **A.** no salt and **B.** salt and yield stresses of **C.** no salt and **D.** salt heat-sintered electrospun PDLA/PLLA scaffolds. * $p<0.05$ from 1.0 PDLA NS, % $p<0.05$ from 0.25 PDLA NS, and @ $p<0.05$ from 0.25 PDLA NS and 1.0 PDLA NS.

3.4.2 *Compressive tests*

Five different groups were heat sintered and mechanically tested in compression: PLA (PDLA/PLLA) Dry, PLA Wet, PLA S Wet, PLGA Dry, and PLGA Wet. Wet samples were tested at 37°C in PBS, while dry samples were tested at 22°C. Compressive tests of electrospun cylinders showed that wetting the samples in PBS at 37°C and the addition of salt lowered the compressive modulus and compressive yield stress of the structures. Specifically, the PLA Wet

is significantly lower than the PLA Dry, but PLA Wet is significantly larger than the PLA S Wet. The yield stress of PLGA Dry was significantly larger than PLGA Wet; however, there was not a significant difference in their moduli. In addition, the PLGA cylinders were significantly weaker compared to their PLA counterparts (Figure 3.6).

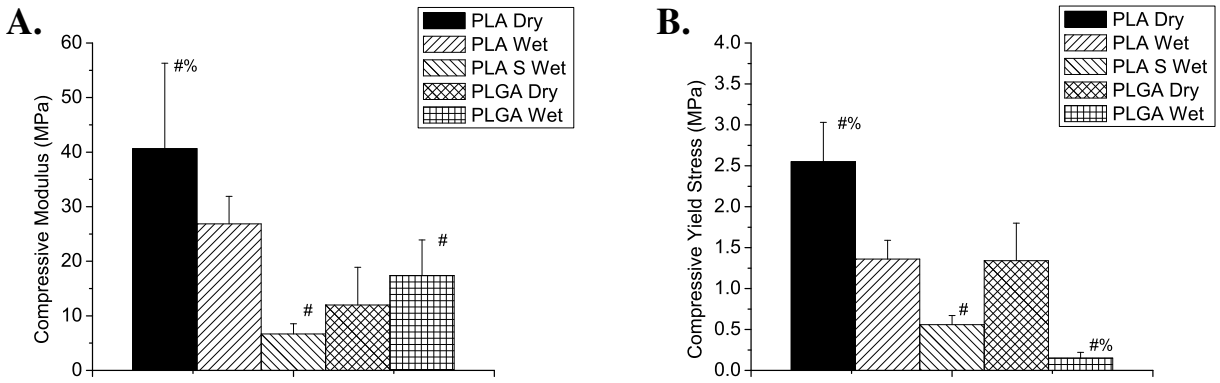

Figure 3.6. Compressive **A.** modulus and **B.** yield stress of heat sintered PDLA/PLLA and PLGA electrospun cylinders. # $p<0.05$ from PLA Wet and % $p<0.05$ from PLGA Dry.

3.4.3 *Scanning Electron Microscopy (SEM)*

Electrospun sintered materials were cross-sectioned and imaged by SEM to view the relationship of the electrospun layers (Figure 3.7). The individual layers were not easily distinguishable from one another. The sintering process created unions between adjacent fibers of PDLA; thus, adjacent mats were fused together by the PDLA fiber layers (Figure 3.7). The sintering process is successful if fusion between adjacent mats occurs (verified by mechanical tests) but fiber structure is maintained. Exposure to solvent vapor for too long begins to destroy the PDLA fiber architecture. Exposure to the solvent vapors for 12 minutes instead of 10 minutes can lead to loss of fiber structure of PDLA while the PLLA fibers are unaffected (Figure 3.8). The loss of fibrous structure is unacceptable because it reduces the porosity of the material

and can prevent diffusion through the material and cell infiltration into the material. The exposure time of the vapor sintering must be stringently controlled to prevent this occurrence.

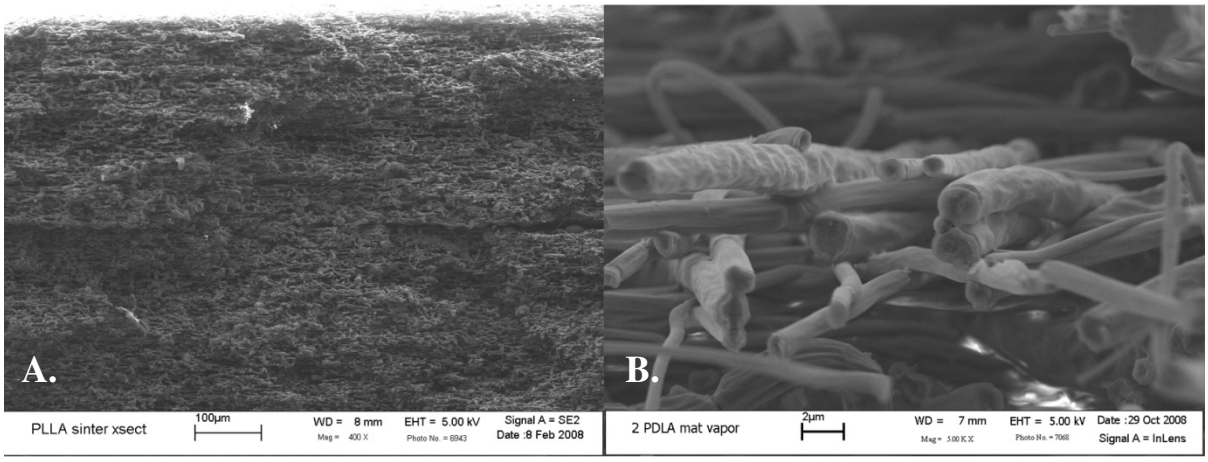

Figure 3.7. Electron micrographs of the cross-section of **A.** several PDLA/PLLA electrospun mats sintered together and of **B.** adjacent PDLA fibers coupled.

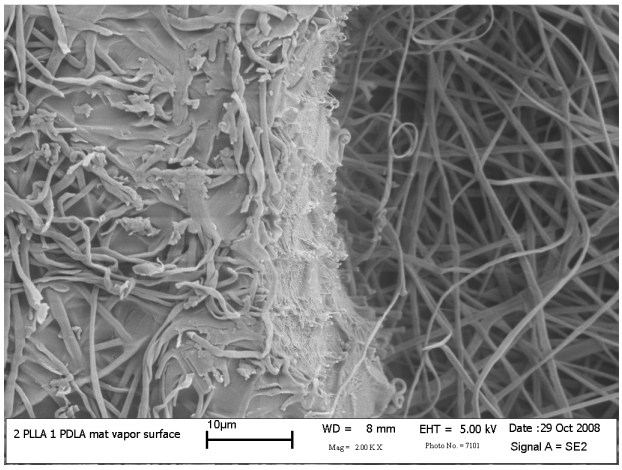

Figure 3.8. Electron micrograph of a PDLA/PLLA electrospun mat exposed to solvent vapor too long. The long exposure of PDLA on the left side has caused it to lose its fiber structure, while the PLLA on the right is unaffected.

SEM was also used to measure average fiber diameters of the PDLA and PLLA electrospun layers. PLLA and PDLA had an average fiber diameter of 766.0±260.4 µm and 1081.8±757.0 µm, respectively. PLLA fiber diameters ranged from 437.5 µm to 1619 µm,

whereas PDLA ranged from 380.2 µm to 2405 µm. Thus, PDLA had both larger average fiber diameters and a much larger range of fiber diameters compared to PLLA.

3.5 Discussion

Both PDLA/PLLA and PLGA electrospun materials were heated and vapor sintered to determine any advantages or disadvantages one may have compared to the other. PDLA/PLLA required two materials to be electrospun together (PDLA and PLLA) and required a higher temperature for sintering. Although more difficult to fabricate, the PDLA/PLLA material approach does have benefits. PDLA sinters at a lower temperature compared to PLLA. As a result, PDLA sintered at 54°C, while the PLLA was unaffected by the required temperature. Thus, the majority of the electrospun materials was unaffected by the process. In addition, the compressive modulus and yield stress of PLGA were lower than PLA due to its lower crystallinity. These lowered mechanical properties would further be exacerbated if salt leaching were included in the process. Therefore, for some tissue engineering applications that involve bearing loads in tension or compression, the PDLA/PLLA electrospun materials could be superior. PLGA electrospun materials also have a tendency to shrink, particularly in the direction of fiber orientation, under the sintering temperatures. The shrinking leads to nonhomogenous heights of the electrospun materials, which are detrimental to creating larger three-dimensional structures.

The sintering process creates junctions between PDLA (or PLGA) fibers and any fibers adjacent (Figure 3.7). The linking of all the fibers along the surface provides a relatively strong bond between electrospun mats. The bonding allows creation of much larger and unique electrospun structures than traditional electrospinning. Multiple electrospun mats can be layered

on top of one another to produce a thicker material. In addition, unique three-dimensional structures, including cylinders, can be fabricated (Figure 3.2). Three dimensional structures could be used to replicate tissues with multiple layers and varying fiber orientations like articulating cartilage or intervertebral disks.

Electrospun materials were sintered together into strips and cylinders for tension and compression mechanical testing. Two different techniques were utilized, vapor sintering and heat sintering, to produce larger, thicker electrospun materials. The vapor sintering technique used THF vapor to connect the fibers of adjacent electrospun mats. Tension tests were performed on electrospun strips to test the effect of sintering on mechanical properties. Only minor differences were noticed between the vapor-sintered samples and their controls. A small but statistically significant reduction in the tensile modulus was noticed between the control and the vapor-sintered samples. A reduced stiffness may be beneficial for tissues like muscle or skin, whereas it would be detrimental for hard, compressive load bearing tissues like bone.

Heat sintering samples were also tested in tension to help elucidate the best procedure for sintering electrospun materials. The heat sintering process significantly increased the mechanical properties of the electrospun materials, particularly in the samples without salt leaching. The increased prevalence of connections between fibers within the electrospun material may strengthen the material and resist crack propagation. For example, the highest mechanical properties belonged to the 1.0 PDLA NS group with a tensile modulus of 87.89 MPa and a tensile yield stress of 1153 kPa, whereas the control group (PLLA-C) was 40.36 MPa and 676 kPa; the mechanical properties (tensile modulus and tensile yield stress) of the control mats are only half of the 1.0 PDLA NS group. All of the sintered groups without salt had larger elastic moduli and tensile yield stresses compared to the control.

The 0.25 PDLA NS and the 1.0 PDLA NS groups had the largest shear mechanical properties in addition to the largest tensile properties. Specifically, the 0.75 PDLA NS and 0.5 PDLA NS had significantly lower shear moduli and shear yield stresses compared to the 1.0 PDLA NS and 0.25 PDLA NS groups. The actual amount of PDLA used does not seem to play a dramatic role in the sintering process. Instead, the most important factor for providing strong shear properties is a robust bonding between the electrospun layers. As a result, a thicker PDLA layer provides a solid platform to create a strong bonding layer, which is why the 1.0 PDLA NS typically had the highest mechanical properties. It is important to note that the samples could possibly fail in tension or shear, which is why both tensile and shear properties were analyzed.

The leaching of salt significantly decreased the mechanical properties of all electrospun samples. The elastic moduli and yield stresses of salt control samples were one-fifth and one-half of PLLA controls, respectively. There was also a statistical decrease in the tensile yield stress between the PLLA salt control (PLLA-SC) group and the salt-sintered groups that were sintered before leaching. However, leaching the salt before sintering (0.75 PDLA L S) removed this effect. Removing the salt prior to sintering allows for an increased surface area for sintering. Bumps in the mat are present when the salt is still embedded, reducing the surface area in contact with the adjacent mat. In addition, the 0.75 PDLA L S group had a significantly higher modulus compared to the salt control and the salt-sintered groups. There were no significant differences in the shear moduli or shear yield stresses among any of the salt-sintered groups. Therefore, the sintering process tends to increase the mechanical properties while the salt leaching process decreases the mechanical properties of electrospun scaffolds.

Compressive mechanical tests were performed on electrospun scaffolds that were heat sintered. Both PDLA/PLLA and PLGA samples had significantly higher elastic moduli and

yield stresses for samples under dry conditions at 22°C compared to physiological conditions (37°C in PBS). In addition, the PDLA/PLLA samples that incorporated salt leaching had significantly lower modulus and yield stress compared to unmodified PDLA/PLLA. Lastly, the PLGA cylinders were significantly weaker compared to their PDLA/PLLA counterparts in both moduli and yield stresses. The compressive mechanical properties of the cylinders are comparable to some load bearing tissues, specifically articulating cartilage. Kurkijarvi *et al.* measured elastic and dynamic moduli of full-thickness, cartilage-bone cylinders of human (nonarthritic) knees to range from 0.15-2.14 MPa and 0.8-15.58 MPa, respectively (the elastic modulus of PLA S Wet was 6.69 MPa) [113]. Therefore, electrospun sintered materials do have applications for tissue engineering of large load bearing tissues. Dynamic and viscoelastic mechanical tests will need to be performed to further elucidate similarities and differences between the electrospun samples and specific tissues.

The heat sintering process has several key advantages compared to vapor sintering. Vapor sintering requires an organic solvent in addition to very high heat (240°C), whereas the heat sintering method requires only moderate heat (54°C for PDLA/PLLA). Thus, the vapor sintering method is more complex and less efficient. In addition, the vapor sintering process requires much more stringent time constraints. If the sample is left just a few seconds too long, it results in degradation of the fibrous structure of the PDLA material (Figure 3.8). This result can significantly reduce the porosity of the material and severely limit infiltration of cells through the tissue engineered scaffold. In contrast, the heat sintering time constraints are much more flexible (several minutes), which can help prevent fiber structure degradation. The mechanical properties of vapor-sintered samples may be less consistent (larger standard errors) because of this property. Replicating the same effective sintering parameters can be difficult for vapor sintering,

which can affect the resulting sample mechanics. A final advantage of heat sintering is that a large number of samples can be sintered at one time in an oven. In contrast, the vapor sintering procedure requires that the materials be subjected to the solvent vapor in a confined space, limiting the number of samples that can be sintered at one time. Although neither process negatively affects the mechanical properties drastically, heat sintering is a more efficient technique to combine poly(lactide) or poly(lactide-co-glycolide) electrospun materials.

3.6 Conclusion

This study fabricated three-dimensional structures of electrospun mats through two distinct sintering processes. The mechanical properties were not drastically affected by either of the techniques used and the fiber architecture remained intact. However, heat sintering is advantageous because it is more easily controlled and does not require a solvent or high temperature. The sintering process allows electrospinning to be a valid tissue engineering processing technique for scaffolds of large tissues, including cartilage and bone. The sintering process in conjunction with electrospinning with salt could provide an excellent 3-D, porous, and fibrous scaffold for tissue engineering.

Acknowledgement

The authors would like to thank the Wallace H. Coulter Foundation for funding this study.

Chapter IV: Electrospun PDLA/PLLA and Hydrogel Scaffold for Tissue Engineered Cartilage

4.1 Introduction

Articulating cartilage is important for successful load transmission and mobility within a diarthroidal joint. Damage to articulating cartilage, in the form of localized defects or primary osteoarthritis, can lead to significant pain and loss of mobility [114]. Cartilage tissue engineering attempts to repair or replace cartilage by utilizing biomaterials, cells, and/or bioactive molecules [35,42,45]. The goal of cartilage tissue engineering is to replace the function of the damaged tissue until cells can regenerate it. Thus, the scaffold must support and allow for tissue regeneration by the cells, while also providing the mechanical properties necessary for the scaffold to be functional.

Collagen type II and proteoglycans, two vital types of extracellular matrix (ECM) molecules, give articulating cartilage its function. Collagen type II is a fibrillar protein that provides cartilage with its resiliency and is the primary structural protein of the cartilage ECM [9,10,35]. Proteoglycans are important for attracting water into cartilage, as the resident water can then be extruded through the tissue to dissipate energy when the cartilage is compressed [9-11,35]. Therefore, both collagen type II and proteoglycans are vital to cartilage's mechanical properties. Choosing appropriate biomaterials and processing techniques that can adequately replicate the functions of both collagen and proteoglycans is an important step in the tissue engineering of cartilage.

We hypothesize that a composite scaffold of electrospun fibers and an embedded hydrogel could replicate functions of both the collagens and proteoglycans. Electrospinning produces materials that are very similar in shape to collagen fibers, polymer fibers with diameters in the nanometer or micrometer range [43,45]. Therefore, a scaffold composed of electrospun fibers could replace collagen's function in cartilage if the fibers are aligned similarly to cartilage. An embedded hydrogel could imbibe a significant amount of water into the scaffold, replicating the function of the proteoglycans.

Specifically this study utilizes a thermal and pH sensitive chitosan hydrogel to perform the role of the proteoglycans. Derived from chitin, the main component of crustacean

exoskeletons and the second most abundant natural polymer [115], chitosan is composed of D-glucosamine and N-acetyl-D-glucosamine and is both biodegradable and biocompatible [116]. Chitosan can be cross-linked with several different agents including dialdehydes, citrates, polyphosphates, and anionic polymers [117-120]. Nair *et al*. previously described using inorganic phosphate salts to create a chitosan solution that would gelate under physiological conditions. The hydrogel displayed no cytotoxic effects and showed promise as a cell carrier [121]. As a result, we have created a scaffold for cartilage tissue engineering composed of an electrospun cylinder of polylactide and a thermally crosslinking chitosan hydrogel.

4.2 Materials and Methods

4.2.1 *Electrospinning*

Poly(l-lactide) (PLLA) was purchased from Sigma-Aldrich (St. Louis, MO, USA). Poly(d,l-lactide) (PDLA) and poly(lactide-co-glycolide) (PLGA) were purchased from Lakeshore Biomaterials (Birmingham, AL, USA). Dichloromethane (DCM), dimethylformamide (DMF), and tetrahydrofuran (THF) were purchased from Fisher Scientific (Pittsburgh, PA, USA). PLLA was mixed with a 3:1 ratio of DCM and DMF to yield a total polymer weight percent of 7% (w/v). PDLA was mixed with a 3:1 ratio of THF and DMF to yield a total polymer weight percent of 22% (w/v).

To create the PDLA/PLLA (PLA) mats, the PDLA solution was first electrospun onto a rotating mandrel (~1100 RPM) with a diameter of 5 cm. An electric field was applied to the PDLA solution (13kV and -10kV) forcing the polymer from the syringe onto the rotating mandrel 20cm away. After 1mL of PDLA was electrospun onto the mandrel, PLLA was electrospun onto the PDLA. An applied electric field (12kV and -9kV) caused PLLA to electrospin onto a rotating mandrel (1100 RPM) 5cm away. During PLLA electrospinning, NaCl crystals (with a diameter of < 710 μm) were released from a rotating drum above the collection mandrel onto the electrospun materials, as previously described by Wright *et al.* [109].

4.2.2 *Salt leaching and sintering*

Electrospun mats were then soaked in deionized water to leach NaCl from mats with salt crystals embedded. The mats were placed in deionized water under a vacuum for 2 hours, during

which the water was replaced three times. After leaching, electrospun mats were sintered into cylinders as described by Wright *et al.* [122]. Electrospun mats were cut into strips 1cm tall and wrapped around a 20 gauge blunt tip needle until the diameter was 0.5cm, creating a 2:1 height to diameter ratio. If one strip was not sufficient to obtain the appropriate diameter, two strips were sintered together by heat before being wrapped around the needle. The cylinder was then taped to prevent unwinding and sintered for 40 minutes at 54°C. The sintering process fuses the different layers of the cylinder into one structure by creating cross-links between the PDLA fibers and the adjacent layer.

4.2.3 *Hydrogel addition*

A chitosan hydrogel, previously described by Nair *et al*., was created and combined with the electrospun scaffold [121]. Specifically, 10mL of chitosan hydrogel was placed into a beaker and cooled in ice along with an ammonium hydrogen phosphate (AHP) solution for 15 minutes. The chitosan hydrogel was then stirred while on ice as 180µL of AHP was added drop-wise. The solution was then mixed for 1 minute before the electrospun scaffold was added to the solution. The scaffold/hydrogel was then placed under vacuum for 5 minutes to improve infiltration of the hydrogel into the electrospun scaffold. The scaffold and hydrogel were next placed into a 37°C water bath overnight to crosslink the hydrogel. The final group names for all scaffolds are listed in Table 1.

Table 4.1. Nomenclature for scaffold cylinders tested in compression.

	No hydrogel	**Hydrogel**
1mL PDLA, 5mL PLLA, Dry Test	PLA dry	PLA-H dry
1mL PDLA, 5mL PLLA, Physiologic Test	PLA wet	PLA-H wet
1ml PDLA, 5mL PLLA, NaCl leach, Physiologic Test	PLA-S wet	PLA-S-H wet

4.2.4 *Mechanical testing*

Compression samples were tested in PBS at 37°C and under dry conditions at 22°C. The cylinders were compressed at a rate of 1mm/min (10% strain/min) until failure on an Instron 5869 with a BioPuls bath. The compressive yield stress and compressive modulus were then

calculated and compared for analysis. The compressive yield stress was defined as the stress at the end of the linear (elastic) region. The compressive modulus was calculated by determining the slope of the stress vs. strain graph in the linear region. Statistical significance was determined by a Student's T test with $\alpha=0.05$.

4.3 Results

Six different groups were mechanically tested in compression: PLA dry, PLA wet, PLA-H dry, PLA-H wet, PLA-S wet, and PLA-S-H wet. Wet samples were tested at 37°C in PBS while dry samples were tested at 22°C. The compressive moduli for the scaffolds were: 40.64±15.66 MPa for PLA dry, 26.86±5.05 MPa for PLA wet, 28.56±4.67 MPa for PLA-H dry, 25.07±6.47 MPa for PLA-H wet, 6.69±1.85 MPa for PLA-S wet, and 11.77±2.44 MPa for PLA-S-H wet (Figure 4.1). Compressive tests showed that the addition of the hydrogel to the electrospun scaffold did not significantly affect the compressive modulus of PLA scaffolds, but did increase the modulus for PLA-S scaffolds significantly. In addition, the moduli of the PLA wet scaffolds were significantly lower than the PLA dry and the PLA-S wet had significantly lower moduli compared to the PLA wet.

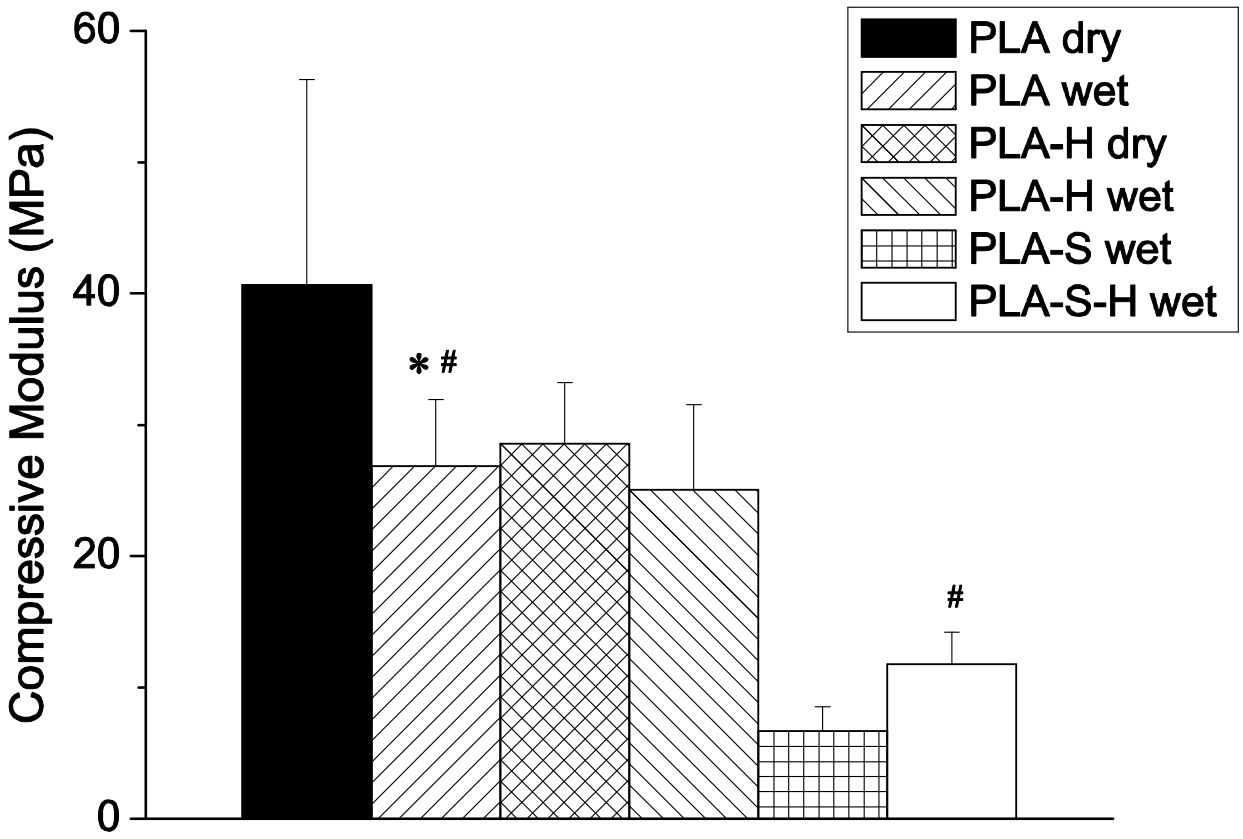

Figure 4.1. Compressive moduli of scaffold cylinders. * $p<0.05$ from PLA dry and # $p<0.05$ from PLA-S wet

The compressive yield stresses for the scaffolds were: 2.55±0.48 MPa for PLA dry, 1.36±0.23 MPa for PLA wet, 1.62±0.25 MPa for PLA-H dry, 1.36±0.11 MPa for PLA-H wet, 0.56±0.11 MPa for PLA-S wet, and 0.92±0.09 MPa for PLA-S-H wet (Figure 4.2). The tests showed that the addition of the hydrogel to the electrospun scaffold did not significantly affect the compressive yield stress of PLA scaffolds, but did increase the yield stress for PLA-S scaffolds significantly. In addition, the PLA wet was significantly lower than the PLA dry, and the PLA-S wet had significantly lower yield stresses compared to the PLA wet.

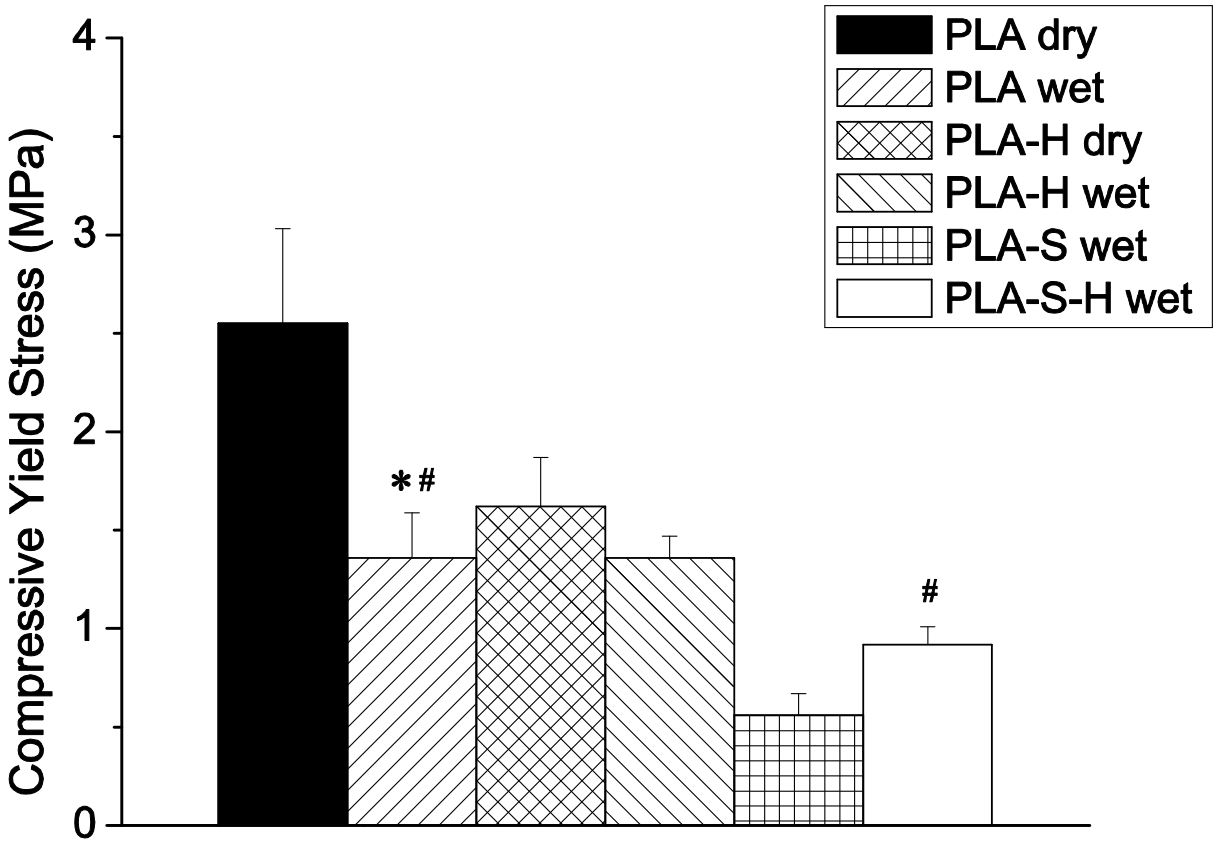

Figure 4.2. Compressive yield stresses of scaffold cylinders. * $p<0.05$ from PLA dry and # $p<0.05$ from PLA-S wet.

4.4 Discussion

Electrospun PDLA/PLLA cylinders were combined with a thermosetting chitosan based hydrogel to create scaffolds for cartilage tissue engineering. The hydrogel is composed of chitosan and ammonium hydrogen phosphate and crosslinks at approximately 37°C. Therefore, this hydrogel can also be used as a cell carrier when implanting the scaffold into the defect of articulating cartilage. The electrospun material can be placed into the defect and then the hydrogel and cells can be injected into the implant site. The body temperature of the patient would then cause the hydrogel to crosslink.

Electrospun cylinders with and without hydrogel were mechanically tested in compression to determine the effect of the hydrogel on the scaffolds' properties. PDLA/PLLA cylinders without salt leaching displayed no significant difference in mechanical properties between scaffolds with or without hydrogel. However, cylinders with salt leaching and the

hydrogel had higher compressive moduli and yield stresses compared to cylinders with salt leaching but no hydrogel. The pores created by the salt leaching process most likely let more hydrogel infiltrate the electrospun material, allowing the hydrogel to have a larger impact on the mechanical properties of the scaffold.

The electrospun PDLA/PLLA cylinders with salt leaching and hydrogel had a compressive modulus of 11.77 MPa. This value is very similar to the compressive modulus found in articular cartilage (approximately 10 MPa) by Slivka *et al.* under similar conditions [13]. Having a similar modulus greatly benefits the scaffold's potential for cartilage tissue engineering. A modulus comparable to surrounding cartilage tissue would help prevent stress-shielding effects after implantation, which lowers the risk of tearing at the scaffold tissue interface, and could be more likely to encourage cells to produce matrix similar to normal cartilage ECM [123]. A modulus similar to cartilage tissue and an ability to produce cartilage-like ECM are very important for the success of the scaffold and initial patient recovery, especially as the scaffold degrades and regenerated ECM takes over the scaffold's functions.

4.5 Scaffold Change

After performing the above experiments, preliminary dynamic mechanical tests were performed on electrospun cylinders with and without hydrogel. After testing, an unfortunate trend was evident. The cylinders displayed limited to no recovery when tested under dynamic conditions. After a series of cycles (~50 at 0.5 Hz) the cylinders showed no recovery from the tests, even after several minutes had passed. This characteristic is a significant limitation for the scaffold to be a reasonable cartilage tissue engineering construct. The scaffold needs to recover so that the scaffold can repeatedly perform its role of resisting and transferring load throughout its lifetime. Therefore, it was determined that changes must be made to the scaffold design to improve recovery during dynamic loading. Polylactides are relatively stiff biodegradable polymers, thus, utilizing a more elastic polymer could significantly improve the recovery of the scaffold. An elastic polymer typically will have a greater strain value before it exits the elastic region. As a result, the material should be able to be strained further and still return to its original size.

Acknowledgements

The authors would like to thank the Walter H. Coulter Foundation for funding this study and Lakshmi Nair and Zhanwu Cui for providing the chitosan hydrogel.

Chapter V: Electrospun PDLA/PCL and Hydrogel Scaffold for Tissue Engineered Cartilage

5.1 Introduction

Articulating cartilage is a tissue that undergoes repetitive loading. While walking and running, for example, cartilage is subjected to numerous loading and unloading conditions [86,124]. The tissue must resist the stresses it is subjected during a loading phase and then recover for another loading cycle during the unloading phase. As a result, the dynamic mechanical properties of any articulating cartilage replacement are very important. The replacement must be capable of resisting multiple loading cycles in close proximity to one another.

Although having cells present and growing in the scaffold is important for an effective tissue engineered replacement, ultimately the cells must be able to produce appropriate ECM for regeneration of the tissue [125,126]. The ECM produced should be capable of handling the physiological loading conditions that it will be subjected to as the scaffold degrades [35,40,126,127]. Therefore, creating a scaffold that encourages production of appropriate ECM is an important factor to developing a successful tissue engineered cartilage replacement.

Electrospun poly(d,l-lactide) (PDLA) and poly(l-lactide) (PLLA) electrospun scaffold with chitosan hydrogel showed promise as a scaffold for articulating cartilage. The scaffolds had a compressive modulus very similar to articulating cartilage as described in chapter 4. However, the scaffold did not perform well under dynamic loading; its recovery was essentially nonexistent. Therefore, a determination was made to change one of the primary polymer components, PLLA, to a more elastic material, polycaprolactone (PCL). A more elastic material should allow the scaffold better capability of recovery. Therefore, we hypothesize that a scaffold composed of PDLA/PLLA electrospun cylinder and a chitosan hydrogel will have improved dynamic mechanical properties while providing an environment for cells to grow and regenerate cartilage tissue.

5.2 Materials and Methods

5.2.1 *Electrospinning*

Poly(d,l-lactide) (PDLA) was purchased from Lakeshore Biomaterials (Birmingham, AL, USA). Dichloromethane (DCM), dimethylformamide (DMF), tetrahydrofuran (THF), and polycaproloctone (PCL) were purchased from Fisher Scientific (Pittsburgh, PA, USA). PCL was mixed with a 1:1 ratio of DCM and DMF to yield a total polymer weight percent of 50% (w/v). PDLA was mixed with a 3:1 ratio of THF and DMF to yield a total polymer weight percent of 22% (w/v).

To create the PDLA/PCL mats, the PDLA solution was first electrospun onto a rotating mandrel (~600 RPM) with a diameter of 5 cm. An electric field was applied to the PDLA solution (13kV and -10kV) forcing the polymer from the syringe and onto the rotating mandrel 20cm away. After 1mL of PDLA was electrospun onto the mandrel, PCL was electrospun onto the PDLA. An applied electric field (12kV and -9kV) caused PCL to electrospin onto a rotating mandrel (~600 RPM) 17cm away from the syringe. During PCL electrospinning, NaCl crystals were released from a rotating drum above the collection mandrel onto the electrospun materials as described in 2.3.1. The salt was then leached from the electrospun mats and sintered as described in 4.2.1.2, except that they were sintered for 45 minutes. A thermosetting chitosan hydrogel was then added to some of the scaffold cylinders as described in 4.2.3. Specifically, 10mL of chitosan hydrogel was placed into a beaker and cooled in ice along with an ammonium hydrogen phosphate (AHP) solution for 15 minutes. The chitosan hydrogel was then stirred while on ice as 180µL of AHP was added dropwise. The solution was then mixed for one minute before the electrospun scaffold was added to the solution. The scaffold/hydrogel was then placed under vacuum for 5 minutes to improve infiltration of the hydrogel into the electrospun scaffold. The scaffold and hydrogel were next placed into a 37°C water bath overnight to crosslink the hydrogel.

5.2.2 *PDLA/PCL failure tests*

PDLA/PCL cylinder scaffolds with salt pores, both with (S+H) and without hydrogel (S), and scaffolds without salt pores (NS) were then tested on the Instron 5869 with Biopuls Bath (Norwood, MA, USA) in PBS at 37°C. The cylinders (n=6) were compressed at a rate of

1mm/min (10% strain/min) until failure. The compressive yield stress and compressive modulus were then calculated and compared for analysis. Statistical significance was tested by one way ANOVA with a Tukey's test with α=0.05.

5.2.3 *Dynamic compression*

The dynamic mechanical properties of the scaffolds were determined using an Instron 5589 with a Biopuls bath system with PBS at 37˚C. PDLA/PCL scaffolds with salt pores with and without chitosan hydrogel were created as described in 4.2.3 and 5.3.1. PDLA/PCL scaffolds without salt pores served as a control. The scaffolds (n=6) were subjected to dynamic mechanical tests with an amplitude of 0.4mm at 0.5Hz for 500 cycles after a pre-load of 0.2N. The storage and loss modulus were calculated as described by Verteramo and Seehom. Specifically, the storage modulus (G') and loss modulus (G'') for cycles 1, 2, 50, 100, and 500 were calculated from the measured values of the peak compressive stress (σ_0), corresponding peak amplitude of cartilage strain (ε_0), and the phase angle (δ) between the two signals at each cycle as follows:

$$G' = \frac{\sigma_0}{\varepsilon_0}\cos\delta, \quad G'' = \frac{\sigma_0}{\varepsilon_0}\sin\delta \qquad \text{Eq. 1}$$

In addition, the recovery of the scaffolds during the dynamic tests was obtained by determining strain at which the stress begins to increase. The lower the strain is when the stress increased, the higher the recovery capability of the scaffolds. The change in peak stress during the course of the dynamic mechanical tests was also calculated. The minimum stress was subtracted from the peak stress and then divided by the peak stress of cycle 1 and multiplied by 100% for cycles 2, 50, 100 and 500. Statistical significance was tested by one way ANOVA with a Tukey's test with α=0.05.

5.2.4 *In vitro static study*

5.2.4.1 Scaffold fabrication

Three groups of electrospun scaffolds were created as described in 5.3.1: salt pores/ no hydrogel cylinders (NH), salt pores/ hydrogel cylinders (H), and a single PDLA/PCL electrospun mat layer with salt pores (2D). Cells cultured on tissue culture polystyrene (TCP) served as a

control. After sintering, the 3D scaffolds were embedded in OCT, cut to a height of 1 cm, and then sterilized by soaking in ethanol for 30 minutes, followed by exposure to UV light for 30 minutes twice. The 3D scaffolds were then glued to Ultra low attachment 24 well plates (Corning Inc., Corning, NY, USA) with Silastic® Medical Adhesive and allowed to dry overnight. The 2D scaffolds were glued to TCP 24-well plates. The wells were then rinsed with sterile PBS and soaked in DMEM/F12 (Invitrogen, Carlsbad, CA, USA) with 10% FBS and 1% pen/strep overnight.

Primary canine chondrocytes (Cell Applications, Inc) were seeded onto the scaffolds at a concentration of 200,000/well at passage 4. During the four-week study, DMEM/F12 media (with 10% FBS, 1% pen/strep, and 0.2 mM p-ascorbic acid) was exchanged three times per week.

5.2.4.2 MTS

The CellTiter 96 AQueousOne Solution Cell Proliferation (MTS) Assay (n=4) was performed after days 7, 14, 21, and 28 to assess cellular activity and cytotoxicity of the cells, through measurement of mitochondrial activity, on the electrospun scaffolds and TCP. First the media was removed from all wells; the 2D scaffolds were placed into a fresh 24-well plate. Next, 80 µL of the MTS reagent and 400 µL of DMEM was added to each well and incubated at 37°C. After three hours of incubation, 200 µL of the solution was then removed from each well and placed into a 48-well plate. Finally, 200 µL of DI water was added to each well before measuring the light absorbance at 490 nm using a SpectraMax M2e spectrophotometer (Sunnyvale, CA, USA). Statistical significance was tested by a one way ANOVA with Tukey's test with α=0.05.

5.2.4.3 Dimethylmethylene blue assay

The concentration of proteoglycans was measured by the dimethylmethylene blue (DMMB) assay (n=3) previously described by Billington, et al [128]. Specifically, the scaffolds were removed from wells and placed into microcentrifuge tubes. Samples cultured on TCP were scraped to obtain the ECM within those wells before being placed into the microcentrifuge tubes. 350 µL of PBS, 100 µL papain solution (0.25 g/10 mL PBS), 50µL cysteine-HCl (0.078 g/10 mL PBS), and 50 µL EDTA (0.19 g/10 mL PBS) were added to each tube and vortex mixed. The

cap of each tube was then pierced with a syringe needle and incubated at 65°C overnight. Then 450µL of PBS was added to each tube and the tubes were stored at 4°C. 40 µL of digested samples or standards were added into a microtiter plate; standards of 0, 5, 10, 15, 20, 25, 30, 35, 40 µg/mL were used. 250 µL of DMMB solution (16 mg DMMB, 5 mL ethanol, 2 mL formic acid, 2.0 g sodium formate) was then added to each well, and the plate was read at 525 nm on a SpectraMax M2e spectrophotometer. Statistical significance was tested by a one way ANOVA with a Tukey's test with α=0.05.

5.2.4.4 ELISA

A Type II Collagen ELISA Kit (Chondrex, Inc, Redmond, WA, USA) (n=3) was used to determine the production of collagen type II by the chondrocytes. The assay was performed according to the manufacturer's protocol.

5.2.4.5 Frozen sectioning protocol for scaffolds

Scaffolds were sectioned in OCT to allow florescent staining of cross-sections. The scaffolds were first removed from the wells, placed into cryomolds, and OCT compound was added. The cryomolds were then vacuumed for 5 minutes to encourage OCT infiltration into the scaffolds and then placed into -80°C for storage. The frozen scaffolds blocks were later sectioned (10-15µm), mounted on slides, and stored at -80°C. Before staining, the slides were warmed to room temperature and fixed in cold acetone for 5 minutes. Slides were allowed to dry for 30 minutes at room temperature and then washed with PBS.

5.2.4.6 Immunostaining

Scaffolds were stained with a collagen II immunoflorescent stain to determine relative production and distribution of collagen II. Specifically, sectioned samples were washed with cold PBS twice. The sections were then fixed with 3.7% paraformaldehyde in PBS for 15 minutes and then washed with PBS twice. The sections were next incubated with 0.5% Triton X-100 in PBS at room temperature for 15 minutes and then washed with PBS twice. Then the sections were incubated at room temperature with 5% normal donkey sera (Santa Cruz Biotechnology, Inc, Santa Cruz, CA, USA) in PBS for 1 hour. The sections were then exposed to the collagen II primary antibody solution (Santa Cruz Biotechnology, Inc) in 1.5% normal sera

in DI water and incubated at 4°C overnight. The collagen II primary antibody is reported by the company to be reactive with canine collagen. Before being incubated with secondary antibody in the dark for 1 hour, the sections were first washed with PBS twice. The sections were washed with PBS twice and then mounted with Vectashield® with DAPI (Vector Laboratories, Burlingame, CA, USA) to stain cell nuclei. Images were then obtained on a Leica DMI 6000B microscope (Lecia Microsystems, Wetzlar, Germany). Maximum pixel intensity and average pixel intensity was measured for each image with ImageJ. Statistical significance was tested by a Student's T test with α=0.05.

5.3 Results

5.3.1 *Mechanical tests*

Electrospun PDLA/PCL materials were sintered into cylinders and mechanically tested in compression. Cylinders were compressed to failure at 10% strain/minute to determine the compressive modulus and compressive yield stress of the materials. They were also tested in dynamic compression to determine their recovery capability and dynamic properties.

Three groups of electrospun cylinders were mechanically tested to failure in compression: no salt pores (NS), salt pores (S), and salt pores with hydrogel (S+H). The elastic moduli of the scaffolds were 4.570±0.617 MPa, 2.606±0.452 MPa, and 2.041±0.549 MPa, respectively. Specifically, the elastic modulus of the NS scaffolds was significantly higher than the elastic moduli of the S and the S+H cylinders (Figure 5.1). The compressive yield stresses for the NS, S, and S+H scaffolds were 255.8±40.2 kPa, 223.3±28.6 kPa, and 161.7±29.8 kPa. The S+H cylinders had a significantly lower compressive yield stress compared to the NS and S groups (Figure 5.2).

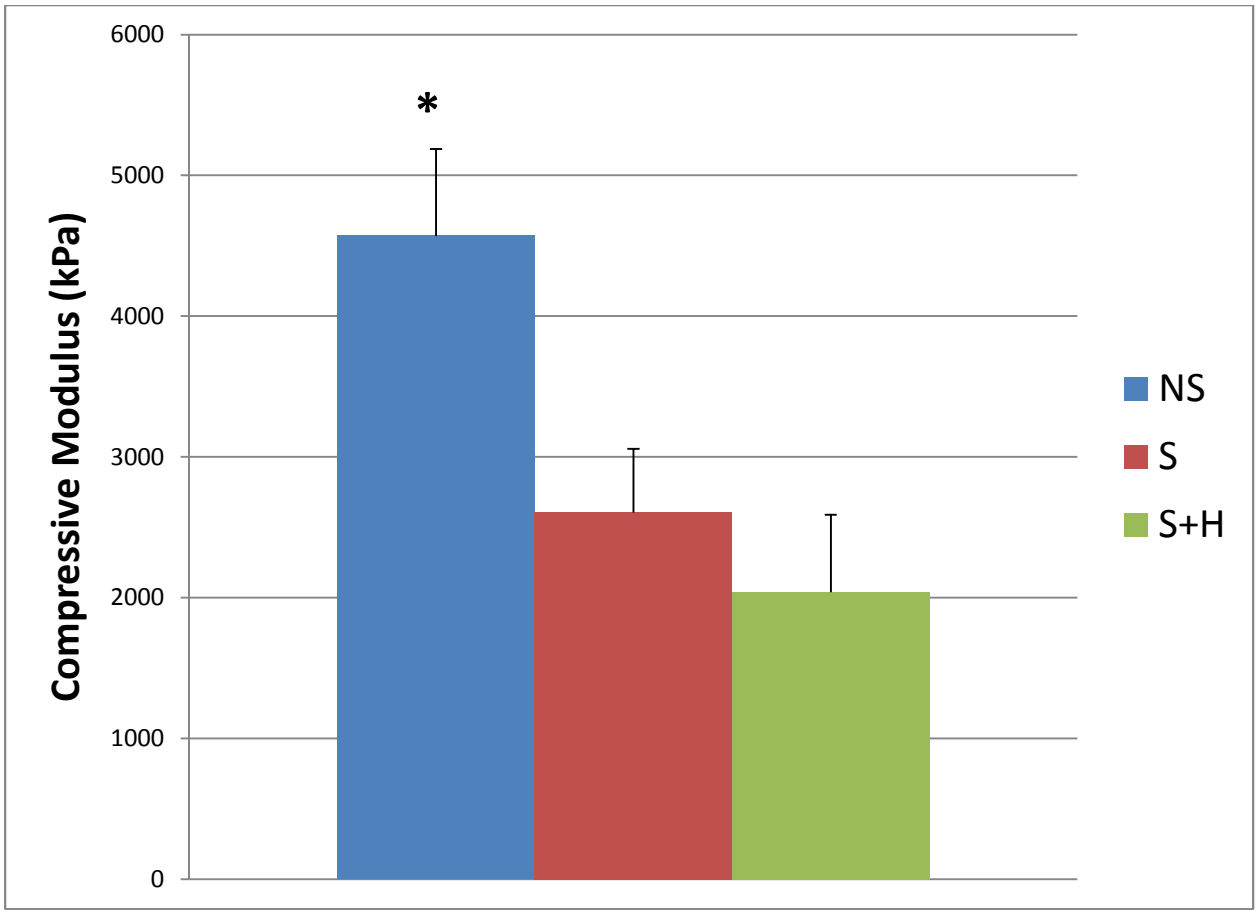

Figure 5.1. Compressive modulus of electrospun cylinders with no salt pores (NS), salt pores (S), and salt pores and hydrogel (S+H). * $p<0.05$ from S and S+H.

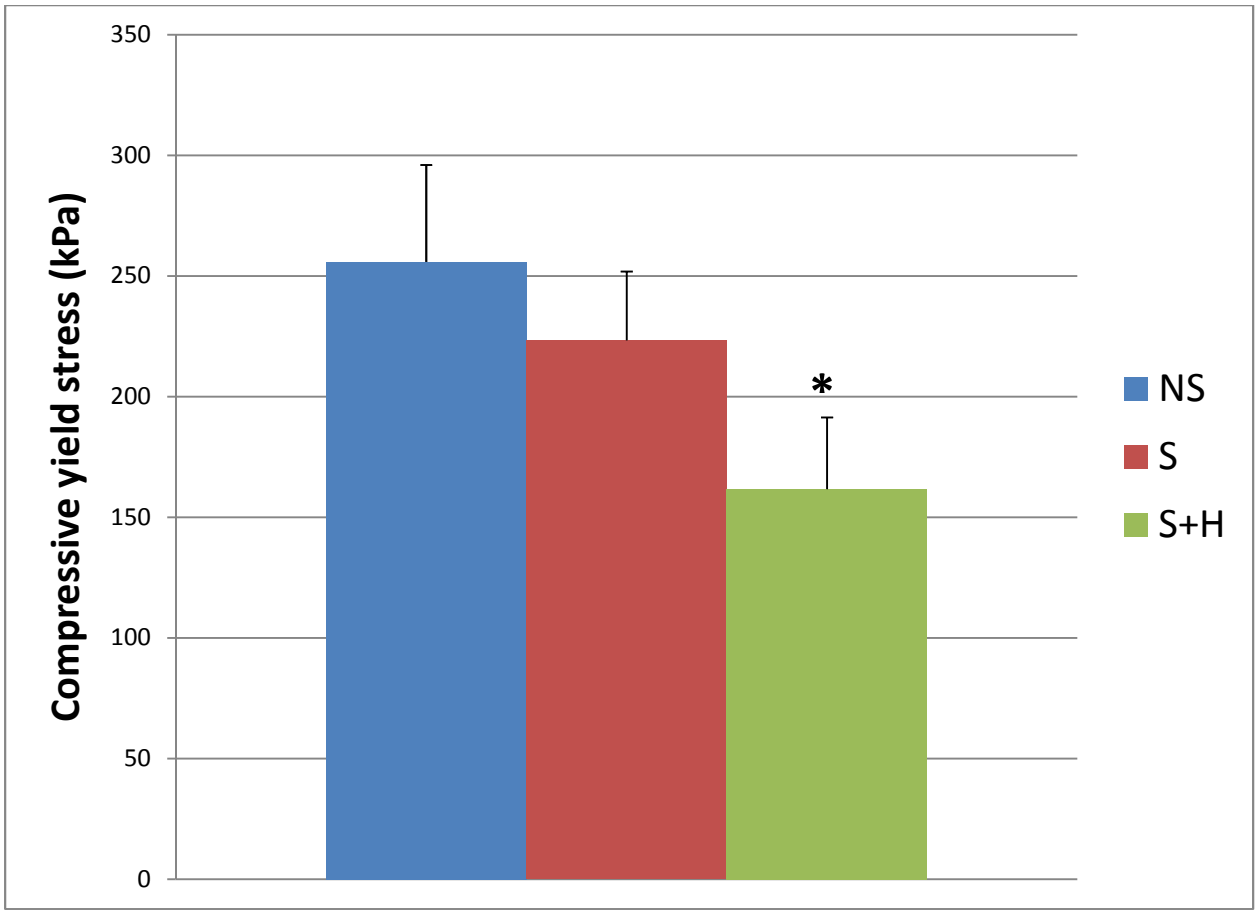

Figure 5.2. Compressive yield stress of electrospun cylinders with no salt pores (NS), salt pores (S), and salt pores and hydrogel (S+H). * $p<0.05$ from NS and S.

Electrospun PDLA/PCL cylinder scaffolds were also tested in dynamic compression to determine their dynamic properties and recovery capability. The storage and loss moduli were calculated for scaffolds without salt pores, scaffolds with salt pores, and scaffolds with salt pores and with hydrogel. There were no significant differences in the storage or loss moduli between the groups. In addition, among all cycles and groups the loss modulus was essentially zero (data not shown). Another metric used to measure recovery was the amount of strain required before the stress increased during a cycle. Thus, samples with lower strain values when the stress begins to increase have better recovery capability during dynamic loading. For cycles 2 and 50 the NS cylinders showed significantly higher strains compared to the S and S+H cylinders. At cycles 100 and 500 the NS cylinders had significantly higher strains compared to the S+H cylinders (Figure 5.3).

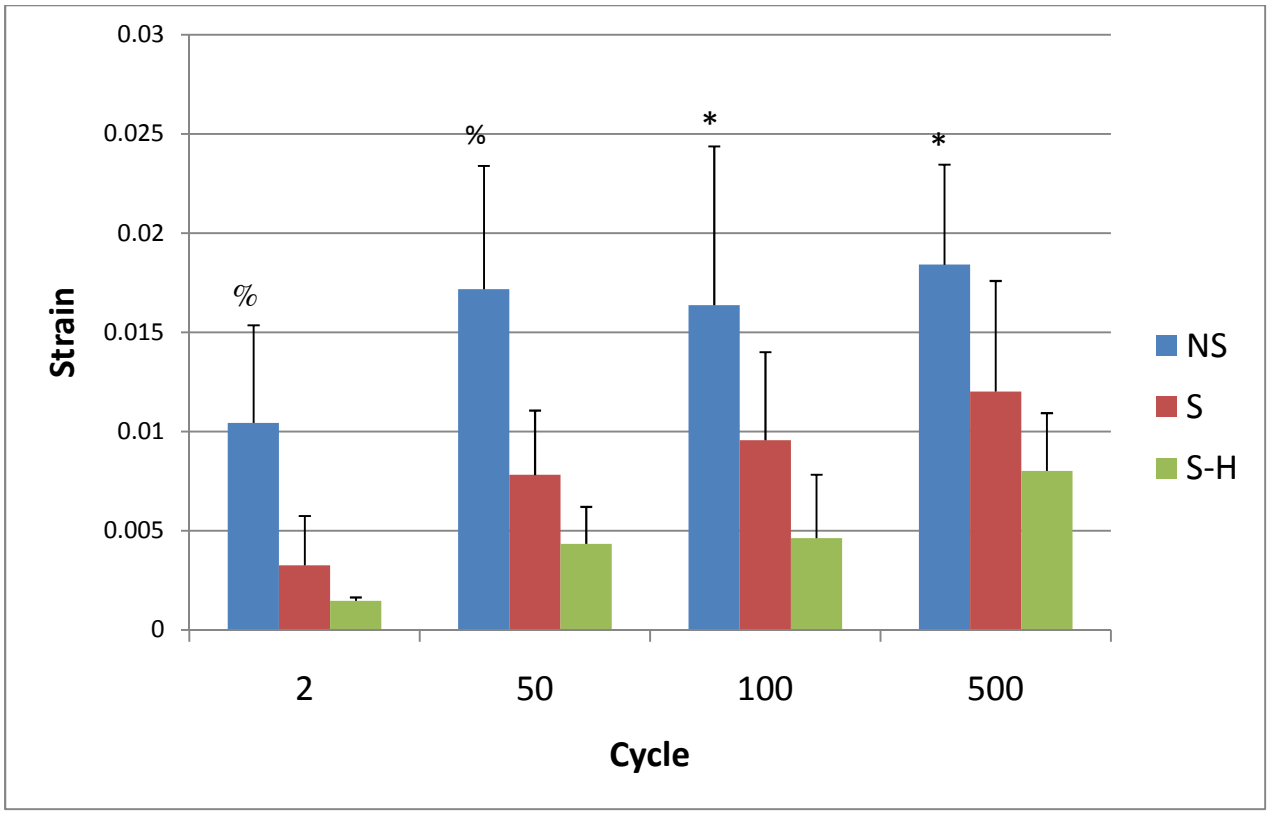

Figure. 5.3. Amount of strain before stress increases for electrospun cylinders with no salt pores (NS), salt pores (S), and salt pores and hydrogel (S+H). % $p<0.05$ from S and S-H of same cycle and * $p<0.05$ from S-H of same cycle.

Another metric measured during dynamic compressive tests was the percent of max stress the cylinders reached at a given cycle. The metric is a comparison of the maximum stress at a given cycle compared to the maximum stress during cycle 1 (100% would represent that the cylinder obtained a maximum stress at a given cycle equal to its maximum stress at cycle 1). The only statistical difference between the groups occurred at cycle 500 where the S scaffolds have a significantly higher percent of maximum stress compared to the S+H scaffolds (Figure 5.4).

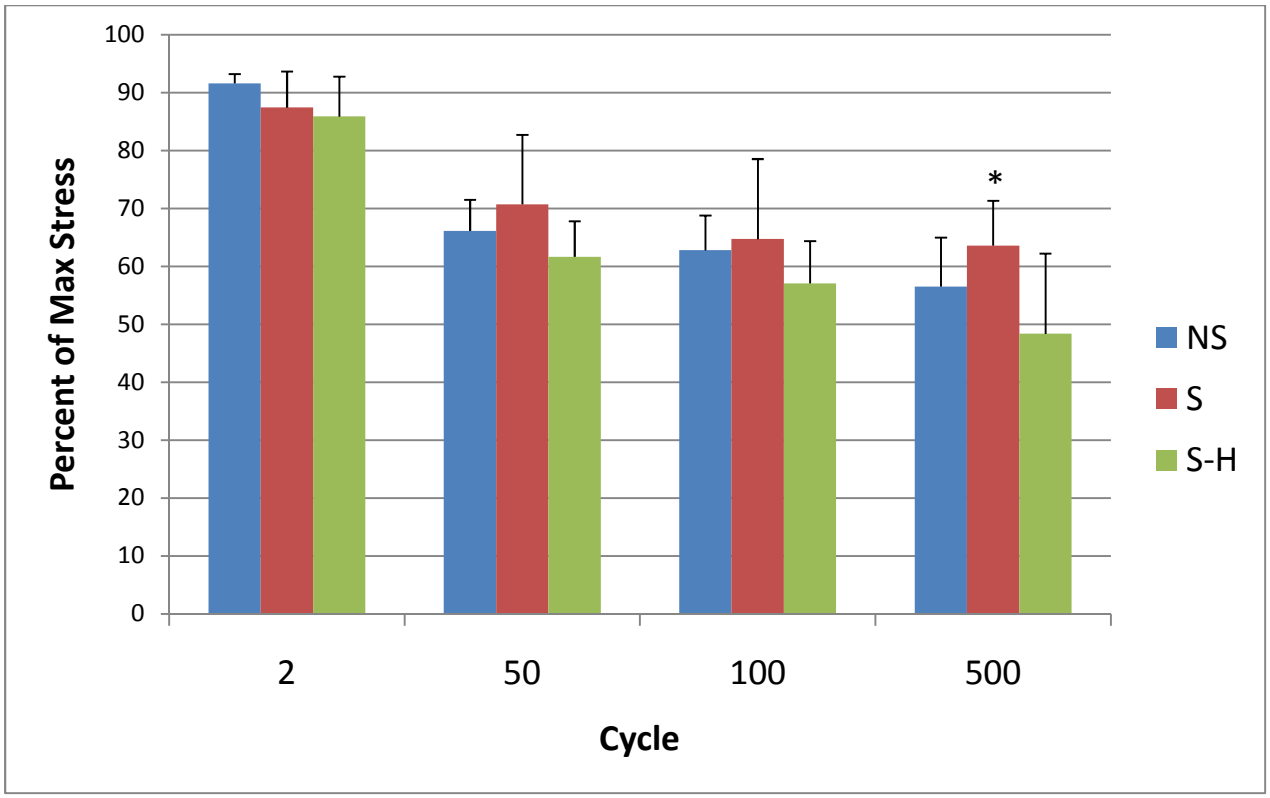

Figure 5.4. Percent of max stress of electrospun cylinders under dynamic tests with no salt pores (NS), salt pores (S), and salt pores and hydrogel (S+H). * $p<0.05$ from S-H of same cycle.

5.3.2 *In vitro static study*

A cell study with primary canine chondrocytes was used to investigate the effect of electrospun scaffolds with or without chitosan hydrogel on chondrocyte growth and ECM deposition. An MTS assay was used to determine cytotoxicity and cell activity on electrospun PDLA/PCL cylinder scaffolds with salt pores with (H) or without (NH) chitosan hydrogel, a flat electrospun PDLA/PCL sheet (2D), and on tissue culture polystyrene (TCP). At day 7 the TCP group had a significantly higher absorbance compared to all other groups. TCP was also significantly higher than the H and NH scaffolds at day 21. By day 28, the 2D group had significantly higher absorbance compared to the H, NH, and TCP groups. Over the course of the study, the 2D group showed large increases in absorbance, the H and NH groups showed moderate increases, and the TCP remained relatively constant (Figure 5.5).

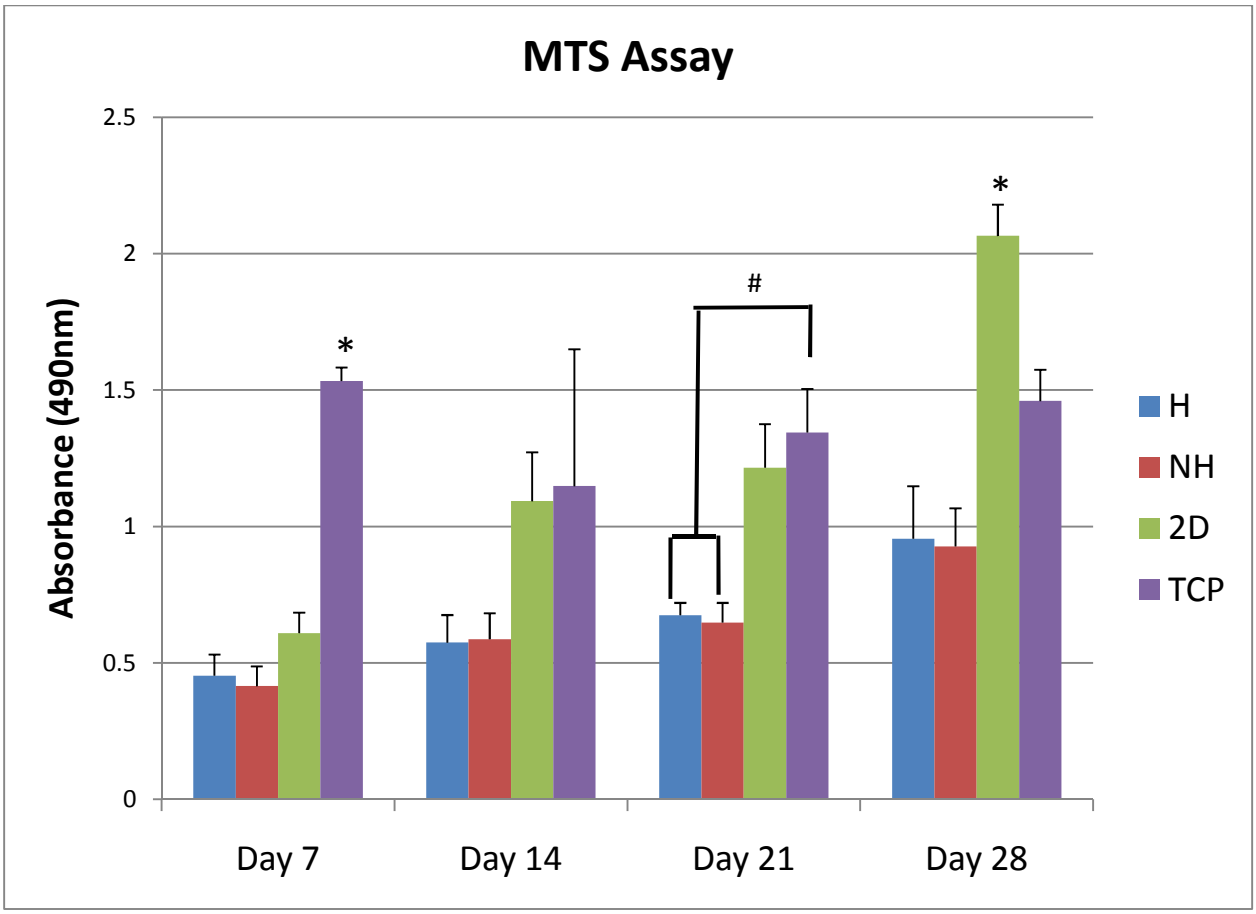

Figure 5.5. Absorbance after MTS assay of electrospun cylinders with hydrogel (H), without hydrogel (NH), two-dimensional mat without hydrogel (2D), and on tissue culture polystyrene (TCP). * $p<0.05$ from all other members of same day, # $p<0.05$ TCP from H and NH of day 21.

At days 7, 14, 21, and 28 the dimethylmethylene blue assay (DMMB) was performed on the scaffolds/TCP. Throughout the study the cells cultured on the TCP produced the most proteoglycans. Specifically, at day 28 the TCP had significantly more proteoglycans compared to the H and NH scaffolds (Figure 5.6).

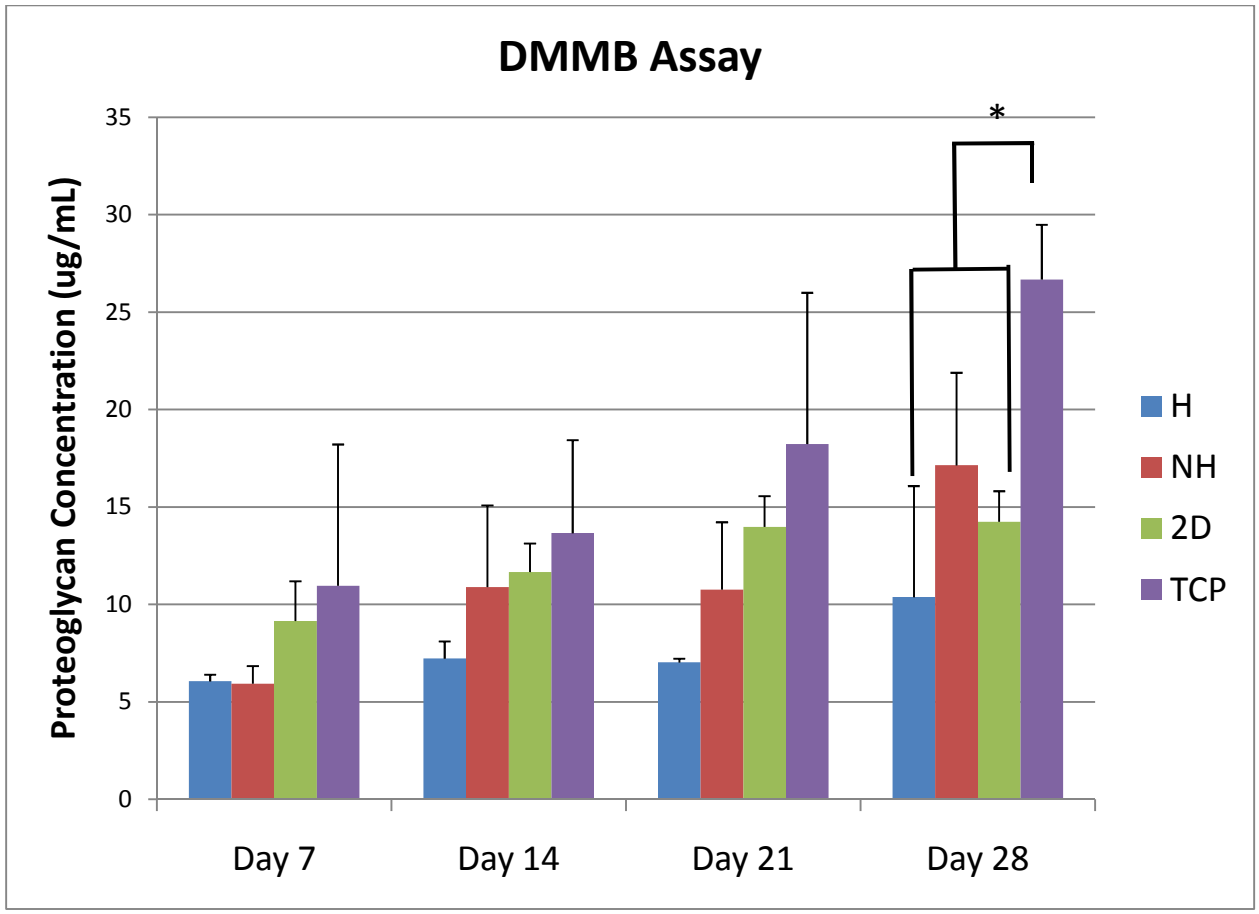

Figure 5.6. Proteoglycan concentration of electrospun cylinders with hydrogel (H), without hydrogel (NH), two-dimensional mat without hydrogel (2D), and on tissue culture polystyrene (TCP) determined by dimethlymethlyene blue assay on days 7, 14, 21, 28. * $p<0.05$ TCP from H and NH of day 28.

Immunoflorescent staining was used to determine the production of collagen type II on the scaffolds. Florescent images were taken and then the mean and maximum pixel intensity was calculated. The mean pixel intensity for PDLA/PCL cylinder scaffolds with salt pores and hydrogel (H) was 7.24±0.32 (pixel intensity units) with a collagen II primary antibody (n=3) and 2.49±0.63 without a collagen II primary antibody (n=4). The mean intensity of the cylinder scaffolds with salt pores without hydrogel (NH) was 4.64±1.34 with the collagen II primary (n=6) and 2.45±0.87 without (n=6). The mean intensity of a two-dimensional PDLA/PCL mat (2D) was 7.72±2.62 with the collagen II antibody (n=6) and 1.57±0.99 without (n=8). The H, NH, and 2D scaffolds with the primary collagen II antibody were all significantly larger than

their counterparts without the antibody. In addition, the NH scaffold was significantly lower than the 2D and H scaffolds with the collagen II primary antibody (Figure 5.7).

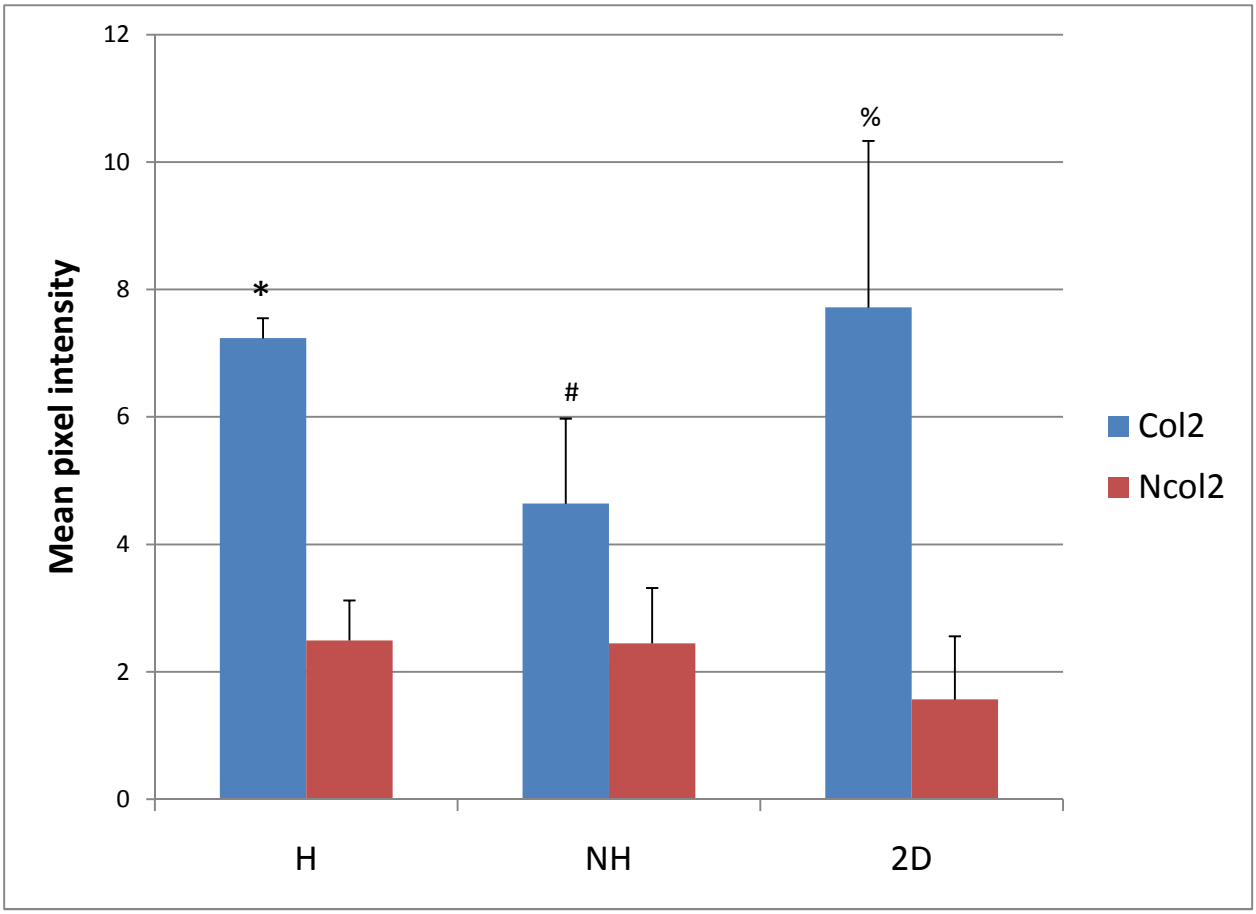

Figure 5.7. Mean pixel intensity of collagen type II florescent stain of electrospun cylinders with hydrogel (H), without hydrogel (NH), and two-dimensional mat without hydrogel (2D). The images were taken of samples provided with a primary antibody to bind collagen II (Col2) and one that does not bind collagen II (Ncol2). * $p<0.05$ from Ncol2 of H scaffolds, # $p<0.05$ from Ncol2 of NH scaffolds, % $p<0.05$ from Ncol2 of 2D scaffolds.

The maximum pixel intensity H scaffolds was 87.0±51.5 with a collagen II primary antibody and 26.0±6.8 without a collagen II primary antibody. The max intensity of the NH cylinder scaffolds was 79.2±16.4 with the collagen II primary and 22.8±1.7 without. The mean intensity of a 2D mat was 62.3±52.1 with the collagen II antibody and 24.9±7.0 without. The H, NH, and 2D scaffolds with the primary collagen II antibody were all significantly larger than their counterparts without the antibody (Figure 5.8).

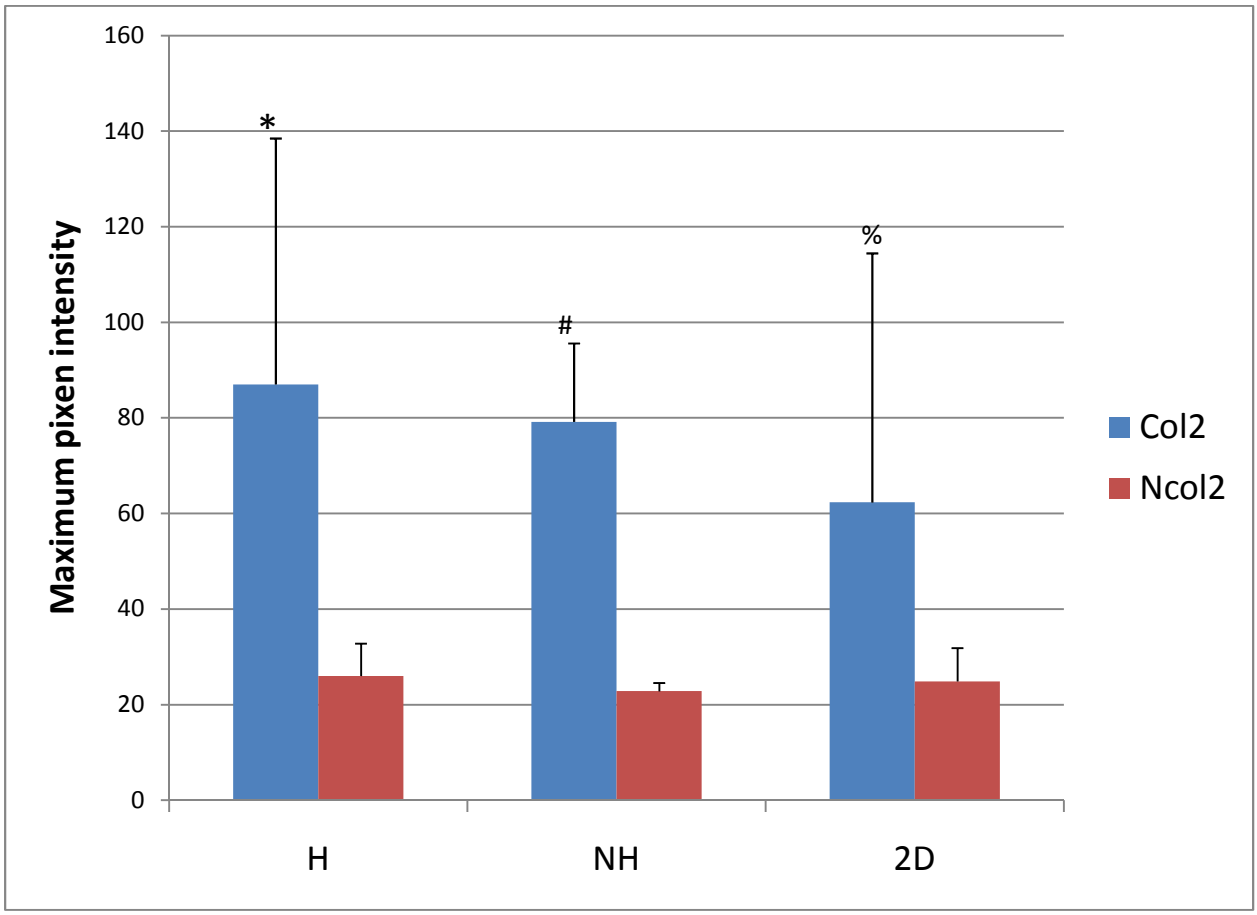

Figure 5.8. Maximum pixel intensity of collagen type II florescent stain of electrospun cylinders with hydrogel (H), without hydrogel (NH), and two-dimensional mat without hydrogel (2D). The images were taken of samples provided with a primary antibody to bind collagen II (Col2) and one that does not bind collagen II (Ncol2).). * $p<0.05$ from Ncol2 of H scaffolds, # $p<0.05$ from Ncol2 of NH scaffolds, % $p<0.05$ from Ncol2 of 2D scaffolds.

5.4 Discussion

Electrospun cylinder scaffolds were made from PDLA/PCL and chitosan hydrogel. Electrospun PDLA/PCL mats were sintered together with heat into cylinders. Chitosan hydrogel was then vacuumed into the scaffold and crosslinked at 37°C. The scaffolds were then mechanically tested to determine their compressive moduli, compressive yield stress, and dynamic mechanical properties. The compressive moduli of scaffolds with salt pores (S) and

scaffolds with salt pores and chitosan hydrogel (S+H) were significantly reduced compared to the scaffolds without salt pores or hydrogel (NS) (Figure 5.1). In addition, the S+H scaffold had significantly lower yield stress compared to the S and NS scaffolds. The S+H scaffold had much lower compressive modulus compared to articular cartilage which is over 10 MPa under similar conditions [13].

In contrast to the mechanical tests to failure, the addition of the hydrogel did improve some of the dynamic mechanical properties of the scaffolds. Specifically, the S+H scaffolds displayed improved recovery during dynamic testing. The S+H scaffolds had significantly lower strain values when stress increased during dynamic testing compared to NS throughout the tests. This translated to significantly improved recovery compared to the NS scaffolds. In addition, for cycles 2 and 50 the S scaffolds also had significantly improved recovery compared to the NS scaffolds. For all cycles the S+H scaffolds had the best recovery (Figure 5.3). A comparison of the percent of max stress during dynamic testing showed that S+H scaffolds had the lowest values for all cycles, although only significantly lower at cycle 500 compared to S scaffolds (Figure 4).

Primary canine chondrocytes were cultured on electrospun scaffolds with salt pores and with or without hydrogel, on 2D electrospun mats, and on TCP. The MTS assay performed showed that cells were able to grow and proliferate on the scaffolds and TCP. The 2D scaffolds showed the greatest increase in MTS absorbance over the course of the study. The H and NH 3D scaffolds showed moderate increases in absorbance over time, while the TCP absorbance remained relatively constant throughout the study. The constant values of absorbance for TCP are due to the wells being confluent from day 7; 200,000 cells/well is a very high concentration for culturing on TCP. The 2D scaffolds showed the highest increase in absorbance in the study because a larger number of cells can attach more easily on 2D scaffolds than the 3D scaffolds. In addition, the 2D scaffolds have a greater surface area for growth than the TCP.

The DMMB assay performed on the scaffolds showed that cells were able to produce proteoglycans. Throughout the study, cells on TCP produced the greatest amount of proteoglycans while the H scaffolds produced the least. The proteoglycans produced by the cells are comparable to a study performed by Bonakdar *et al*. which used polyvinyl alcohol hydrogels crosslinked with prepolyurethane. Their study obtained concentrations of 8-10 ug/mL with

human chondrocytes at day 14 [129] which is consistent with day 14 results of 7.22 µg/mL and 10.89 µg/mL for H and NH scaffolds, respectively.

Immunostaining for collagen II illustrated that cells produced collagen II. The staining performed with a primary antibody for collagen II was compared to one performed with a primary antibody not for collagen II. For all groups, the max pixel intensity and the average pixel intensity were significantly larger for the staining with collagen II antibody. This verifies that the staining procedure has no autofluorescent or nonspecific binding. Attempting to compare the different groups in max pixel and average pixel intensity is difficult within this study. The images were not of a confluent monolayer of cells. Instead large portions of the images were composed of regions without cells. Since the amount of space in each image composed of noncellular regions was not the same, making a comparison between the groups based on pixel intensities would be unadvised. However, it should be noted that the number of images for N and H scaffolds were not the same. The H scaffolds had fewer images taken (3 versus 6) because there were fewer regions that could be used. This fact leads us to believe that there are fewer locations where cells reside in the scaffold. The most likely cause of this result is reduced infiltration of cells into the scaffolds with hydrogel due to the hydrogel reducing the porosity of the scaffold when it crosslinks. Therefore, cells may be required to degrade the chitosan hydrogel as they infiltrate the scaffold, which could inhibit tissue engineering applications.

Acknowledgements

The authors would like to thank the Walter H. Coulter Foundation for funding this study and Lakshmi Nair and Zhanwu Cui for providing the chitosan hydrogel and performing the *in vivo* study.

Chapter VI: Future Directions

6.1 Introduction

Cartilage tissue engineering has been hampered by an inability to create a scaffold that encourages regeneration and replicates the mechanical properties of the cartilage tissue. Two common techniques used to create scaffolds for tissue engineering are electrospinning and hydrogel formation. Both of these techniques, however, have limitations to effectively tissue engineer cartilage as discussed in chapter 1. Combining the electrospun scaffold with a hydrogel has allowed us to create a composite that has begun to overcome some of the limitations of both electrospinning and hydrogels. We added salt to poly(l-lactide) (PLLA) electrospun mats to increase cell infiltration into the electrospun mesh. We were able to increase the average pore size and distribution as well as increase the amount of cell infiltration into electrospun mats. Later, three dimensional (3D) structures were created from poly(d,l-lactide) (PDLA)/PLLA electrospun mats which allowed the creation of electrospun scaffolds with unique architectures including cylinders for cartilage tissue engineering. Following the creation of 3D structures we introduced a thermosetting chitosan hydrogel scaffold into a PDLA/PLLA electrospun cylinder scaffold with larger pores and improved the mechanical properties of the scaffold. However, the dynamic mechanical properties of the PDLA/PLLA with hydrogel scaffold were very poor. Thus, the PLLA was exchanged with polycaprolactone (PCL) which improved dynamic mechanical properties but decreased the mechanical properties in failure tests. In addition cells cultured on the electrospun PDLA/PCL scaffolds with and without hydrogel were able to produce cartilage extracellular matrix.

Continued work on this composite scaffold is necessary to create a viable cartilage tissue engineering scaffold. The scaffold needs to be capable of regenerating cartilage tissue *in vivo* in addition to regenerating tissue *in vitro*. Scaffold components may also needed to be changed to improve performance, with respect to both mechanics and regenerative capability. Chapter 6 will discuss the *in vivo* study currently being performed with the composite scaffolds as well as possible future directions of this project.

6.2 Materials and Methods

6.2.1 *Electrospinning*

Poly(d,l-lactide) (PDLA) was purchased from Lakeshore Biomaterials (Birmingham, AL, USA). Dichloromethane (DCM), dimethylformamide (DMF), tetrahydrofuran (THF), and polycaproloctone (PCL) were purchased from Fisher Scientific (Pittsburgh, PA, USA). PCL was mixed with a 1:1 ratio of DCM and DMF to yield a total polymer weight percent of 50% (w/v). PDLA was mixed with a 3:1 ratio of THF and DMF to yield a total polymer weight percent of 22% (w/v).

To create the PDLA/PCL mats, the PDLA solution was first electrospun onto a rotating mandrel (~600 RPM) with a diameter of 5 cm. An electric field was applied to the PDLA solution (13kV and -10kV) forcing the polymer from the syringe and onto the rotating mandrel 20cm away. After 1mL of PDLA was electrospun onto the mandrel, PCL was electrospun onto the PDLA. An applied electric field (12kV and -9kV) caused PCL to electrospin onto a rotating mandrel (~600 RPM) 17cm away from the syringe. During PCL electrospinning, NaCl crystals were released from a rotating drum above the collection mandrel onto the electrospun materials as described in 2.3.1. The salt was then leached from the electrospun mats and sintered as described for 45 minutes into cylinders with a diameter of 1.5mm. Afterwards the cylinders were embedded in OCT, frozen, and cut to heights of 2 cm. The OCT was then leached out of the scaffold with deionized water and allowed to dry. Next, the cylinders were sterilized by soaking the cylinders in ethanol for 30 minutes and then exposing them to UV for 30 minutes twice. A thermosetting chitosan hydrogel was then added to some of the scaffold cylinders as described in 4.2.3. Specifically, 10mL of chitosan hydrogel was placed into a beaker and cooled in ice along with an ammonium hydrogen phosphate (AHP) solution for 15 minutes. The chitosan hydrogel was then stirred while on ice as 180µL of AHP was added dropwise. The solution was then mixed for one minute before the electrospun scaffold was added to the solution. The scaffold/hydrogel was then placed under vacuum for 5 minutes to improve infiltration of the hydrogel into the electrospun scaffold.

6.2.2 *In vivo study*

Electrospun cylinders, with and without hydrogel, were placed into the knees of rats to determine the effectiveness of the scaffolds. A defect in the knee with no scaffold served as the control. Cylinders were created by first electrospinning with 1mL of 22% PDLA followed by 5mL of 50% PCL. Salt was added to the electrospun mats and then leached out. The electrospun mats were then sintered into cylinders with a diameter of 1.5 mm as previously described in 5.3.1. Hydrogel was then added to one group of scaffolds as described in 4.2.3.

Rats were prepared by shaving the fur of the animal in the leg region and then prepping the skin with betadine solution. For anesthesia, animals received 2-3% continuous isoflurane by inhalation. Sedation was confirmed through tail pinch. The groove between the femoral condyles was then identified and a medial parapatellar incision of 1.5 to 2 cm was performed using a sterile blade. The knee joint was then maximally flexed to expose the weight-bearing portion of the lateral femoral chondyle. A sterilized microdrill was used to create a 1.5 mm diameter by 2-3mm deep defect through the articular cartilage and subchondral bone of the lateral hemichondyle. The scaffold was then used to fill the defect; a defect with no scaffold served as the control. Next the skin was closed in a single layer using 4-0 Vicryl-R sutures. Buprenorphine (0.05-0.2 mg/kg) was administered to every rat immediately following recovery and every 8-12 hours for 2 days to help moderate pain.

After 6 weeks (n=4) and 15 weeks (n=5) the effectiveness of the scaffolds was determined by histology. These time points were chosen because based on previous data it was estimated that at 6 weeks some initial regeneration would have occurred, while the 15 week time point should provide a point at which significant healing has occurred but difference between groups should still remain. At the designated time point the rats were sacrificed by carbon dioxide inhalation and the knee samples were collected. The samples were fixed in 10% formalin phosphate for 4-5 days and then decalcified in 14% EDTA solution for 4-6 weeks. Afterwards, the tissue samples were dehydrated in a series of ethanol solution, a mixture of xylene and paraffin solution (1:1 v/v), and paraffin solution. Finally, the samples were embedded in paraffin. The samples were then sectioned at 5 μm per slide and stained by H & E. The tissue repair was evaluated by histology.

6.3 Preliminary Results

Electrospun cylinders, with and without hydrogel, were placed into the knees of rats to determine the effectiveness of the scaffolds. A defect in the knee with no scaffold served as the control. After 6 and 15 weeks histology was performed on the knees. Preliminary results show that at 6 weeks the control has some fibrous tissue formation around the defect site. Compared to the control there was a larger inflammatory response and greater cell infiltration with the electrospun scaffold without hydrogel. The defect filled with an electrospun scaffold and hydrogel seemingly has a less severe inflammatory response (Figure 6.1).

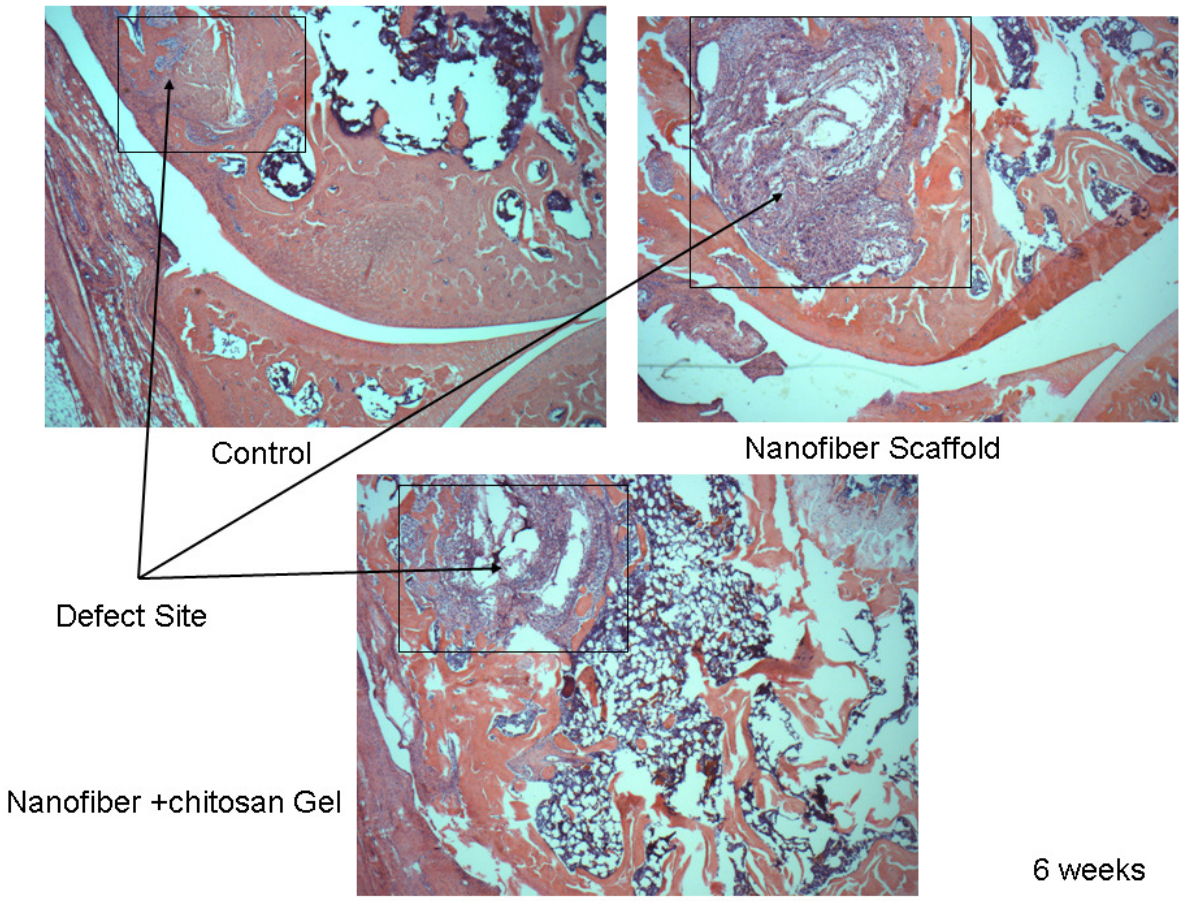

Figure 6.1. Histology of defect in rat knees with no scaffold (control), nanofiber scaffold, and nanofiber scaffold with chitosan hydrogel after 6 weeks.

Preliminary results at 15 weeks portray that the control has no visible fibrous tissue, while there is still an inflammatory response and fibrous tissue presence for the defect filled with

both the scaffold with and without hydrogel. However, the scaffold with hydrogel does displays less severe inflammatory response and better integrates with surrounding tissue compared to the scaffold without hydrogel (Figure 6.2). Further histology and analysis of this study will be performed to elucidate the scaffold's effectiveness.

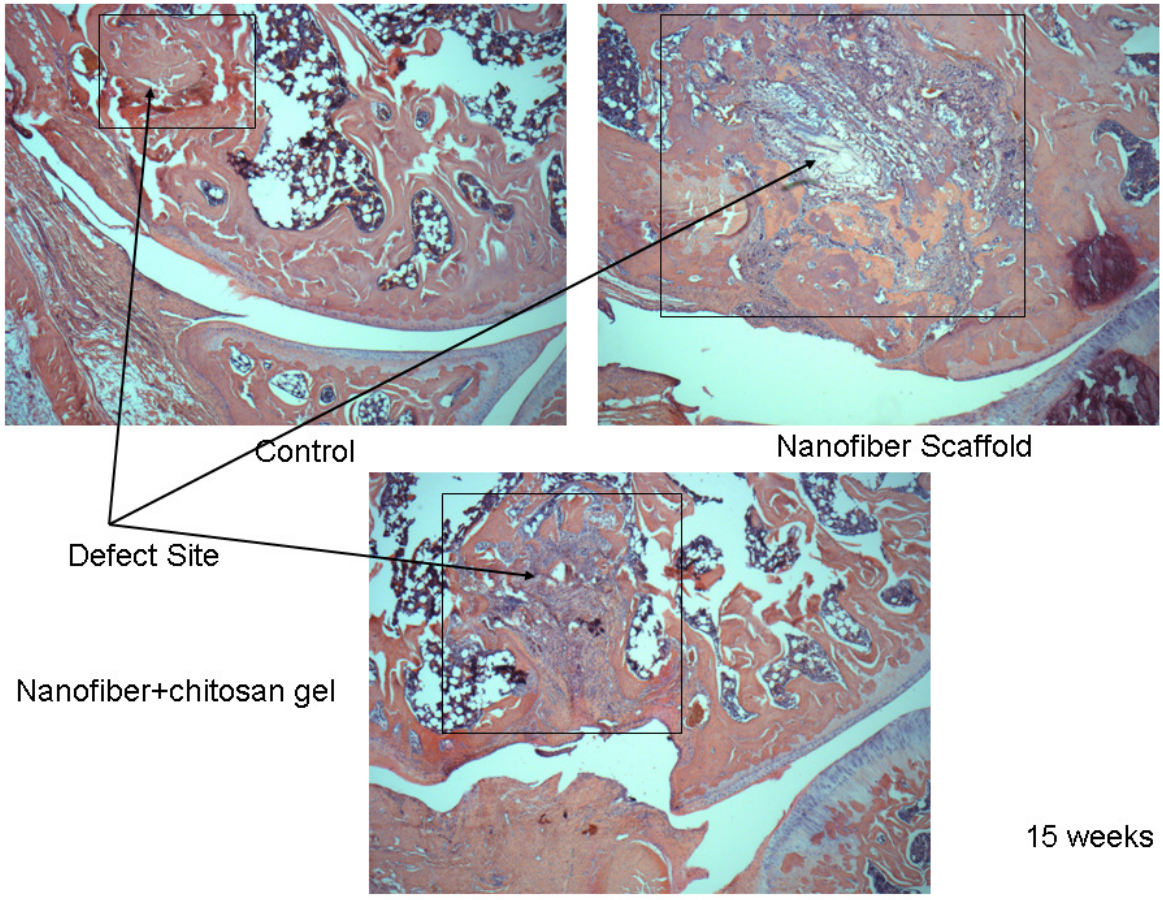

Figure 6.2. Histology of defect in rat knees with no scaffold (control), nanofiber scaffold, and nanofiber scaffold with chitosan hydrogel after 15 weeks.

6.4 Future Directions

This project can potentially continue in two distinct directions. The first possible direction is to adjust the electrospun polymer components of the scaffold to better mimic the mechanical properties of articulating cartilage. The current design of PDLA/PCL with chitosan hydrogel does show improved dynamic properties, but at the cost of reduced yield stress and compressive modulus. In addition, the dynamic properties are not optimal compared to

articulating cartilage. Changing the construction to PCL did improve recovery; however, the hydrogel seems to have less of an impact on mechanics with the PCL compared to one with PLLA. One theory is that since the PCL fibers pack tighter due to a greater range in fiber diameters compared to PLLA when electrospun, less hydrogel can penetrate the scaffold and therefore the hydrogel has less of an impact. Thus, one could postulate that using a more elastic polymer than PLLA but stiffer than PCL could benefit the overall mechanics of the scaffold. Another theory is that the lower mandrel speed reduced the compressive modulus and yield stress of the electrospun cylinders. The mandrel speed had to be lowered to obtain adequate incorporation of salt during electrospinning PCL. Switching polymers may allow the mandrel speed to be higher during salt incorporation which could improve the mechanics. One candidate would be to create either a blend of PLLA and PCL or a block copolymer of PLLA and PCL. The combination of the two polymers should produce a material that has improved recovery compared to PLLA and improved modulus and yield stress compared to PCL.

Another avenue of change for the scaffold would be to switch hydrogel polymers. The degree of cross-linking of the chitosan hydrogel cannot be well adjusted. Utilizing a hydrogel polymer that can cross-link more densely may increase the stiffness of the scaffold. Increased stiffness of the hydrogel should cause the compressive modulus and compressive yield stress to be higher, hopefully more similar to that of articulating cartilage. Chemically binding the hydrogel to the electrospun scaffold could also improve the mechanical properties of the scaffold and create a construct more similar to cartilage tissue. Proteoglycans, including aggrecan, are bound and interact to the collagen matrix in cartilage through various mechanisms [130]. The interactions between the two molecules can help prevent the proteoglycans from being extruded and lost during compression. Similarly, binding the hydrogel to the electrospun polymer may help prevent removal of the hydrogel during compression. Thus, during compression only water would be extruded which can be reabsorbed during unloading.

A different direction for the project would be to continue utilizing the PDLA/PCL scaffold with chitosan hydrogel and investigate its success in larger animals (canines or sheep). Although the scaffold is not mechanically perfect, it may display good success *in vivo*. Investigating the capabilities of the scaffold in larger animals would provide a better idea of the possibilities of the scaffold in eventual human use. In addition, the penetration of cells into the

scaffold could be improved by improved cell seeding techniques. As mentioned, the *in vivo* study involved no cell seeding of the scaffolds. Thus, cells must infiltrate into the scaffold from surrounding tissue for adequate tissue repair. Although the *in vitro* study did incorporate cell seeding, better techniques may improve cell distribution within the scaffold and facilitate more homogenous tissue regeneration; static seeding did not provide a homogenous distribution of cells in the scaffold. One method to improve cell seeding would be to place the cells in the hydrogel before it is crosslinked. The hydrogel would then be added to the scaffold, vacuumed into the scaffold, and crosslinked; the hydrogel would serve as a cell carrier. Similarly, investigating benefits of chemical factors within the scaffold would also be beneficial. Chemical factors could be used to promote cell localization and infiltration (chemotaxis) into the scaffold in addition to promoting production of ECM [131-133]. Insulin-like growth factor-1 (IGF-1) has been shown to have both a chemotactic effect and increase production of ECM, while transforming growth factor-β (TGF-β) has been shown to improve ECM production and platelet-derived growth factor (PDGF) displays a strong chemotactic effect [133-135].

References

1. Buckwalter, J.A., C. Saltzman, and T. Brown, *The Impact of Osteroarthritis: Implications for Research.* Clinical Orthopaedics and Related Research, 2004. **427**: p. s6-s15.
2. Lawrence, R.C., D.T. Felson, C.G. Helmick, L.M. Arnold, H. Choi, R.A. Deyo, S. Gabriel, R. Hirsch, M.C. Hochberg, G.G. Hunder, J.M. Jordan, J.N. Katz, H.M. Kremers, F. Wolfe, and W. Natl Arthritis Data, *Estimates of the prevalence of arthritis and other rheumatic conditions in the United States.* Arthritis and Rheumatism, 2008. **58**(1): p. 26-35.
3. Hootman, J.M. and C.G. Helmick, *Projections of US prevalence of arthritis and associated activity limitations.* Arthritis and Rheumatism, 2006. **54**(1): p. 226-229.
4. Kotlarz, H., C.L. Gunnarsson, H. Fang, and J.A. Rizzo, *Insurer and out-of-pocket costs of osteoarthritis in the US: Evidence from national survey data.* Arthritis and Rheumatism, 2009. **60**(12): p. 3546-3553.
5. Mahajan, A., S. Verma, and V. Tandon, *Osteoarthritis.* Journal of the Association of Physicians of India, 2005. **53**: p. 634-41.
6. Mazieres, B., B. Jamard, E. Verrouil, A. Constantin, M. Laroche, and A. Cantagrel, *The therapeutic approach to osteoarthritis.* Aging Clinical and Experimental Research, 2003. **15**(5): p. 405-12.
7. Huch, K., *Knee and ankle: human joints with different susceptibility to osteoarthritis reveal different cartilage cellularity and matrix synthesis in vitro.* Archives of Orthopaedic and Trauma Surgery, 2001. **121**(6): p. 301-6.
8. Goldring, M.B. and S.R. Goldring, *Osteoarthritis.* Journal of Cellular Physiology, 2007. **213**(3): p. 626-634.
9. Cowin, S.C., -, *Tissue mechanics*, ed. S.B. Doty. Vol. xvi, 682 p. :. 2007, New York, NY :: Springer.
10. Poole, A.R., T. Kojima, T. Yasuda, F. Mwale, M. Kobayashi, and S. Laverty, *Composition and structure of articular cartilage - A template for tissue repair.* Clinical Orthopaedics and Related Research, 2001(391): p. S26-S33.
11. Huber, M., S. Trattnig, and F. Lintner, *Anatomy, biochemistry, and physiology of articular cartilage.* Investigative Radiology, 2000. **35**(10): p. 573-580.
12. Alford, J.W. and B.J. Cole, *Cartilage restoration, part 1 - Basic science, historical perspective, patient evaluation, and treatment options.* American Journal of Sports Medicine, 2005. **33**(2): p. 295-306.
13. Slivka, M.A., N.C. Leatherbury, K. Kieswetter, and G.G. Niederauer, *Porous, resorbable, fiber-reinforced scaffolds tailored for articular cartilage repair.* Tissue Engineering, 2001. **7**(6): p. 767-780.
14. McAlindon, T., M. Formica, M. LaValley, M. Lehmer, and K. Kabbara, *Effectiveness of glucosamine for symptoms of knee osteoarthritis: Results from an internet-based randomized double-blind controlled trial.* The American Journal of Medicine, 2004. **117**(9): p. 643-649.
15. Pelletier, J.P. and J. Martel-Pelletier, *Therapeutic targets in osteoarthritis: from today to tomorrow with new imaging technology.* Ann Rheum Dis, 2003. **62**(90002): p. 79ii-82.
16. *Total Knee Replacement*. Joint Replacement April 2009 [cited 2010 February 22, 2010]; Available from: http://orthoinfo.aaos.org/topic.cfm?topic=A00389.

17. McClelland, J.A., K.E. Webster, and J.A. Feller, *Gait analysis of patients following total knee replacement: A systematic review.* Knee, 2007. **14**(4): p. 253-263.
18. Rand, J.A., R.T. Trousdale, D.M. Ilstrup, and W.S. Harmsen, *Factors affecting the durability of primary total knee prostheses.* Journal of Bone and Joint Surgery-American Volume, 2003. **85A**(2): p. 259-265.
19. *Total Knee Replacement*. Fred Philips Orthopaedic Surgeon [cited 2010 February 22, 2010]; Available from: http://www.fredphillips.co.nz/orthopaedic-wellington/knee-replacement.html.
20. Alford, J.W. and B.J. Cole, *Cartilage restoration, part 2 - Techniques, outcomes, and future directions.* American Journal of Sports Medicine, 2005. **33**(3): p. 443-460.
21. Kish, G., L. Modis, and L. Hangody, *Osteochondral mosaicplasty for the treatment of focal chondral and osteochondral lesions of the knee and talus in the athlete - Rationale, indications, techniques, and results.* Clinics in Sports Medicine, 1999. **18**(1): p. 45.
22. Duchow, J., T. Hess, and D. Kohn, *Primary stability of press-fit-implanted osteochondral grafts - Influence of graft size, repeated insertion, and harvesting technique.* American Journal of Sports Medicine, 2000. **28**(1): p. 24-27.
23. Hangody, L. and P. Fules, *Autologous osteochondral mosaicplasty for the treatment of full-thickness defects of weight-bearing joints - Ten years of experimental and clinical experience.* Journal of Bone and Joint Surgery-American Volume, 2003. **85A**: p. 25-32.
24. Chu, C.R., F.R. Convery, W.H. Akeson, M. Meyers, and D. Amiel, *Articular cartilage transplantation - Clinical results in the knee.* Clinical Orthopaedics and Related Research, 1999(360): p. 159-168.
25. Lyle J. Micheli, M., M. Jon E. Browne, M. Christoph Erggelet, PhD, M. Freddie Fu, M. Bert Mandelbaum, M. J. Bruce Moseley, and P. David Zurakowski, *Autologous Chondrocyte Implantation of the Knee: Multicenter Experience and Minimum 3-Year Follow-Up.* Clinical Journal of Sports Medicine, 2001. **11**: p. 223-228.
26. Jackson, D.W. and T.M. Simon, *Chondrocyte transplantation.* Arthroscopy: The Journal of Arthroscopic & Related Surgery, 1996. **12**(6): p. 732-738.
27. Gillogly, S.D., M. Voight, and T. Blackburn, *Treatment of articular cartilage defects of the knee with autologous chondrocyte implantation.* Journal of Orthopaedic & Sports Physical Therapy, 1998. **28**(4): p. 241-251.
28. Minas, T. and L. Peterson, *Advanced techniques in autologous chondrocyte transplantation.* Clinics in Sports Medicine, 1999. **18**(1): p. 13-+.
29. Mithofer, K., L. Peterson, B.R. Mandelbaum, and T. Minas, *Articular cartilage repair in soccer players with autologous chondrocyte transplantation - Functional outcome and return to competition.* American Journal of Sports Medicine, 2005. **33**(11): p. 1639-1646.
30. *Carticel Surgical Procedure*. 2003; Available from: http://www.arthroscopy.com/sp08029.htm.
31. Matsumoto, T., T. Okabe, T. Ikawa, T. Iida, H. Yasuda, H. Nakamura, and S. Wakitani, *Articular Cartilage Repair With Autologous Bone Marrow Mesenchymal Cells.* Journal of Cellular Physiology, 2010. **225**(2): p. 291-295.
32. Kuroda, R., K. Ishida, T. Matsumoto, T. Akisue, H. Fujioka, K. Mizuno, H. Ohgushi, S. Wakitani, and M. Kurosaka, *Treatment of a full-thickness articular cartilage defect in the femoral condyle of an athlete with autologous bone-marrow stromal cells.* Osteoarthritis and Cartilage, 2007. **15**(2): p. 226-231.

33. Nejadnik, H., J.H. Hui, E.P.F. Choong, B.C. Tai, and E.H. Lee, *Autologous Bone Marrow-Derived Mesenchymal Stem Cells Versus Autologous Chondrocyte Implantation An Observational Cohort Study.* American Journal of Sports Medicine, 2010. **38**(6): p. 1110-1116.
34. Rosenberger, R.E., A.H. Gomoll, T. Bryant, and T. Minas, *Repair of Large Chondral Defects of the Knee With Autologous Chondrocyte Implantation in Patients 45 Years or Older.* American Journal of Sports Medicine, 2008. **36**(12): p. 2336-2344.
35. Cheung, H.-Y., K.-T. Lau, T.-P. Lu, and D. Hui, *A critical review on polymer-based bio-engineered materials for scaffold development.* Composites Part B: Engineering, 2007. **38**(3): p. 291-300.
36. Eisenbarth, E., *Biomaterials for Tissue Engineering.* Advanced Engineering Materials, 2007. **9**(12): p. 1051-1060.
37. Agrawal, C.M. and R.B. Ray, *Biodegradable polymeric scaffolds for musculoskeletal tissue engineering.* Journal of Biomedical Materials Research, 2001. **55**(2): p. 141-150.
38. Mikos, A.G., G. Sarakinos, S.M. Leite, J.P. Vacanti, and R. Langer, *Laminated 3-Dimensional Biodegradable Foams for use in Tissue Engineering.* Biomaterials, 1993. **14**(5): p. 323-330.
39. Mooney, D.J., D.F. Baldwin, N.P. Suh, J.P. Vacanti, and R. Langer, *Novel approach to fabricate porous sponges of poly(-lactic-co-glycolic acid) without the use of organic solvents.* Biomaterials, 1996. **17**(14): p. 1417-1422.
40. Hutmacher, D.W., *Scaffolds in tissue engineering bone and cartilage.* Biomaterials, 2000. **21**(24): p. 2529-2543.
41. Giordano, R.A., B.M. Wu, S.W. Borland, L.G. Cima, E.M. Sachs, and M.J. Cima, *Mechanical properties of dense polylactic acid structures fabricated by three dimensional printing.* Journal of Biomaterials Science-Polymer Edition, 1996. **8**(1): p. 63-75.
42. Lannutti, J., D. Reneker, T. Ma, D. Tomasko, and D. Farson, *Electrospinning for tissue engineering scaffolds.* Materials Science and Engineering: C, 2007. **27**(3): p. 504-509.
43. Huang, Z.M., Y.Z. Zhang, M. Kotaki, and S. Ramakrishna, *A review on polymer nanofibers by electrospinning and their applications in nanocomposites.* Composites Science and Technology, 2003. **63**(15): p. 2223-2253.
44. Pham, Q.P., U. Sharma, and A.G. Mikos, *Electrospun poly(epsilon-caprolactone) microfiber and multilayer nanofiber/microfiber scaffolds: Characterization of scaffolds and measurement of cellular infiltration.* Biomacromolecules, 2006. **7**(10): p. 2796-2805.
45. Martins, A., R.L. Reis, and N.M. Neves, *Electrospinning: processing technique for tissue engineering scaffolding.* International Materials Reviews, 2008. **53**(5): p. 257-274.
46. Deitzel, J.M., J.D. Kleinmeyer, J.K. Hirvonen, and N.C. Beck Tan, *Controlled deposition of electrospun poly(ethylene oxide) fibers.* Polymer, 2001. **42**(19): p. 8163-8170.
47. Deitzel, J.M., J. Kleinmeyer, D. Harris, and N.C.B. Tan, *The effect of processing variables on the morphology of electrospun nanofibers and textiles.* Polymer, 2001. **42**(1): p. 261-272.
48. Megelski, S., J.S. Stephens, D.B. Chase, and J.F. Rabolt, *Micro- and Nanostructured Surface Morphology on Electrospun Polymer Fibers.* Macromolecules, 2002. **35**(22): p. 8456-8466.
49. Demir, M.M., I. Yilgor, E. Yilgor, and B. Erman, *Electrospinning of polyurethane fibers.* Polymer, 2002. **43**(11): p. 3303-3309.

50. Baumgarten, P.K., Journal Colloid Interface Science, 1971. **36**.
51. Subbiah, T., G.S. Bhat, R.W. Tock, S. Parameswaran, and S.S. Ramkumar, *Electrospinning of nanofibers.* Journal of Applied Polymer Science, 2005. **96**(2): p. 557-569.
52. Srinivasarao, M., D. Collings, A. Philips, and S. Patel, *Three-Dimensionally Ordered Array of Air Bubbles in a Polymer Film.* Science, 2001. **292**(5514): p. 79-83.
53. Formhals, A., U.S.P.a.T. Office, Editor. 1934.
54. Taylor, G., *Disintegration of Water Drops in an Electric Field.* Proceedings of the Royal Society of London. Series A. Mathematical and Physical Sciences, 1964. **280**(1382): p. 383-397.
55. Annis, D., *Materials for Arterial Grafts.* British Polymer Journal, 1978. **10**(4): p. 238-240.
56. Reneker, D.H. and I. Chun, *Nanometre diameter fibres of polymer, produced by electrospinning.* Nanotechnology, 1996(3): p. 216.
57. Baker, B.M. and R.L. Mauck, *The effect of nanofiber alignment on the maturation of engineered meniscus constructs.* Biomaterials, 2007. **28**(11): p. 1967-1977.
58. Lee, C.H., H.J. Shin, I.H. Cho, Y.-M. Kang, I.A. Kim, K.-D. Park, and J.-W. Shin, *Nanofiber alignment and direction of mechanical strain affect the ECM production of human ACL fibroblast.* Biomaterials, 2005. **26**(11): p. 1261-1270.
59. Yang, F., R. Murugan, S. Wang, and S. Ramakrishna, *Electrospinning of nano/micro scale poly(L-lactic acid) aligned fibers and their potential in neural tissue engineering.* Biomaterials, 2005. **26**(15): p. 2603-2610.
60. Ayres, C.E., G.L. Bowlin, R. Pizinger, L.T. Taylor, C.A. Keen, and D.G. Simpson, *Incremental changes in anisotropy induce incremental changes in the material properties of electrospun scaffolds.* Acta Biomaterialia, 2007. **3**(5): p. 651-661.
61. Bashur, C.A., L.A. Dahlgren, and A.S. Goldstein, *Effect of fiber diameter and orientation on fibroblast morphology and proliferation on electrospun poly(d,l-lactic-co-glycolic acid) meshes.* Biomaterials, 2006. **27**(33): p. 5681-5688.
62. Li, W.-J., R.L. Mauck, J.A. Cooper, X. Yuan, and R.S. Tuan, *Engineering controllable anisotropy in electrospun biodegradable nanofibrous scaffolds for musculoskeletal tissue engineering.* Journal of Biomechanics, 2007. **40**(8): p. 1686-1693.
63. Jalili, R. and M. Morshed, *Fundamental parameters affecting electrospinning of PAN nanofibers as uniaxially aligned fibers.* Journal of Applied Polymer Science, 2006. **101**: p. 4350-4357.
64. Li, D., Y.L. Wang, and Y.N. Xia, *Electrospinning nanofibers as uniaxially aligned arrays and layer-by-layer stacked films.* Advanced Materials, 2004. **16**(4): p. 361-366.
65. Teo, W.-E., R. Gopal, R. Ramaseshan, K. Fujihara, and S. Ramakrishna, *A dynamic liquid support system for continuous electrospun yarn fabrication.* Polymer, 2007. **48**(12): p. 3400-3405.
66. Smit, E., U. Buttner, and R.D. Sanderson, *Continuous yarns from electrospun fibers.* Polymer, 2005. **46**(8): p. 2419-2423.
67. Huang, Z.M., Y.Z. Zhang, and S. Ramakrishna, *Double-layered composite nanofibers and their mechanical performance.* Journal of Polymer Science Part B-Polymer Physics, 2005. **43**(20): p. 2852-2861.

68. Jiang, H.L., Y.Q. Hu, P.C. Zhao, Y. Li, and K.J. Zhu, *Modulation of protein release from biodegradable core-shell structured fibers prepared by coaxial electrospinning.* Journal of Biomedical Materials Research Part B-Applied Biomaterials, 2006. **79B**(1): p. 50-57.
69. Li, D. and Y.N. Xia, *Direct fabrication of composite and ceramic hollow nanofibers by electrospinning.* Nano Letters, 2004. **4**(5): p. 933-938.
70. Nam, J., Y. Huang, S. Agarwal, and J. Lannutti, *Improved cellular infiltration in electrospun fiber via engineered porosity.* Tissue Engineering, 2007. **13**(9): p. 2249-2257.
71. Kim, T.G., H.J. Chung, and T.G. Park, *Macroporous and nanofibrous hyaluronic acid/collagen hybrid scaffold fabricated by concurrent electrospinning and deposition/leaching of salt particles.* Acta Biomaterialia, 2008. **4**(6): p. 1611-1619.
72. Mathews, J., G. Wnek, D. Simpson, and G. Bowlin, *Electrospinning of Collagen Type II: A Feasibility Study.* Journal of Bioactive and Compatible Polymers, 2003. **18**(March): p. 125-134.
73. Wise, J.K., A.L. Yarin, C.M. Megaridis, and M. Cho, *Chondrogenic Differentiation of Human Mesenchymal Stem Cells on Oriented Nanofibrous Scaffolds: Engineering the Superficial Zone of Articular Cartilage.* Tissue Engineering Part A, 2009. **15**(4): p. 913-921.
74. Subramanian, A., D. Vu, G.F. Larsen, and H.Y. Lin, *Preparation and evaluation of the electrospun chitosan/PEO fibers for potential applications in cartilage tissue engineering.* Journal of Biomaterials Science-Polymer Edition, 2005. **16**(7): p. 861-873.
75. Li, W.-J., R. Tuli, C. Okafor, A. Derfoul, K.G. Danielson, D.J. Hall, and R.S. Tuan, *A three-dimensional nanofibrous scaffold for cartilage tissue engineering using human mesenchymal stem cells.* Biomaterials, 2005. **26**(6): p. 599-609.
76. Karageorgiou, V. and D. Kaplan, *Porosity of 3D biomaterial scaffolds and osteogenesis.* Biomaterials, 2005. **26**(27): p. 5474-5491.
77. Nisbet, D.R., J.S. Forsythe, W. Shen, D.I. Finkelstein, and M.K. Horne, *Review Paper: A Review of the Cellular Response on Electrospun Nanofibers for Tissue Engineering.* Journal of Biomaterials Applications, 2009. **24**(1): p. 7-29.
78. Slaughter, B.V., S.S. Khurshid, O.Z. Fisher, A. Khademhosseini, and N.A. Peppas, *Hydrogels in Regenerative Medicine.* Advanced Materials, 2009. **21**(32-33): p. 3307-3329.
79. Varghese, S. and J.H. Elisseeff, *Hydrogels for musculoskeletal tissue engineering*, in *Polymers for Regenerative Medicine*. 2006, Springer-Verlag Berlin: Berlin. p. 95-144.
80. Gong, J.P., Y. Katsuyama, T. Kurokawa, and Y. Osada, *Double-network hydrogels with extremely high mechanical strength.* Advanced Materials, 2003. **15**(14): p. 1155.
81. Yasuda, K., N. Kitamura, J.P. Gong, K. Arakaki, H.J. Kwon, S. Onodera, Y.M. Chen, T. Kurokawa, F. Kanaya, Y. Ohmiya, and Y. Osada, *A Novel Double-Network Hydrogel Induces Spontaneous Articular Cartilage Regeneration in vivo in a Large Osteochondral Defect.* Macromolecular Bioscience, 2009. **9**(4): p. 307-316.
82. Suri, S. and C.E. Schmidt, *Photopatterned collagen-hyaluronic acid interpenetrating polymer network hydrogels.* Acta Biomaterialia, 2009. **5**(7): p. 2385-2397.
83. Miljkovic, N.D., Y.C. Lin, M. Cherubino, D. Minteer, and K.G. Marra, *A novel injectable hydrogel in combination with a surgical sealant in a rat knee osteochondral defect model.* Knee Surgery Sports Traumatology Arthroscopy, 2009. **17**(11): p. 1326-1331.

84. Miller, R.E., A.J. Grodzinsky, E.J. Vanderploeg, C. Lee, D.J. Ferris, M.F. Barrett, J.D. Kisiday, and D.D. Frisbie, *Effect of self-assembling peptide, chondrogenic factors, and bone marrow-derived stromal cells on osteochondral repair.* Osteoarthritis and Cartilage, 2010. **18**(12): p. 1608-1619.
85. Kisiday, J., M. Jin, B. Kurz, H. Hung, C. Semino, S. Zhang, and A.J. Grodzinsky, *Self-assembling peptide hydrogel fosters chondrocyte extracellular matrix production and cell division: Implications for cartilage tissue repair.* Proceedings of the National Academy of Sciences of the United States of America, 2002. **99**(15): p. 9996-10001.
86. Wang, P.Y., H.H. Chow, J.Y. Lai, H.L. Liu, and W.B. Tsai, *Dynamic Compression Modulates Chondrocyte Proliferation and Matrix Biosynthesis in Chitosan/Gelatin Scaffolds.* Journal of Biomedical Materials Research Part B-Applied Biomaterials, 2009. **91B**(1): p. 143-152.
87. Barnes, C.P., S.A. Sell, E.D. Boland, D.G. Simpson, and G.L. Bowlin, *Nanofiber technology: Designing the next generation of tissue engineering scaffolds.* Advanced Drug Delivery Reviews, 2007. **59**(14): p. 1413-1433.
88. Furth, M.E., A. Atala, and M.E. Van Dyke, *Smart biomaterials design for tissue engineering and regenerative medicine.* Biomaterials, 2007. **28**(34): p. 5068-5073.
89. Rutledge, G.C. and S.V. Fridrikh, *Formation of fibers by electrospinning.* Advanced Drug Delivery Reviews, 2007. **59**(14): p. 1384-1391.
90. Vaz, C.M., S. van Tuijl, C.V.C. Bouten, and F.P.T. Baaijens, *Design of scaffolds for blood vessel tissue engineering using a multi-layering electrospinning technique.* Acta Biomaterialia, 2005. **1**(5): p. 575-582.
91. Buttafoco, L., N.G. Kolkman, P. Engbers-Buijtenhuijs, A.A. Poot, P.J. Dijkstra, I. Vermes, and J. Feijen, *Electrospinning of collagen and elastin for tissue engineering applications.* Biomaterials, 2006. **27**(5): p. 724-734.
92. Dai, X. and S. Shivkumar, *Electrospinning of hydroxyapatite fibrous mats.* Materials Letters, 2007. **61**(13): p. 2735-2738.
93. Duan, B., X. Yuan, Y. Zhu, Y. Zhang, X. Li, Y. Zhang, and K. Yao, *A nanofibrous composite membrane of PLGA-chitosan/PVA prepared by electrospinning.* European Polymer Journal, 2006. **42**(9): p. 2013-2022.
94. Duling, R.R., R.B. Dupaix, N. Katsube, and J. Lannutti, *Mechanical characterization of electrospun polycaprolactone (PCL): A potential scaffold for tissue engineering.* Journal of Biomechanical Engineering-Transactions of the ASME, 2008. **130**(1).
95. Geng, X., O.-H. Kwon, and J. Jang, *Electrospinning of chitosan dissolved in concentrated acetic acid solution.* Biomaterials, 2005. **26**(27): p. 5427-5432.
96. Huang, Z.-M., Y.Z. Zhang, S. Ramakrishna, and C.T. Lim, *Electrospinning and mechanical characterization of gelatin nanofibers.* Polymer, 2004. **45**(15): p. 5361-5368.
97. Ji, Y., K. Ghosh, X.Z. Shu, B. Li, J.C. Sokolov, G.D. Prestwich, R.A.F. Clark, and M.H. Rafailovich, *Electrospun three-dimensional hyaluronic acid nanofibrous scaffolds.* Biomaterials, 2006. **27**(20): p. 3782-3792.
98. Liang, D., B.S. Hsiao, and B. Chu, *Functional electrospun nanofibrous scaffolds for biomedical applications.* Advanced Drug Delivery Reviews, 2007. **59**(14): p. 1392-1412.
99. Kumbar, S.G., R. James, S.P. Nukavarapu, and C.T. Laurencin, *Electrospun nanofiber scaffolds: engineering soft tissues.* Biomedical Materials, 2008. **3**(3).

100. Li, W.-J., R. Tuli, X. Huang, P. Laquerriere, and R.S. Tuan, *Multilineage differentiation of human mesenchymal stem cells in a three-dimensional nanofibrous scaffold.* Biomaterials, 2005. **26**(25): p. 5158-5166.
101. Zhong, S.P., W.E. Teo, X. Zhu, R. Beuerman, S. Ramakrishna, and L.Y.L. Yung, *Development of a novel collagen-GAG nanofibrous scaffold via electrospinning.* Materials Science and Engineering: C, 2007. **27**(2): p. 262-266.
102. Stitzel, J., L. Liu, S.J. Lee, M. Komura, J. Berry, S. Soker, G. Lim, M. Van Dyke, R. Czerw, J.J. Yoo, and A. Atala, *Controlled fabrication of a biological vascular substitute.* Biomaterials, 2006. **27**(7): p. 1088-1094.
103. Yang, F., C.Y. Xu, M. Kotaki, S. Wang, and S. Ramakrishna, *Characterization of neural stem cells on electrospun poly(L-lactic acid) nanofibrous scaffold.* Journal of Biomaterials Science-Polymer Edition, 2004. **15**(12): p. 1483-1497.
104. Bhattarai, S.R., N. Bhattarai, H.K. Yi, P.H. Hwang, D.I. Cha, and H.Y. Kim, *Novel biodegradable electrospun membrane: scaffold for tissue engineering.* Biomaterials, 2004. **25**(13): p. 2595-2602.
105. Baker, B.M., A.O. Gee, R.B. Metter, A.S. Nathan, R.A. Marklein, J.A. Burdick, and R.L. Mauck, *The potential to improve cell infiltration in composite fiber-aligned electrospun scaffolds by the selective removal of sacrificial fibers.* Biomaterials, 2008. **29**(15): p. 2348-2358.
106. Hayes, W.C. and T.N. Gerhart, *Biomechanics of bone: Applications for assessment of bone strength.* Bone and Mineral Research, 1985: p. 259-294.
107. Manschot, J.F.M. and A.J.M. Brakkee, *The measurement and modeling of the mechanical-properties of human-skin in vivo.* Journal of Biomechanics, 1986. **19**(7): p. 511-515.
108. Lee, S.J., J.J. Yoo, G.J. Lim, A. Atala, and J. Stitzel, *In vitro evaluation of electrospun nanofiber scaffolds for vascular graft application.* Journal of Biomedical Materials Research Part A, 2007. **83A**(4): p. 999-1008.
109. Wright, L.D., T. Andric, and J.W. Freeman, *Utilizing NaCl to increase the porosity of electrospun materials.* Materials Science & Engineering C-Materials for Biological Applications, 2011. **31**(1): p. 30-36.
110. Li, W.-J., J.J.A. Cooper, R.L. Mauck, and R.S. Tuan, *Fabrication and characterization of six electrospun poly([alpha]-hydroxy ester)-based fibrous scaffolds for tissue engineering applications.* Acta Biomaterialia, 2006. **2**(4): p. 377-385.
111. Li, W.J., C.T. Laurencin, E.J. Caterson, R.S. Tuan, and F.K. Ko, *Electrospun nanofibrous structure: A novel scaffold for tissue engineering.* Journal of Biomedical Materials Research, 2002. **60**(4): p. 613-621.
112. Kumbar, S.G., R. James, S.P. Nukavarapu, and C.T. Laurencin, *Electrospun nanofiber scaffolds: engineering soft tissues.* Biomedical Materials, 2008. **3**(3): p. 034002.
113. Kurkijarvi, J.E., M.J. Nissi, I. Kiviranta, J.S. Jurvelin, and M.T. Nieminen, *Delayed gadolinium-enhanced MRI of cartilage (dGEMRIC) and T-2 characteristics of human knee articular cartilage: topographical variation and relationships to mechanical properties.* Magnetic Resonance in Medicine, 2004. **52**(1): p. 41-46.
114. Buckwalter, J.A., *Articular cartilage: injuries and potential for healing.* Journal of Orthopopaedic Sports and Physical Therapy, 1998. **28**(4): p. 192-202.
115. Khor, E., *Chitin: fulfilling a biomaterials promise*. 2001, New York: Elsevier Science Ltd.

116. Kumar, M., *A review of chitin and chitosan applications.* Reactive & Functional Polymers, 2000. **46**(1): p. 1-27.
117. Chen, S.C., Y.C. Wu, F.L. Mi, Y.H. Lin, L.C. Yu, and H.W. Sung, *A novel pH-sensitive hydrogel composed of N,O-carboxymethyl chitosan and alginate cross-linked by genipin for protein drug delivery.* Journal of Controlled Release, 2004. **96**(2): p. 285-300.
118. Berger, J., M. Reist, J.M. Mayer, O. Felt, N.A. Peppas, and R. Gurny, *Structure and interactions in covalently and ionically crosslinked chitosan hydrogels for biomedical applications.* European Journal of Pharmaceutics and Biopharmaceutics, 2004. **57**(1): p. 19-34.
119. Shu, X.Z. and K.J. Zhu, *A novel approach to prepare tripolyphosphate/chitosan complex beads for controlled release drug delivery.* International Journal of Pharmaceutics, 2000. **201**(1): p. 51-8.
120. Berger, J., M. Reist, J.M. Mayer, O. Felt, and R. Gurny, *Structure and interactions in chitosan hydrogels formed by complexation or aggregation for biomedical applications.* European Journal of Pharmaceutic Biopharmaceutics, 2004. **57**(1): p. 35-52.
121. Nair, L.S., T. Starnes, J.W. Ko, and C.T. Laurencin, *Development of injectable thermogelling chitosan-inorganic phosphate solutions for biomedical applications.* Biomacromolecules, 2007. **8**(12): p. 3779-85.
122. Wright, L.D., R.T. Young, T. Andric, and J.W. Freeman, *Fabrication and mechanical characterization of 3D electrospun scaffolds for tissue engineering.* Biomedical Materials, 2010. **5**(5).
123. Waldman, S.D., C.G. Spiteri, M.D. Grynpas, R.M. Pilliar, and R.A. Kandel, *Long-term intermittent compressive stimulation improves the composition and mechanical properties of tissue-engineered cartilage.* Tissue Engineering, 2004. **10**(9-10): p. 1323-1331.
124. Park, S., C.T. Hung, and G.A. Ateshian, *Mechanical response of bovine articular cartilage under dynamic unconfined compression loading at physiological stress levels.* Osteoarthritis and Cartilage, 2004. **12**(1): p. 65-73.
125. Martin, I., S. Miot, A. Barbero, M. Jakob, and D. Wendt, *Osteochondral tissue engineering.* Journal of Biomechanics, 2007. **40**(4): p. 750-765.
126. Temenoff, J.S. and A.G. Mikos, *Review: tissue engineering for regeneration of articular cartilage.* Biomaterials, 2000. **21**(5): p. 431-440.
127. Vinatier, C., D. Mrugala, C. Jorgensen, J. Guicheux, and D. Noël, *Cartilage engineering: a crucial combination of cells, biomaterials and biofactors.* Trends in Biotechnology, 2009. **27**(5): p. 307-314.
128. Billington, C.J., *Cartilage proteoglycan release assay.* Methods in molecular biology (Clifton, N.J.), 2001. **151**: p. 451-6.
129. Bonakdar, S., S.H. Emami, M.A. Shokrgozar, A. Farhadi, S.A.H. Ahmadi, and A. Amanzadeh, *Preparation and characterization of polyvinyl alcohol hydrogels crosslinked by biodegradable polyurethane for tissue engineering of cartilage.* Materials Science and Engineering: C, 2010. **30**(4): p. 636-643.
130. Hedlund, H., E. Hedbom, D. Heinegard, S. Mengarelli-Widholm, F.P. Reinholt, and O. Svensson, *Association of the aggrecan keratan sulfate-rich region with collagen in bovine articular cartilage.* Journal of Biological Chemistry, 1999. **274**(9): p. 5777-5781.
131. Takahashi, T., T. Ogasawara, J. Kishimoto, G. Liu, H. Asato, T. Nakatsuka, E. Uchinuma, K. Nakamura, H. Kawaguchi, U.-i. Chung, T. Takato, and K. Hoshi,

Synergistic Effects of FGF-2 With Insulin or IGF-I on the Proliferation of Human Auricular Chondrocytes. Cell Transplantation, 2005. **14**: p. 683-693.
132. van der Kraan, P.M., P. Buma, T. van Kuppevelt, and W.B. van Den Berg, *Interaction of chondrocytes, extracellular matrix and growth factors: relevance for articular cartilage tissue engineering.* Osteoarthritis and Cartilage, 2002. **10**(8): p. 631-637.
133. Morales, T.I., *Chondrocyte moves: clever strategies?* Osteoarthritis and Cartilage, 2007. **15**(8): p. 861-871.
134. Chang, C., D.A. Lauffenburger, and T.I. Morales, *Motile chondrocytes from newborn calf: migration properties and synthesis of collagen II.* Osteoarthritis and Cartilage, 2003. **11**(8): p. 603-612.
135. Mishima, Y. and M. Lotz, *Chemotaxis of human articular chondrocytes and mesenchymal stem cells.* Journal of Orthopaedic Research, 2008. **26**(10): p. 1407-1412.